universität wien

MASTERARBEIT / MASTER'S THESIS

Titel der Masterarbeit / Title of the Master's Thesis

„Nanodisc embedded proteins as biorecognition elements on a graphene-based field-effect transistor for biosensing applications - A proof of principle investigation“

verfasst von / submitted by

Marie-Helene Polt BA BSc

angestrebter akademischer Grad / in partial fulfilment of the requirements for the degree of

Master of Science (MSc)

Wien, 2022 / Vienna, 2022

Studienkennzahl lt. Studienblatt / degree programme code as it appears on the student record sheet:	UA 066 834
Studienrichtung lt. Studienblatt / degree programme as it appears on the student record sheet:	Masterstudium Molekulare Biologie
Betreut von / Supervisor:	Univ.-Prof. Dr. Bojan Zagrovic, BA

Acknowledgements

I would hereby like to take the opportunity to thank everyone who enabled this work and who supported me along the way.

First of all I would like to thank Dr. Wolfgang Knoll from the AIT, who encouraged me to seek beyond my own scientific constraints. Further my thanks go to Dr. Sabine Szunerits for welcoming me at the University of Lille, France and for giving me the opportunity to learn and profit from her well-positioned lab. I would also like to thank Dr. Bojan Zagrovic for accepting to supervise this master thesis, although the topic is not within his usual scientific interest. I want to especially thank Adrien Hugo for the many hours of input and discussions and for taking the time to teach me so many valuable lessons. It really was a great pleasure working alongside you. Although it is a stand-alone effort, any work is driven by the support of the people close to you. Therefore, I would like to thank my friends for listening to my concerns and encouraging me, even if they don't always understand what exactly I am doing. Furthermore, I would like to thank my parents for their constant support and trust in me to find my own way. Finally, the biggest thanks goes to my partner Klaus, for having my back and believing in me when I doubt myself.

Abstract

As the recent years have shown, fast and individualized diagnostic tools are essential for guaranteeing and maintaining global health. Because of that, the need for reliable real-time detection of biomolecules related to diseases is a fundamental issue of our time. One way of tackling this issue is developing biosensing devices for medical applications. Within the vast field of biosensors graphene-based field-effect transistors (gFETs) stand out due to their high sensitivity. To additionally make them selective towards respective biomolecules their surface has to be modified with bioreceptors. One particularly relevant group of bioreceptors are situated within the cell membrane of human cells. Using these receptors as biosensing moieties would allow the specific detection of a wide range of biomolecules. However, how to immobilize these receptors on the graphene surface remains a challenging quest. Further those membrane bioreceptors request a particular environment, which is only provided when embedding them in lipid nanodiscs. Therefore the aim of the work of this thesis was to investigate a successful immobilization strategy for nanodisc embedded proteins on a gFET and to test them as biosensing units. This was done by characterizing the modified devices using atomic force miroscopy (AFM), Raman spectroscopy, X-ray photoelectron spectroscopy (XPS), as well as electrical measurements in a liquid environment.

Kurzfassung

In den letzten Jahren hat sich gezeigt, dass schnelle und individualisierte Diagnose-tools unerlässlich sind um die globale Gesundheit zu gewährleisten und aufrechtzuerhalten. Daher ist die zuverlässige Echtzeit-Detektion von Biomolekülen, die mit Krankheiten in Verbindung stehen, ein grundlegendes Problem unserer Zeit. Eine Möglichkeit, dieses Problem anzugehen, ist die Entwicklung von Biosensoren für medizinische Anwendungen. Innerhalb des breitgefächerten Feldes der Biosensoren zeichnen sich graphenbasierte Feldeffekttransistoren (gFETs) durch ihre hohe Empfindlichkeit aus. Um sie zusätzlich selektiv für entsprechende Biomoleküle zu machen, muss ihre Oberfläche mit Biorezeptoren modifiziert werden. Eine besonders relevante Gruppe von Biorezeptoren befindet sich in der Zellmembran von menschlichen Zellen. Die Verwendung dieser Rezeptoren im Kontext von Biosensoren würde den spezifischen Nachweis einer Vielzahl von Biomolekülen ermöglichen. Die Immobilisierung dieser Rezeptoren auf der Graphenoberfläche stellt jedoch eine Herausforderung dar. Außerdem benötigen diese Membran-Biorezeptoren eine besondere Umgebung, die nur durch die Einbettung in Lipid-Nanodiscs gegeben ist. Ziel dieser Arbeit war es daher, eine erfolgreiche Immobilisierungsstrategie für die, in Nanodiscs eingebettete Proteine, auf einem gFET zu untersuchen und diese als Biosensoren zu testen. Dazu wurden die modifizierten Sensoren mit Hilfe von Atomkraftmikroskopie (AFM), Raman-Spektroskopie, Röntgen-Photoelektronenspektroskopie (XPS) sowie elektrischen Messungen in einer elektrolytischen Umgebung charakterisiert.

Contents

Outline and Objective

At the end of many output-oriented processes there is a final “product”. The finality of the product is, however, only short-lived, as with every day that passes by, innovative ideas can sprout and through that progress alterations are implemented. Hence also the term state-of-the-art. This is especially true for applied research or fields close to that, as the demand of the market further pushes innovation. One of these fields is the one of biosensing. In the here presented work a biosensor will be introduced and discussed. However, the presented thesis would not be able to exists if not for the preceding work of Ciril Reiner-Rozman, Patrik Aspermaier and Adrien Hugo. This concerned "hardware", in the form of already established substrates and equipment, software as well as substantial knowledge about fabrication processes and material properties. Thus their findings greatly make up the foundation for this work here. To thoroughly be able to understand and follow the essence of this work and the presented biosensor, as well as to get an understanding of the presented outline a few fundamental questions have to be contextualized first: What do we mean when talking about biosensing? What actually is a biosensor and is there even such a thing as a/the biosensor? And finally, why is this of relevance for our time and worth scientific investment? To keep this as intelligible and entertaining as possible the practical considerations will be presented alongside the theoretical background. Through this approach the work can be considered a step by step guide to the preparation process and the considerations behind the presented biosensing platform, which is aimed at immobilizing nanodisc embedded proteins onto a graphene based biosensor and testing them towards a ligand with high affinity.
If not indicated otherwise, all graphs, figures and pictures were created or obtained by the author.

1. Background and Theory

1.1. Introduction

This first section will give an introduction to biosensing and aims to contextualise which concepts and principles are essential to consider for the objective of a successful biosensor. The aim is to clarify what a biosensor is, why it is of use and to whom. Further the biochemical concepts that are relevant for biosensing shall be explained in depth, as this will be useful later on for interpreting and understanding the data discussed and presented in this work. Finally the biosensor at the basis of this work will be briefly introduced.

Fundamentals of Biosensing

Biosensing describes the active recording of the presence of a biological compound. This can be accomplished by using a biosensor. In its simplest definition a biosensor is the combination of a biological recognition element with a transducing element [64]. In this constellation the bioreceptor is responsible for recognising a biomolecule of interest and the transducer element converts this recognition event into a recordable signal.

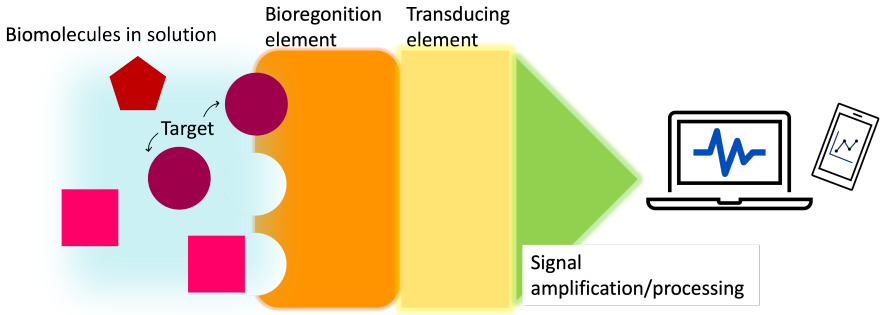

Figure 1.1.: Schematic illustration of the principle of a biosensor (graphic created by the author using PowerPoint ©)

Metaphorically speaking and seen from a biological perspective the whole human body can be considered an enormous biosensor that ultimately contains both recognition events as well as signal transduction in one. This can be illustrated when regarding one of the endocrine signalling pathways of Estradiol (Figure 1.2). Estradiol travels through the bloodstream and might recognise and bind to the extracellular domain of an estradiol receptor, GPER1 located within a cell membrane. Upon binding of the estadiol molecule

to the estradiol receptor this receptor is switched from it's inactive to it's active form. In the case of the G-coupled protein receptor family, to which this specific estradiol receptor, GPER1, belongs to, this leads to the further activation of a trimeric G protein, initiated through the binding of the activated estradiol receptor to the α subunit of the G protein. This binding of the estradiol receptor to the α subunit induces a conformational change which releases the just bound GDP from the nucleotide-binding site of the α subunit, allowing for the binding of GTP. Binding of GTP induces another conformational change, which now results into the dissociation of the α subunit from the $\beta\gamma$ complex. The active α subunit, as well as the active $\beta\gamma$ complex now posses the capacity to induce further downstream signalling cascades, such as cAMP regulation and protein-kinase activation, which ultimately will regulate gene expression [31].

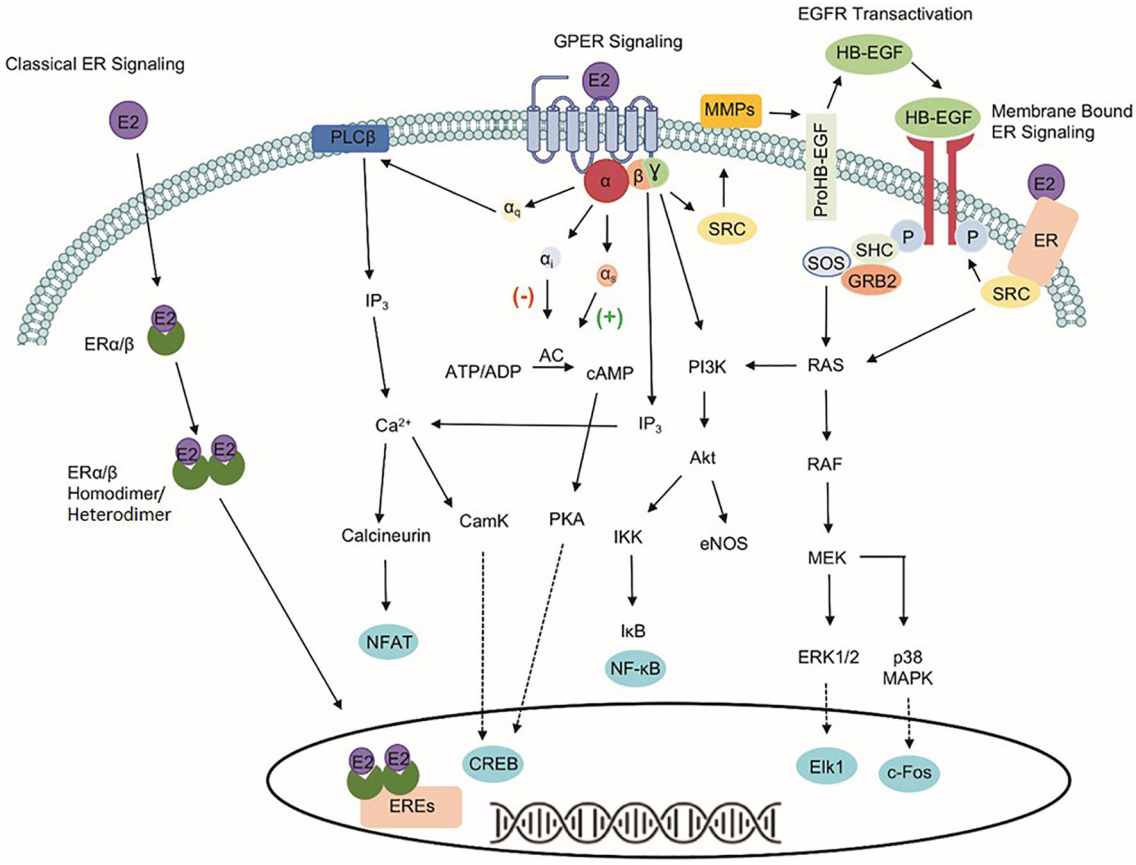

Figure 1.2.: Signalling pathways of estradiol depicting the example of GPER1 (from [22])

This example illustrates the sheer complexity of biological systems where biomolecules are constantly interacting and regulative mechanisms are ongoing non-stop. Within such an environment it's difficult to easily determine how the different components interact with each other and which interactions cause which outcomes. Although understanding

and unravelling those cascades is fascinating in itself, a special subgroup of molecules is of huge general interest for the human population. Referred to as *biomarkers* these molecules are tremendously important within a clinical context, meaning that they can be an indication for medical conditions or the risk of such. As often with those seemingly ubiquitous terms, an ultimate answer to the question "What is a biomarker?" is hard to provide. Therefore the Food and Drug Administration (FDA) and the National Institutes of Health (NIH) joined forces and founded the BEST (Biomarkers, EndpointS, and other Tools) working group to identify clear and suitable working definitions for several types of biomarkers [29]. Those are:

- "Diagnostic Biomarkers: used to dectect or confirm presence of disease or condition of interest or to identify individuals with a subtype of the disease (e.g. Blood sugar - Diabetes Type 2)"
- "Monitoring Biomarkers: measured repeatedly for assessing status of a disease or medical condition or for evidence of exposure to (or effect of) a medical product or an environmental agent (e.g. BNP & proBNP - patients with pulmonary hypertension)"
- "Response Biomarkers: used to show that a biological response, potentially beneficial or harmful, has occured in an individual who has been exposed to a medical product or an environmental agent (e.g. Phospho-AKT levels - anti-cancer PI3K inhibitors)"
- "Predictive Biomarkers: used to identify individuals who are more likely than similar individuals without the biomarker to experience a favourable or unfavorable effect from exposure to a medical product or an environmental agent (e.g. BRCA1/2 - patients response to PARP inhibitors)"
- "Prognostic Biomarkers: used to identify likelihood of a clinical event, disease recurrence or progression in patients who have the disease or medical conditions of interest (e.g. BRCA1/2 - likelihood of second breast cancer outbreak)"
- "Safety Biomarker: measured before or after an exposure to a medical product or an environmental agent to indicate the likelihood, presence, or extent of toxicity as an adverse effect (e.g. Neutrophil count - adjustment of cytotoxic dose in chemotherapy)"
- "Risk Biomarkers: indicate the potential for developing a disease or medical condition in an individual who does not currently have clinically apparent disease or the medical condition (e.g. BRCA1/2 - predisposition for breast cancer)"

It has to noted that, for most of the biomarkers listed above there isn't one exact concentration value that can be consulted, but rather a concentration range. If this range is passed (below or above), this is potentially harmful for the respective individual. Because of this associations with health and well-being a great amount of resources are directed towards sensitive and precise detection methods to monitor biomarkers. This is where biosensors come into play. The biomolecule of interest is therefore in this

context the respective biomarker in question. For the other elements of a biosensor, biorecognition element and transducing element, various approaches and combinations are possible (Figure1.3) and there is no one-size-fits-all-solution. Regardless of which variant is chosen, however, the underlying demands directed towards a biosensor stay the same and are assessed within the categories: Selectivity, reproduciblity, stability, sensitivity and linearity [7]. One key aspect of a well conceptualized biosensor is therefore the reduction of complexity in favour of obtaining straight forward information about the molecule of interest. In order words, in order to be able to match the criteria mentioned above, a biosensor should:

a) only show a signal for the biomolecule of interest (selectivity)
b) this response should always be obtainable with this biosensor when the biomolecule is present (reproducibility)
c) the biosensor and the shown response should be stable over time (stability)
d) the biosensor should show a signal upon the smallest amount of biomolecule (sensitivity) and
e) the response signal should change linearly with the concentration of biomolecule (linearity)

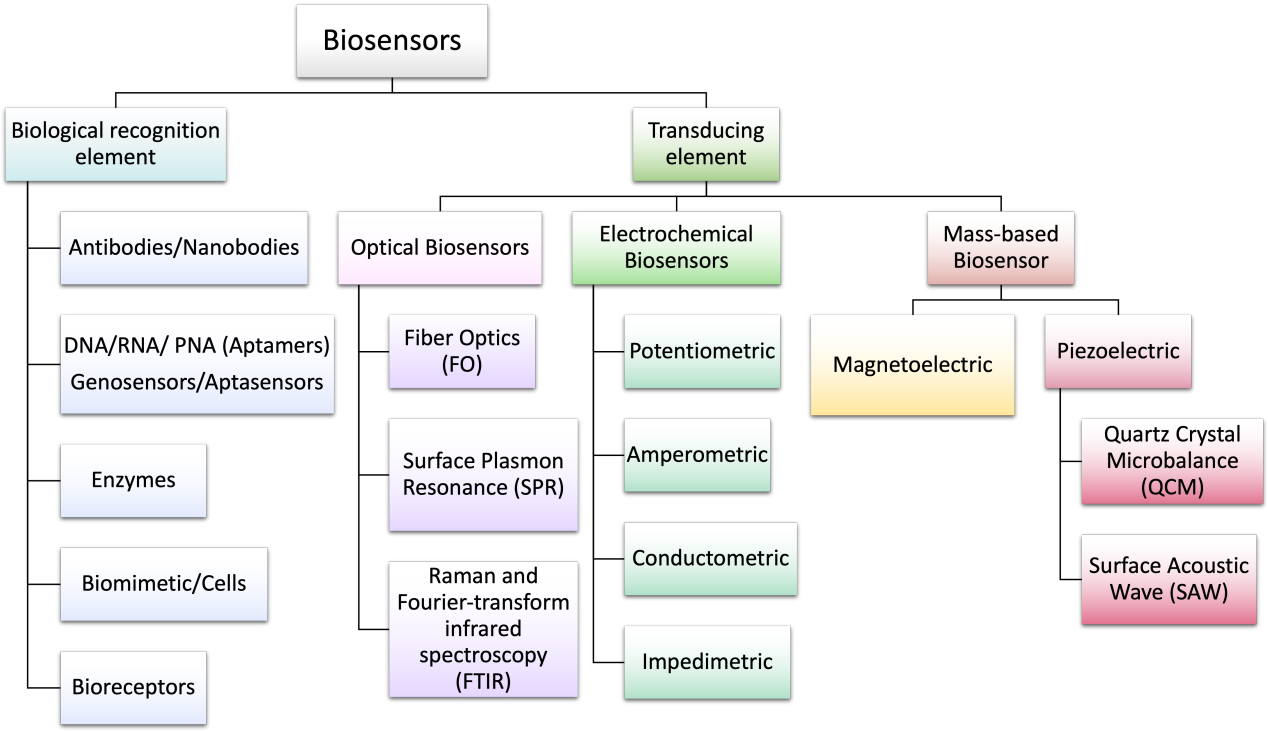

Figure 1.3.: Types of biosensors (adapted from [2])

The example par excellence for biomarker monitoring is the measurement of the blood glucose concentration. Dating back to one of the first ever developed biosensors in 1962, this biomarker - biosensor pair helps people with diabetes worldwide to asses their blood sugar levels on a regular basis, simplifying their life's and granting autonomy. What working principle however is at the basis of this biosensor? Critical for the development of this first biosensor, developed by Clark and Lyons [19] was the already established "Clark" electrode, which allowed for the measurement of the oxygen partial pressure (pO_2) in a liquid reservoir. For the set up of their biosensor the bottom of the reservoir consisted of two membranes enclosing a layer of concentrated glucose oxidase (GOx or GOD). When the liquid reservoir contains glucose, this glucose is able to diffuse through the membrane, thus being exposed to the GOx. Through the enzymatic activity of the GOx the glucose is, under the presence of oxygen, converted to gluconic acid and hydrogen peroxide (H_2O_2) [4]. Due to this reaction oxygen is consumed, leading to a change in (pO_2), which can be tracked via the electrode. Another possibility using the same set-up would be to track the pH using a pH electrode, which would show a decrease in pH with a higher concentration of gluconic acid, allowing for an inference about the concentration of glucose within the reservoir. Alternatively also the concentration of (H_2O_2) could be monitored, yielding information about the concentration of glucose present. In all these scenarios the concentration of glucose is indirectly determined by other parameters. But how does one get from one of these parameters to the concentration of glucose and why is it safe to assume that these reactions even occur in the described manner? In order to answer these questions, it is worth taking a closer look at some of the fundamental concepts of thermodynamics and the consequences for biological systems.
One could begin with raising the question: Why do molecules even interact with each other? In order for molecules to interact they need to be part of the same system. Let's take the state where the molecules are not interacting and call it Y and the state of interaction X. If those states are now compared to one another, they will exhibit differences in their free enthalpy or Gibbs free energy (ΔG). As all systems strive towards having a minimum of free energy, all potential energy present within a system will be converted in either heat or work, as fast as possible, until the minimum state is reached. This minimum state is therefore the state in which equilibrium is reached ($\Delta G = 0$). This relationship is summarised by the ***equilibrium constant K***. If state X is now energetically more favourable than state Y this will result in Y $\rightarrow$ X, with the equilibrium constant being:

$$K = \frac{[X]}{[Y]}$$

where the enumerator and the denominator present the respective concentrations at equilibrium [1]. Thus the Gibbs free energy can be expressed as equation that defines the difference between the current state of the system and its equilibrium:

$$\Delta G = \Delta G^{0\prime} + RTlnK$$

with T being the temperature in Kelvin, R the gas constant (8.314 KJ/mol) and $\Delta G^{0\prime}$ the standard free-energy change.

In the context of the example of the first biosensor the glucose in the solution can be in the unbound state or can be bound to the GOx. Eventually the GOx will, in it's function as enzyme speed up the reaction of glucose into gluconic acic, following the reaction:

$$Glucose + O_2 + H_2O \xrightarrow{Glucoseoxidase} Gluconicacid + H_2O_2$$

but first the glucose itself has to bind to the enzyme. Assuming that this system has no limitation in the availability of substrate, hence there in endless glucose available, it's possible to conclude that in a solution containing these molecules there will always be glucose molecules that associate with the enzyme and then some that dissociate before the enzyme facilitates the break up into gluconic acic and H_2O_2. This relation is expressed through the Michaelis-Menten-Kinetics:

$$E + S \underset{k_{-1}}{\overset{k_1}{\rightleftharpoons}} ES \underset{k_{-cat}}{\overset{k_{cat}}{\rightleftharpoons}} E + P$$

with E being the enzyme, S the substrate, ES the complex of substrate bound to enzyme and P the product. The traditional Michaelis-Menten-equation describes, differently to the depiction here, the reaction from enzyme-substrate complex to product as irreversible. This is a simplification, which, although being a valid assumption for many systems, still should be kept in mind when discussing enzyme biology. The Michaelis-Menten model is, nevertheless, commonly used to characterise enzymes, as the k_{cat} or turnover rate is used to determine the number of substrate molecules processed by each enzyme per second. Further this parameter can be used to determine the Michaelis-Menten-Constant (K_m):

$$K_m = \frac{k_{-1} + k_{cat}}{k_1}$$

which represents the concentration at which the reaction rate is at half of it's maximum:

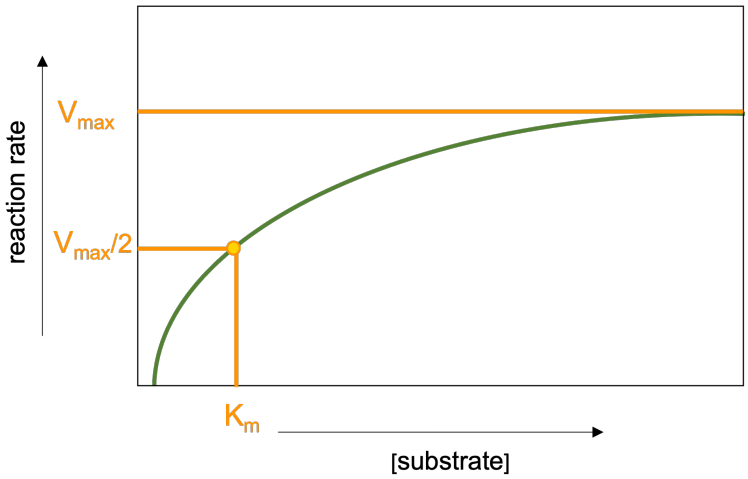

Figure 1.4.: Enzyme kinetics according to Michaelis-Menten (adapted from [1]

The constant K_m is therefore also an indication for the affinity of an enzyme to it's substrate, as a lower K_m value is equivalent to a lower concentration at which half of the V_{max} is reached, which implies a higher affinity, or attraction of the enzyme to bind to it's substrate. The Michaelis-Menten-equation does however, next to describing enzymatic kinetics, hold an even more fundamental principal, as the first part of the equation:

$$E_{nzyme} + S_{ubstrate} \underset{k_{-1}}{\overset{k_1}{\rightleftharpoons}} ES$$

is not only true for enzyme and substrate interactions, but can be more generally applied to interacting biomolecules. The usually used nomenclature refers to a Protein (P) and it's respective ligand (L):

$$L + P \underset{k_{-1}/k_{off}}{\overset{k_1/k_{on}}{\rightleftharpoons}} PL$$

with k_1/k_{on} being the rate of association and k_{-1}/k_{off} being the rate of dissociation. Exactly this rate of dissociation is used under the term dissociation constant or K_d to express the affinity of the ligand-protein interaction. It refers to the ligand concentration at which half of the present proteins are in a bound state and is expressed as:

$$K_d = \frac{[L][P]}{[LP]} = \frac{k_{-1}}{k_1} = \frac{k_{off}}{k_{on}}$$

The rate constants of association and disassociation, as well as it's ratio thereby yield valuable information about the system in question. The rate of association indicates that interaction, and thus non-covalent binding events are occurring. Whereas the rate of dissociation provides more information about how long the molecules stay bound to each other. It can therefore be regarded as a more informative parameter concerning the affinity of those two molecules. This is because non-covalent interactions can easily occur randomly, with each individual interaction only being a minor energetic contribution. In order to achieve some sort of stability, however, numerous of those interactions have to be able to occur, which is only the case if a fitting binding site is present. It can therefore be concluded that a lower rate of dissociation is an indication for more binding events and therefore greater stability. When a system has reached equilibrium K_d represents the concentration at which half of the protein (or receptor) is bound to the ligand and is equivalent to the inverse of the equilibrium constant (K). Therefore equilibrium binding experiments are often the method of choice to investigate the interaction of two biomolecules, as the lower the K_d of a system the higher it's affinity, implying the higher abundance of inter-molecular interactions. In order for two interacting proteins to bind to each other their surfaces need to be able to align in a very specif manner [1]. This can either be via a surface-string interaction, where one protein has an extended polypeptide chain loop contacting the surface of the other protein. Via helix-helix interaction, that form a coil around each other. Or, most commonly, via rigid surface-surface interaction. This surface-surface interaction can be very tight, as numerous of non-covalent binding events can occur. These binding events only grant lasting stability when they occur in a

higher abundance, as the energetic contribution of each individual contribution is only very minor (around 0.4 kJ/mole for van der Waals' interactions, around 4.2 kJ/mole for hydrogen bonds and around 12.6 kJ/mole for charge interactions vs. around 390 kJ/mole for covalent bonds [1]). Therefore only proteins with fitting surfaces or binding sites have the potential to interact in a stable fashion. Because of the convention to use the K_d of two interacting molecules as a measure of affinity, it comes as no surprise that also within the context of biosensing this parameter is regularly used to describe the affinity observed for a specifically developed biosensor. Next to the K_d, another value of interest is the limit-of-detection (LOD) which describes the minimum concentration of protein of interest to which the sensor gives a response that is distinguishable from noise. These values are used to characterise a biosensor and to evaluate it's utility in a medical context. The K_d is relevant as it provides information about the affinity and therefore the specificity and selectivity of the biosensor. Whereas the LOD is important as this determines whether the biosensor is able to detect a concentration that is meaningful in a diagnostic context. Naturally, a lower LOD can be promising for detecting biomolecules at an early point of for example infection. At this point it should be pointed out that, although many biosensor have been reported as being able to detect their target molecule on a femtomolar level, this might not always be the best parameter of quality control for a biosensor. This is because often a concentration range of a biomarker, that may even be patient specific, is more relevant. With that being said, more and more biosensing devices enter the market with the aim to make diagnostics quicker. Next to this clinical relevance biosensor devices also become more prominent in everyday life as they are part of a self-monitoring trend supposedly allowing the users to take control over their health and life. These include devices designed to track sleep quality, monitor sportive efforts and check for fertility [92].
To sum up, the dissociation constant or the K_d is a parameter commonly used to describe the affinity of two molecules to each other. The lower the K_d, the higher the affinity. The unit used to describe this affinity is Molarity or molar concentration (M) in mol/L. In the context of Biosensing this is relevant, because as stated previously a) the concentration of a certain biomolecule in a sample should be determined and b) the limit of detection (LOD) should be provided.

Now that the principles of biosensing are clarified, we shall specify and introduce the biosensor at the core of this master thesis: A graphene based field-effect-transistor with an immobilised lipid-nanodiscs containing a biotynilated Glycophorin A protein (Figure 1.5).

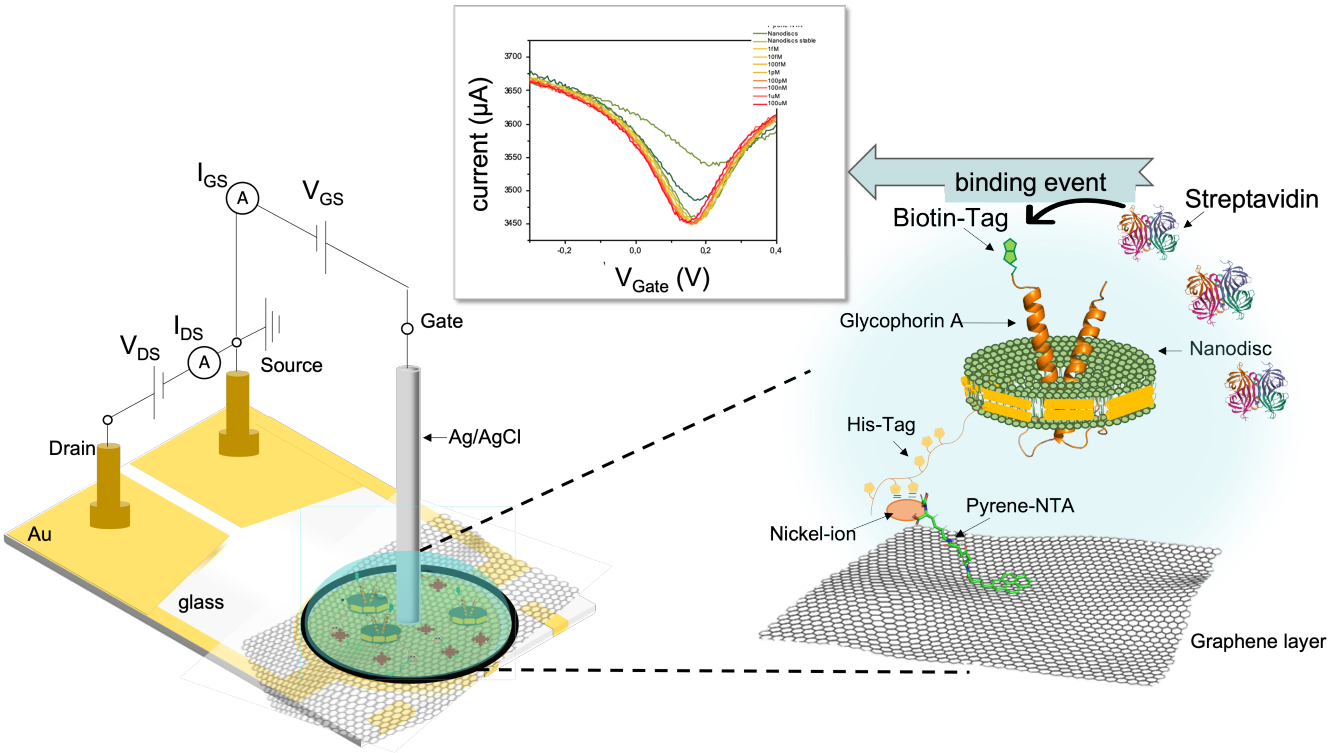

Figure 1.5.: gFET-Nanodisc Biosensor (graphic created by the author using PowerPoint ©, BioRender © and streptavidin molecule taken from the Protein Data Base (PDB) ©)

The presented biosensor is based on a field-effect transistor allowing for the monitoring of current that flows between the source and drain electrode of the device. Thereby a region referred to as sensing area or channel is passed. This area is modified with a graphene film that is functionalised and houses a lipid nanodisc containing a Glycophorin A protein with a biotin-tag. Biotin has a high affinity to the protein streptavidin. Therefore the sensor should show a response to the exposure of increasing concentrations of streptavidin. This is a proof-of-concept approach, as the interaction of biotin and streptavidin is well understood and not really of clinical relevance. Therefore the main aim is to investigate the possibility of using nanodiscs as biorecognition element on this kind of graphene field-effect transistor based biosensing platform. In order to understand the introduced biosensor the next sections will explore the details of the biosensor presented here by dissecting it step-by-step. Beginning with field-effect transistors and their application for biosensing purposes.

1.2. Field-effect transistors (FETs) for biosensing applications

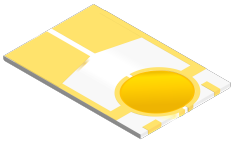

The use of field-effect-transistors (FETs) for biosensing applications (in the form of BioFETs) is considered to be a promising low-cost and fast-forward method on the rise [95]. But what exactly makes FETs suitable for the purpose of biosensing? Traditionally the key components of FETs are referred to as as source (S), drain (D) and gate (G) [123]. Due to an applied voltage at the gate, the conductivity of the semiconductor between the source and the drain is modulated, thus changing the flow of current. The source and drain can therefore be seen as the starting and ending point of charge carriers which are connected via the gate. In the context of biosensing these properties can be used for the detection of biomolecules because the variations in surface potential correspond to molecular binding events. Depending on the design of the respective FET these biomolecular events take place on the gate electrode or on the channel connecting the source and drain. The commonly used detection mechanisms, however, remain the same: the occurrence of a binding event is either measured by tracking the change in source-drain current ($\Delta I/I_0$), the change in conductance (Δ G/G_0) or the shift in Dirac point (in V) (different measurement approaches depicted in Figure 1.6). This principle of charge detection, that is utilised for BioFETs is based on the set-up of the ion-sensitive field-effect transistors (ISFETs) proposed by Bergveld in 1970 [6]. ISEFTs themselves were based on the working principle of metal–oxide–semiconductor field-effect transistors (MOSFETs), making the BioFETs descendants of MOSFETS. Before diving deeper into the specificity's of the BioFET underlying this work, it is valuable to briefly discuss the physical principles and structure of MOSFETs and their "evolution" towards biosensing applications.

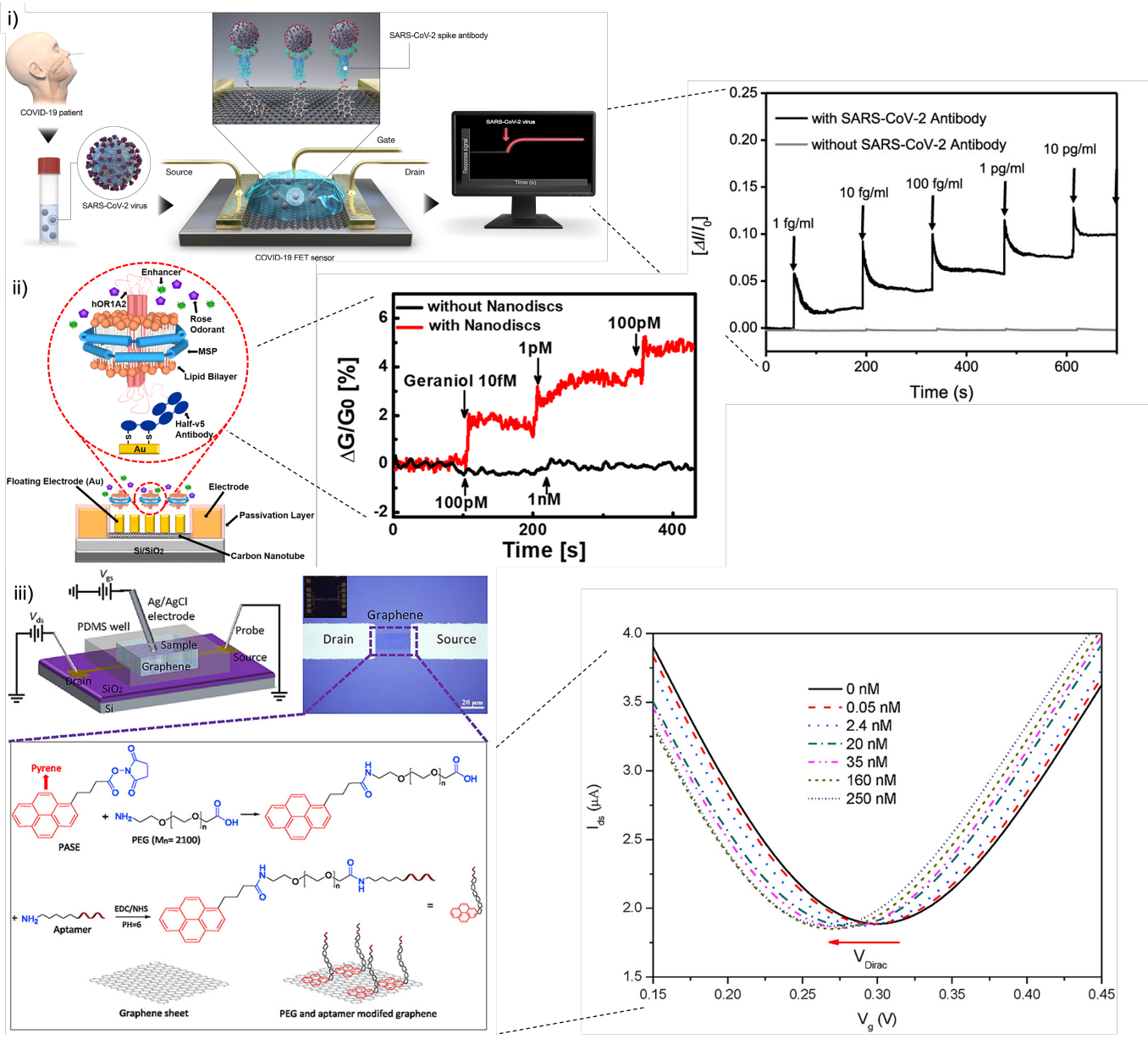

Figure 1.6.: i) SARS-CoV-2 virus detection via ($\Delta I/I_0$) using a graphene FET sensor (from [98]) ii) Carbon nanotube (CNT) based FET functionalized with a nanodisc-embedded olfactory receptor for the detection of a terpene oderant tracked by (Δ G/G$_0$) (from [62]) iii) Aptamer modified graphene FET for IgE detection in human serum following the shift in Dirac point (from [110])

From MOSFETs to BioFETs

In order for electric current to exist as a flow of electric charges, these charges need to be transported by charge carriers (electrons or holes). Whether those charges can be transported depends, however, also on the material that they are exposed to. Solid state materials can be either conductive (metals), semi-conductive (semiconductors) or non-conductive/insulating (insulators). Their nomenclature is due to the relative proximity of the valence and the conduction band in the energy band diagram (Figure 1.7).

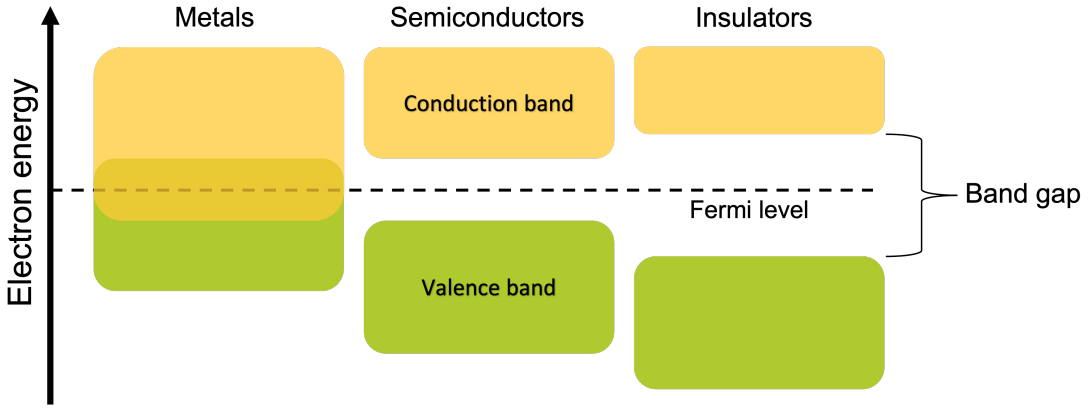

Figure 1.7.: Energy Band Diagram illustrating the concept of valence and conduction band (adapted from [123])

With the valence band being the energy band made up of molecular orbitals occupied by electrons and the conduction band representing the orbitals unoccupied by electrons and are thus potentially available to electrons moving through the lattice. The smaller the energy gap (or band gap) between valence and conduction band the more likely it is for the present electrons to move through the lattice, or from the relative lower energy state to the higher energy state. FETs are, by definition, semiconductive devices [71]. Therefore electrons present in FETs have to be excited in order to move from the valence to the conduction band. Several types of FETs exist, with MOSFETs being one of the most prevalent one. The most commonly used material for MOSFETs is silicon (Si). Silicon is an intrinsic semiconductor and has four electrons in its valence shell. These electrons are also referred to as valence electrons and form bonds with their neighbouring valence electrons. Therefore pure silicon forms a tetrahedral crystal with theoretically semiconducting properties. Because all the valence electrons are participating in bonds however, only a few of them actually contain enough energy to move across the lattice. This makes pure silicon practically an insulator at room temperature. In order to overcome this the silicon that is used as substrate for FETs undergoes *doping*. Doping refers to the purposeful introduction of impurities into the pure crystal which results in an increase in conductivity (S/m). This can either be done as negative-doping (n-doping)

by adding elements acting as electron donors or as positive doping (p-doping) by adding elements possessing less than four valence electrons and thus leave a *hole*, which can subsequently take up an electron. Making holes function as electron acceptors, as they actually represent the absence of electrons within the lattice, making them fictitious positive particles. The terms n- and p-type thus refer to the type of charge that can move within the semiconductor, not the actual charge of the semiconductor, as this remains neutral, due to the protons and electrons from the used elements. MOSEFTs are either constructed as nMOSFETs with n-type wells on a p-type silicon or as pMOSFETs with p-type wells on a n-type silicon (Figure 1.8). The source and the drain electrodes contact the transistor device at the two ends. The gate electrode, however, is insulated from the rest of the circuit using a gate oxide material (e.g. silicon oxide). Looking at the nMOSFET the electrons from the n-type can diffuse into the p-type region (p-n junction), thereby filling the holes. This results in a depletion layer, because the p-type region has drawn all the free electrons from the n-type region and is now negatively charged due to the electrons that diffused into the free holes. This makes it impossible for electric current to flow through the transistor, as the electrons coming from the n-type region now get repelled at the p-type region. This can only be overcome by applying a positive voltage at the gate electrode, creating a conduction channel, which now allows the current to travel from source to drain. The gate electrode therefore electrically bridges the source and the drain whenever a sufficient voltage is applied. For the pMOSFET the polarities are switched, meaning that the gate voltage has to be lower than the voltage of the body and that the charge carriers are holes instead of electrons. It is also possible to combine both nMOSFETs and pMOSFETs on one device, making it a complementary metal-oxide-semiconductor (CMOS).

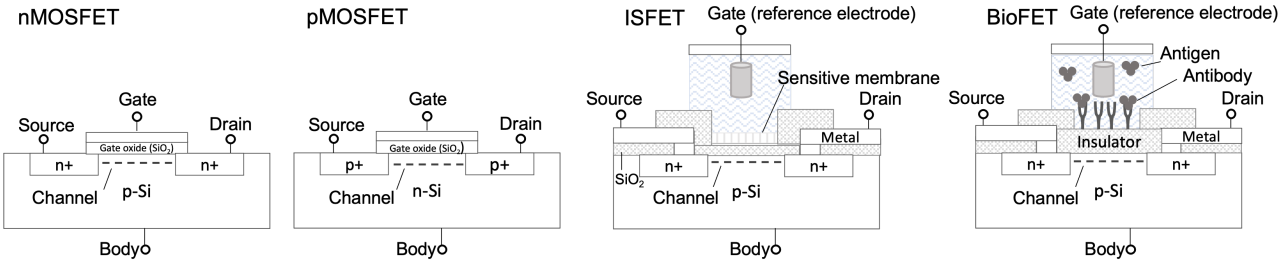

Figure 1.8.: Schematic illustration of MOSFETs, ISFET and BioFET (e.g. ImmunoFET) (adapted from [123] and [96])

Now that the working principle of the MOSFET is specified, it is easy to comprehend how these properties can be utilised for the purpose of biosensing: As charges provide key contributions to the properties, structure and organisation of biomolecules and FETs are sensitive to exactly those charges, they can be used to detect the presence of given biomolecules. For this objective the gate insulator gets modified using specific biomolecular recognition elements. In the case of the ISFETs the gate electrode gets

replaced by an ion-sensitive membrane, an electrolyte solution and a reference electrode [96] (Figure 1.8). They are designed to detect concentrations of ions in a solution. Based on this development the idea arose to not only investigate electrical charge changes caused by ions, but to specifically target biomolecules using biorecognition elements coupled to the ISFET. If it's possible to monitor the electrical changes close to the gate insulator/the interface of the electrolyte using an ISFET, any biochemical/molecular reaction inducing a chemical or electrical change can be detected with the right combination of ISFET + bioreceptor [96]. This lead to a generation of biosensors referred to as BioFETs. Several types of BioFETs have been proposed [123] [96], with their name corresponding to the biorecognition element used: these are ImmunoFETs, with antibodies immobilised on the gate insulator; DNA-FET or GenFET, which have single DNA strands for detection of the specific complementary strands; cell-transistors, for the monitoring of whole cells; and EnFETs, which utilises immobilised enzymes on the sensing area. BioFETs are therefore special as the electrical change that is measured is due to binding events occurring on the surface of the insulating layer of the FET. Since the appearance of the first BioFETs numerous materials and alternative architectures have been proposed that can be utilised in a similar FET-based fashion for biosensing purposes. These innovations were driven by the quest for using more affordable materials while maximising sensitivity and selectivity. Giving some examples these can be more elaborate forms of silicon, like silicon nanowires (SiNW) [32],[102]; conductive polymers [48]; or carbon-based nanomaterials [50], such as carbon-nanotube (CNT) [106], carbon dots (CDs) [58] and graphene [39, 110, 86]. These graphene based field-effect-transistors used for biosensing purposes shall now be discussed further, as we take a look at the State-of-the-Art in the field.

1.2.1. Graphene Field-Effect Transistors (gFETs) - State of the Art

One of the most recent success-stories of gFET based biosensor is a device aimed at the detection of SARS-CoV-2 in human samples [98] (Figure 1.6 i)). Here the authors used a PBASE modified gFET with SARS-CoV-2-spike protein antibodies. They first tested their device against SARS-CoV-2 spike protein in Phosphate-Saline-Buffer (PBS), proceeded with cultured SARS-CoV-2 virus and finally moved to human samples from SARS-CoV-2 positive patients, providing a well-thought-out biosensing device. As Limit-of-detection (LOD) 2.42 x 10^2 copies/ml were reported. This example presents the steps necessary in developing a biosensing device and testing it, as for every added step of complexity respective measurements, as well as control experiments were done (starting with spike protein in PBS buffer, then cultured SARS-CoV-2 virus and finally patients sample). This is mandatory when considering the previously introduced requirements concerning biosensors, as the sensor ought to only respond to SARS-CoV-2, and should also do so if the liquid environment changes from less complex (buffer) to more complex (patients sample in transport medium). For the context of this work also relevant to mention are publications addressing the development of "electronic-nose" devices [57], which in recent publications also functionalize Nanodic-embedded proteins on a CNT-FET [119] [62] [79] and more recently on a gFET device [88] [78] (Figure 1.9). All these approaches are based on the use of odorant-binding-proteins (OBPs) for the

detection of oderants [14]. What is especially intriguing is the use of Nanodisc-embedded proteins as biorecognition elements, allowing the use of membrane in-cooperated proteins for biosensing applications. Membrane proteins represents an immensely interesting subgroup of proteins vital to the communication between extra- and intracellular matrix and determine specific characteristics of a cell type. In the presented example two insect odorant receptors (ORs) from *Drosophila melanogaster* were purified and incubated with phosphatidylcholine dissolved in sodium cholate and the membrane scaffold protein (MSP). The prepared nanodisc containing the respective OR was immobilised on the gFET using a PBASE-solution (this form of surface modifications will be discussed later on) and then tested against the positive and negative ligand with increasing concentrations from 10 fM to 100 nM. Further empty nanodiscs were tested against the positive ligand. The sensor showed a selective and concentration-dependent response to the respective positive ligand for each OR. Both of those more detailed described examples were used in

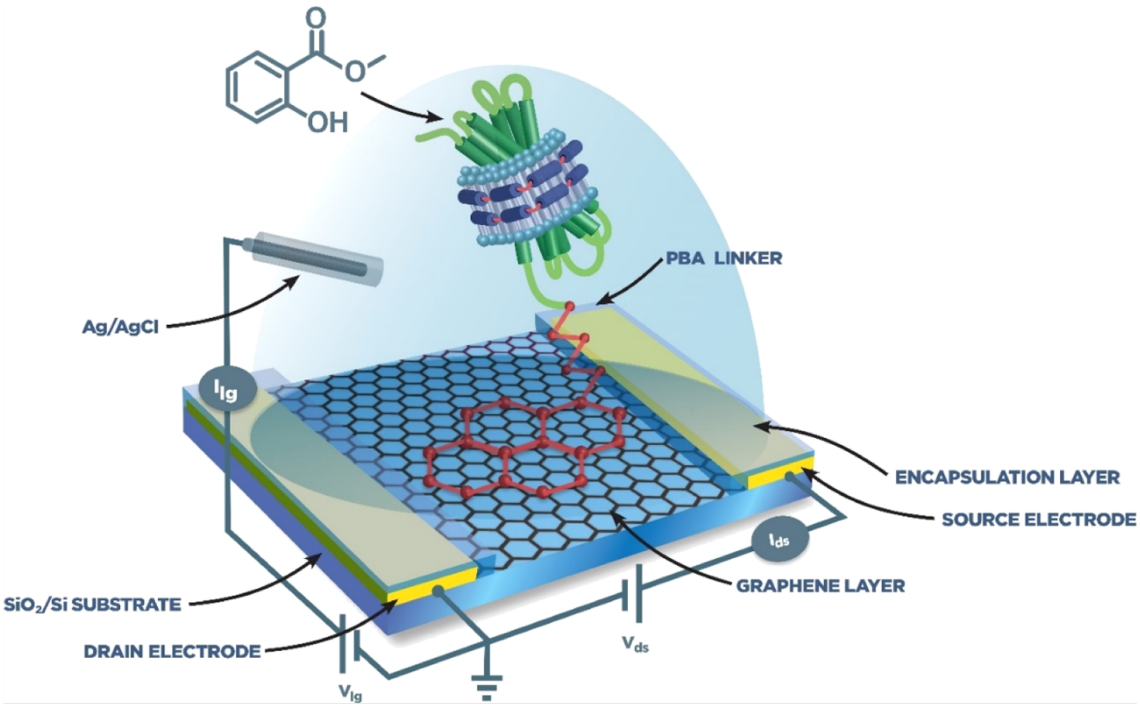

Figure 1.9.: Nanodisc-embedded Odorant Receptor on a gFET device from [78]

an electrolyte-gated or liquid-gated gFET configuration. Alternatively to the liquid-gates configuration, back-gated [83], top-gated and dual-gated gFETs can be used for biosensing purposes [97] (Figure 1.10).

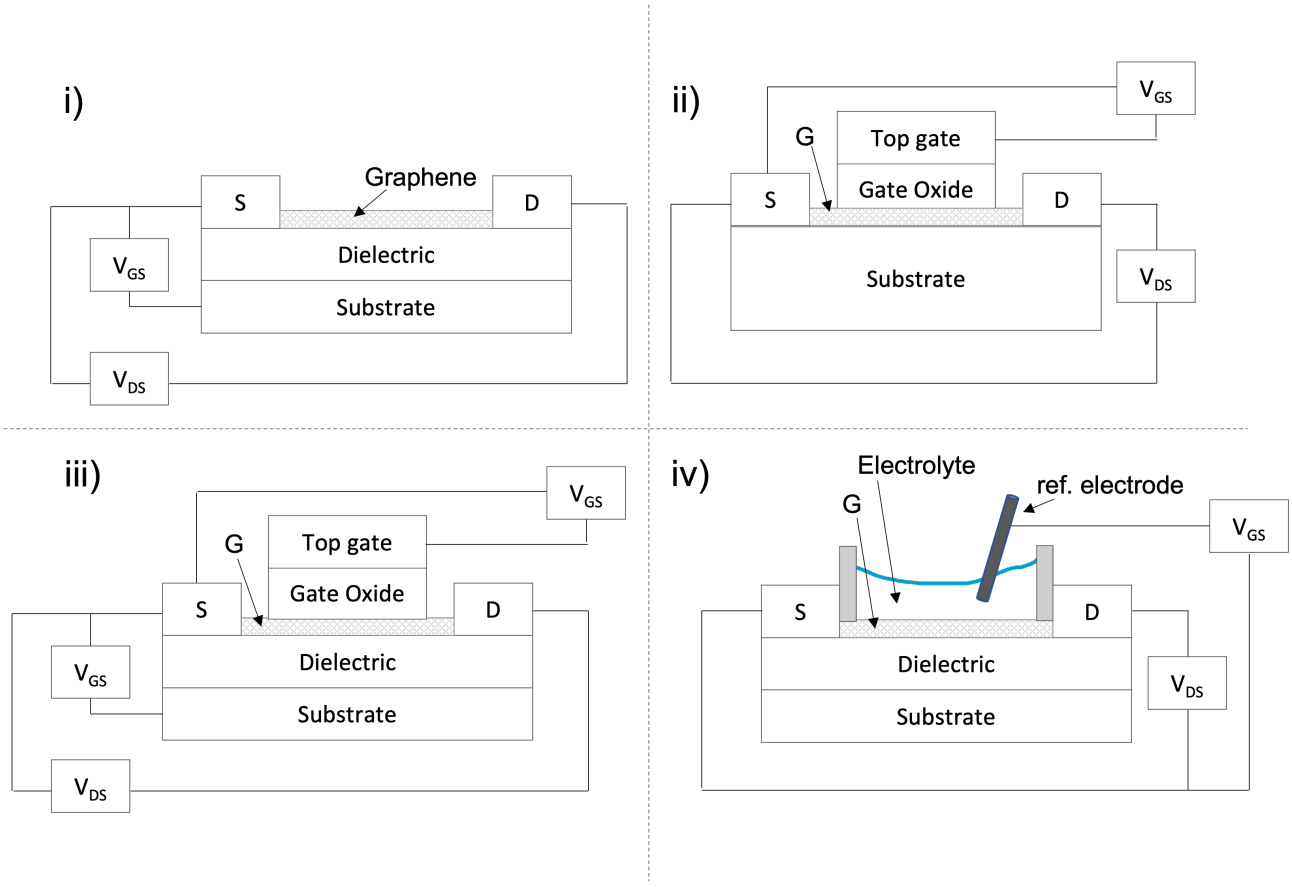

Figure 1.10.: Representation of different gFET configuration i) back-gated GFET; ii) top-gated GFET; iii) dual-gated FET, where the top-gate can also be a liquid-gated FET like in iv); d) liquid/electrolyte-gated FET from [86]

Electrolyte-gated or liquid-gated gFET configuration refers to the set-up where the graphene channel is in direct contact to an electrolyte that contains charges particles. This configuration is popular with the context of biosensing the majority of the biomolecules of interest are found in aqueous environments. Therefore the used electrolyte often mimics the biological fluid. A reference electrode immersed in this electrolyte solution functions as an out-of-plane gate. Through this electrode a fixed potential can be applied, shifting the Fermi level (energy level) in graphene and modulating the drain-source current of the transistor. The applied voltage causes the formation of an electrochemical double-layer (EDL) at the graphene-electrolyte interface which results in a large capacitance. These properties, along with some of the consequences (Debye-Hückel screening phenomena) will be discussed in the section dedicated to graphene later on. It should be noted however that for the gFET the modulation of current does not only occur due to the external gate voltage applied through the gate electrode, but that any change in the electronic

states of graphene itself, caused by the adsorption of molecules or just alterations in the graphene film, can also regulate the current between source and drain.
Although numerous derivatives of graphene are currently used for biosensing purposes [104] this State of the Art paragraph mostly covered chemical vapour deposition fabricated graphene (CVD-graphene) based biosensing approaches. This is because CVD-graphene should, in theory, be defect free and thus grant greater reproducibility. The next section will therefore be dedicated to the properties of graphene and how high quality graphene is characterized.

1.3. Graphene - the honeycomb carbon

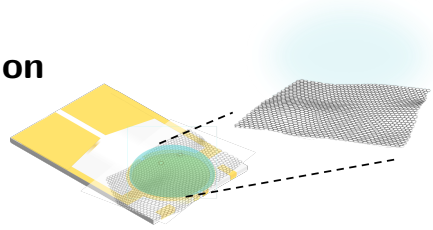

As we have seen now and as already comprehensively summarised [105], [26], [91] different types of graphene based biosensor are available - their common point? They all take advantage of graphenes extraordinary properties. Of which the most relevant for biosensing are its electrical conductivity and high mobility, or ability of charged particles to move through the lattice ($2x10^5 cm^2/Vs$, which is around 200 times higher than silicon) [13], as well as its biocompatibility [51]. Its electrical conductivity and high mobility of charge carriers allow for the detection of the smallest of changes occurring due to charges presented by biomolecules. These unique properties are a result of the structure of graphene. Graphene is a carbon allotrop organised in a two-dimensional manner forming a honeycomb-lattice, while several layers of graphene stacked onto each other form another carbon allotrop called graphite (Figure1.11).

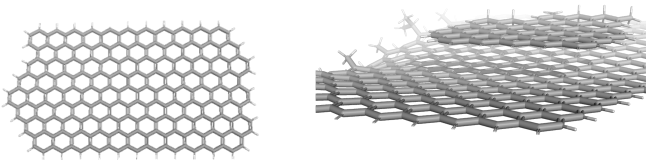

Figure 1.11.: Schematic illustration of the graphene structure on an atomic scale (left) and stacking of graphene layers forming graphite (right) (graphic created by the author using PyMOl ©

This structural speciality is relevant as the electronic structure is highly dependent on the numbers of graphene layers [120]. The nucleus of a carbon is orbited by six electrons, four of which being valence electrons and thus able to interact with neighbouring atoms. These outer electrons of carbon can result in different hybridization states, most importantly: sp, sp^2 or sp^3 (sp^2 or sp^3 shown in Figure1.12). When all the carbon atoms neighbouring each other share sp^2 electrons, they form the planar structure of a single layer graphene sheet. Each carbon atom is thereby covalently bond to three other

carbon atoms (via σ-bonds and in-plane), while the remaining out-of-plane π orbitals form π-bonds. This results in a delocalized network of electrons allowing the electrons to move freely, resulting in graphene being a zero band-gap semiconductor. A zero band-gap semiconductor is characterized by the intersection of the valence and the conduction band, granting constant conductivity. Thereby the conduction band and the valence band touch at the K and K' points (or Dirac points) in the reciprocal lattice space (Figure1.13). These π-bonds also provide the bases for van der Waals interaction leading to the π-stacking making up graphite. This π-stacking property is also useful for the modification of the graphene film later on.

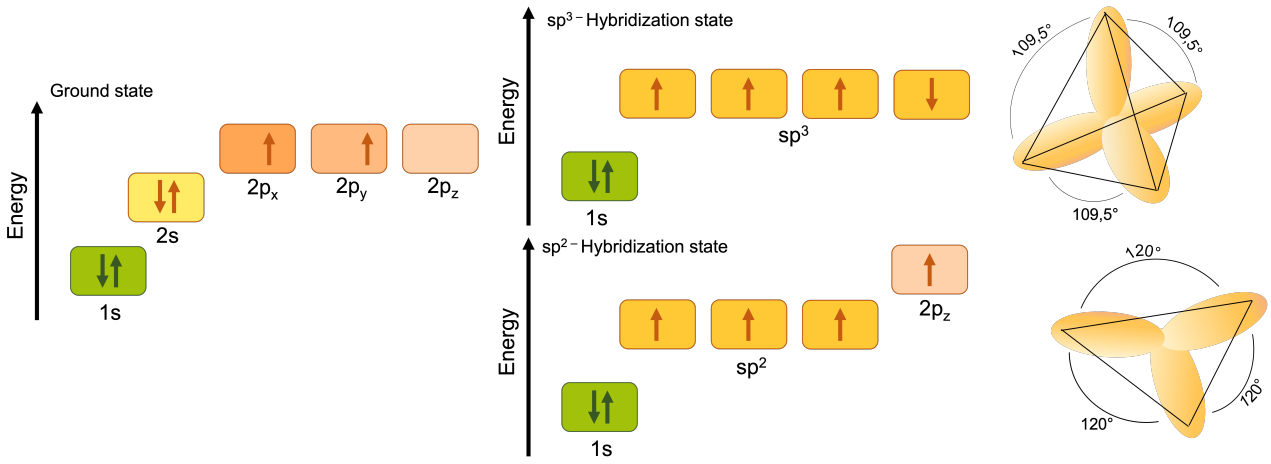

Figure 1.12.: Energy levels of the outer electrons of carbon depending on their hybridization state as well as hybridization states illustrating the respective order of orbitals in space (adapted from [118])

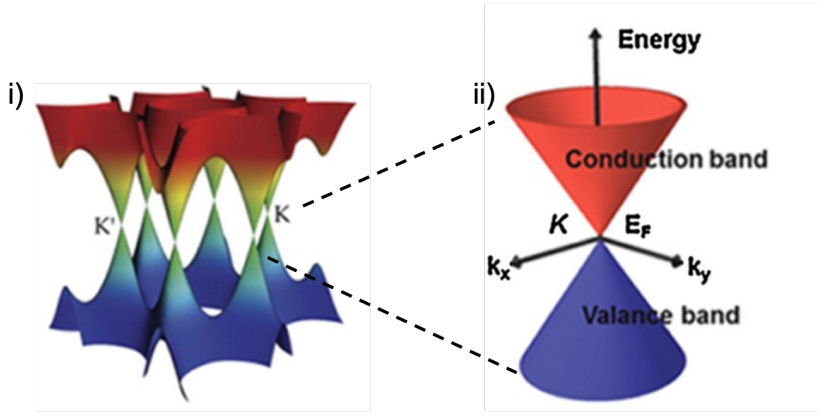

Figure 1.13.: i) Band diagram of graphene ii) Conic energy bands close to the Dirac point (both from [13])

These properties make graphene a contender for biosensing applications as its high electrical conductivity is a promising asset for sensitive detection. The properties are, however, subject to change, as the electronic band structure of graphene is easily altered by defects and disorders in the lattice. Before we dive into the application of graphene for a biosensing field-effect transistor we shall thus first discuss the effects defects can have and which steps can be undertaken regarding quality control.

1.3.1. General properties of graphene

The term graphene, strictly speaking, only refers to one single layer of carbon atoms. The literature, however, also refers to bilayer (BLG) and mulitlayer graphene (MLG) and only starts using the term graphite at 10 layers of graphene [118]. The number of layers thereby determines the band structure that is displayed and therefore the electronic properties. While single layer graphene has zero band-gap, bilayer graphene also has zero band-gap, however with the possibility to be tuned, which grants flexibility in nanoelectronics [124]. If more than two layers are stacked onto each other the electronic properties further change: with increasing layer thickness, which is accompanied by an increase in effective mass, the mobility decreases compared to mono- and bilayer graphene [55]. At this point the conduction and the valence band overlap to a considerable extend showing a parabolic-like band structure. Next to the number of layers, also disruptions in the atomic structure of graphene can alter it's electronic properties. The commonly known disorders are: corrugations, topological defects, adatoms, vacancies and sp^3-defects. Corrugations include: ripples, wrinkles and crumbles (Figure1.14). These corrugations are interesting as graphene actually never seems to be completely flat in any real life circumstance and ripples, that are caused by intrasystem thermal fluctuations are intrinsic features of graphene sheets. Wrinkles and crumbles however are commonly caused during fabrication processes, with wrinkles occurring due to water drainage during the graphene film transfer and crumbles are caused by rapid evaporation [118]. Topological defects are often found in CVD grown graphene. During the growth process of CVD graphene

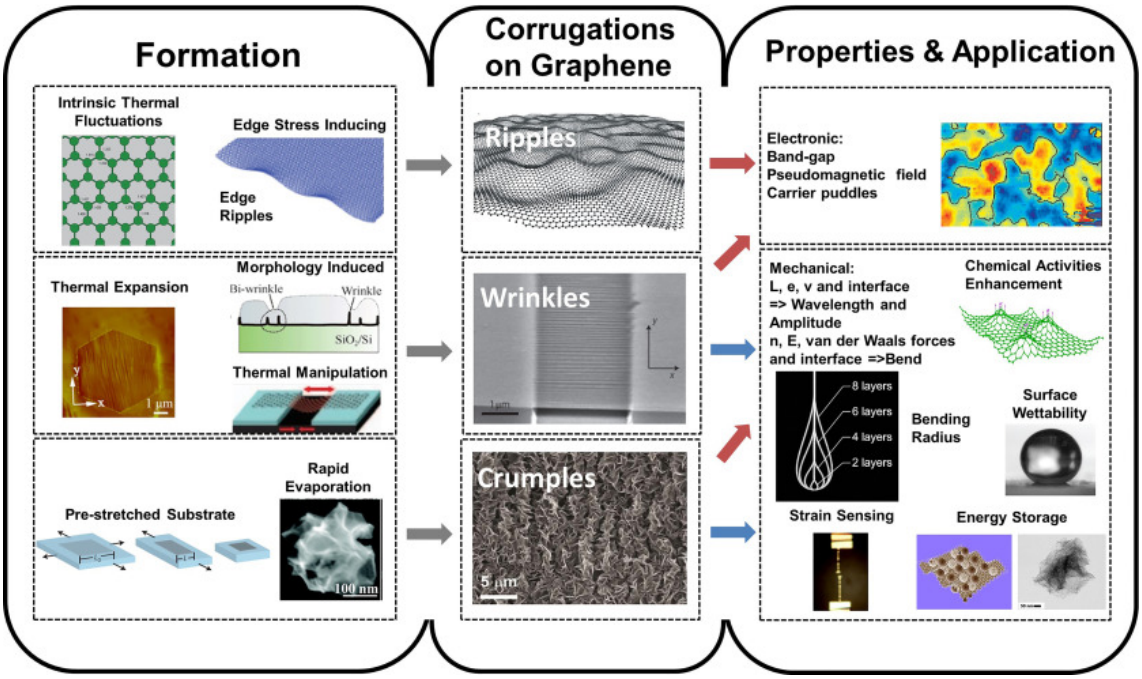

Figure 1.14.: Types of corrugations from [23])

several crystalline structure start to form at different nucleation spots creating topological defects or non-hexagonal rings in the sp^2 carbon network. This results in out-of plane structures to satisfy the bond arrangements. Finally, vacancies, adatoms and sp^3-defects occur when atoms are missing in the lattice, when an atom is absorbed on a graphene sheet and when a carbon atom in the lattice in replaced by another atom (e.g. chlor). All these factors contribute to the respective electrical properties of the graphene sheet, like the opening of the band-gap and some of them even get exploited for biosensing purposes, supposedly increasing the sensitivity [46]. The now discussed defects can arise due to the several fabrication steps required for the processing of graphene. A detail description and illustration of the fabrication process of the devices used in this work can be found in the appendix. To validate and control the properties of graphene used for biosensing application several steps of quality control can be done.

1.3.2. Graphene - quality control

Raman spectroscopy: Raman spectroscopy is a commonly used method to determine the number of graphene layers. For this a laser beam gets focused on the respective sample and upon hitting the sample, interacts with it and gets scattered. This scattering can either be elastic (Rayleigh scattering) or inelastic (Stokes Raman and Anti-Stokes Raman). During

the process of inelastic scattering energy transfer from the photon to the molecule of the sample takes place. The photon therefore either loses energy (Stokes Raman scattering) or gains energy (Anti-Stokes Raman). Because inelastic scattering is a very rare event, the energetic loss/gain is a fingerprint of the specific investigated material, as it is typical for the vibrational modes of the material. For Raman spectroscopy a laser at a certain wavelength (energy) is focused on the sample material. By using an optical filter only the inelastic scattered light (which has a different energy than the laser) is allowed to pass, is sorted by wavelengths and finally encounters a Charge Coupled Device detector (CCD detector). The information can then be presented in a Raman Spectra, which plots the measured light intensity expressed as arbitrary units against the frequency of the scattered light in cm^{-1}, the Raman shift. For each material this spectra will look different, exhibiting peaks at certain light frequency. For graphene the characteristic peaks are referred to as G peak ($\sim$1580 cm^{-1}), 2D peak ($\sim$ 2700 cm^{-1}), D peak($\sim$ 1350 cm^{-1}) as well a sometimes known D' peak (at the right shoulder of the G peak and therefore around 1620 cm^{-1}) [16]. By comparing the location and the shape of the different peaks as well as the ratio of the G peak and the 2D peak intensity (I_2D/I_G) the number of layers, as well as the abundance of defects can be identified [118]. Pristine monolayer graphene displays narrow and well-defined peaks, as well as a 2D peak that shows around two times the intensity compared to the G peak. While with increasing disorder and defects the intensity of the D and the D' peaks increases.

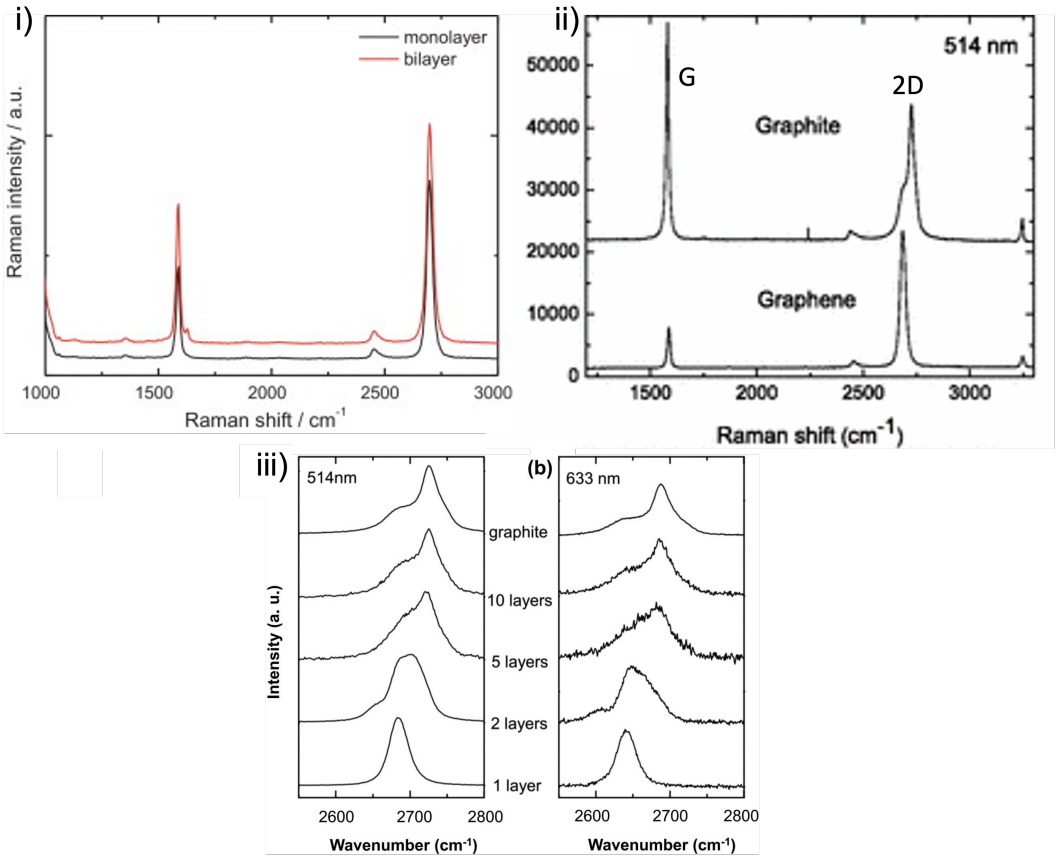

Figure 1.15.: i) Typical Raman spectra for CVD graphene - comparison of monolayer and bilayer graphene (from [107]) ii) G peak and 2D peak comparison for monolayer graphene and graphite iii) 2D peak evolution depending on the number of graphene layers (using two different lasers (514 and 633nm) (both from [118])

Scanning Electron Microscopy (SEM): SEM is a straightforward method to obtain information about the topography of a material/sample. For this an electron beam is focused on a sample under vacuum conditions. The electrons hit the sample and interact with the atoms. This produces various types of electrons, namely Auger electrons, secondary electrons and backscattered electrons. Different detectors are then required to registers this information and finally translation into a picture is done. The obtained pictures allow for a visual evaluation of the graphene film on the respective devices (Figure 1.16).

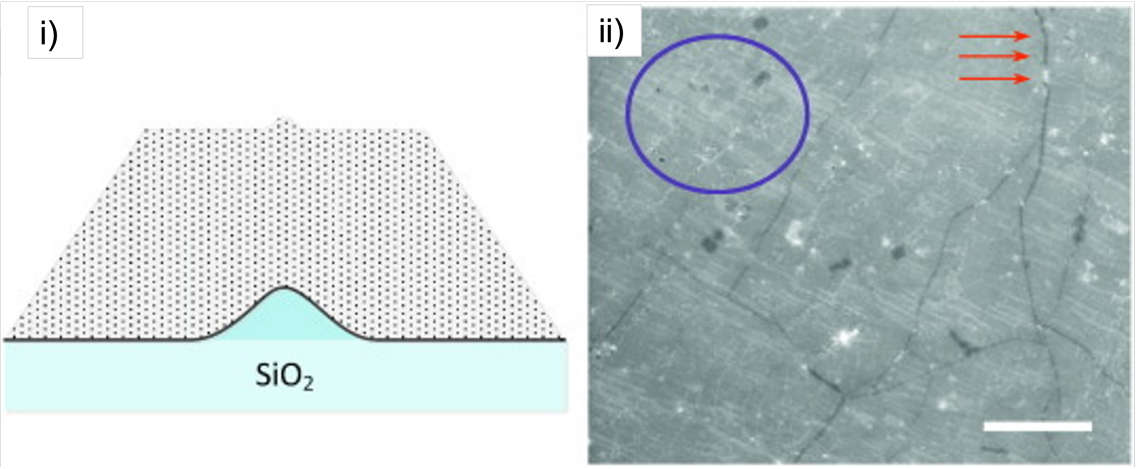

Figure 1.16.: i) Illustration of a graphene wrinkle after graphene transfer onto a SiO_2 substrate ii) SEM images of transferred graphene on a SiO_2/Si substrate (arrows indicating a graphene folding line and circle marking a region with many graphene wrinkles (both from [61])

Atomic Force Microscopy: The Atomic Force Microscope is another tool that is used to obtain further topological information about the sample. This is done via scanning the surface using a cantilever. The cantilever experiences deflection upon coming in contact with the forces between its tip and the sample. The sampling can be done in either contact, non-contact or tapping mode. The tapping mode is very commonly used for samples like those presented here. For this the cantilever is driven to oscillate up and down at or near its resonance frequency. The amplitude, however, is fixed and does only change when the cantilever is exposed to forces from the surface of the sample. From this information a height profile of the sample is generated. Further AFM images often yield more information about residues on the graphene film compared to SEM images. This makes AFM a practical assessment tool when comparing different transfer and cleaning strategies (Figure 1.17).

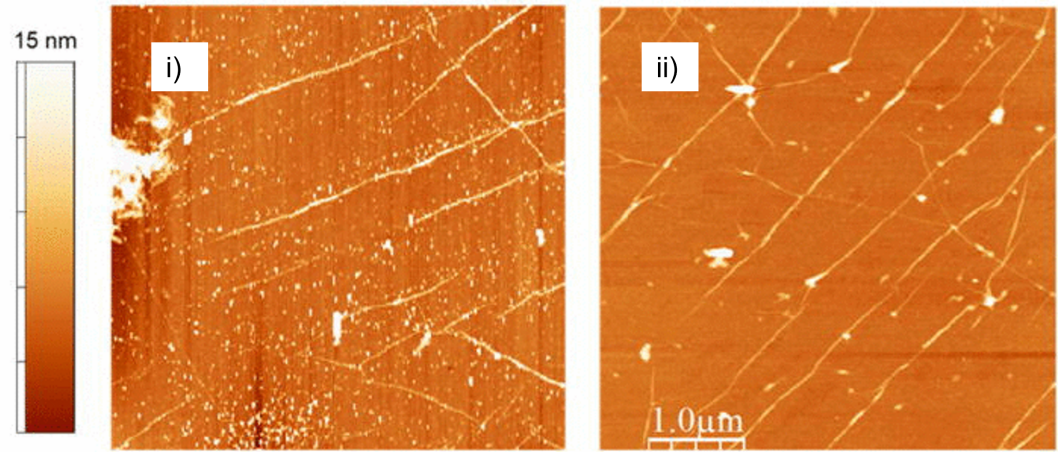

Figure 1.17.: i) ii) AFM images of monolayer graphene on a SiO_2 exhibiting various degrees of residues of polymethyl methacrylate (PMMA) depending on cleaning method used (both from [21])

X-ray photoelectron spectroscopy (XPS): XPS is a spectroscopic technique used to determine the elements present in a sample, as well as their chemical bonds and their oxidation state. This is done by measuring the kinetic energy (electron-volt - eV) of the photo-electrons emitted from a sample, after it is exposed to monochromatic X-rays. For the analysis of graphene this technique can be utilized to assert the hybridisation states of the carbon atoms. For a perfect layer of graphene the C1 spectra will show a narrow and almost symmetric peak at $\sim$ 284.4 eV, corresponding to the sp^2 carbons of the C=C bonds [21]. If lattice defects are present this will introduce sp^3 hybridized carbons (C-C, C-H). These are visible at $\sim$ 285 eV [21]. In practice these peaks not be distinguishable from each other due to the small shift in eV. The shape of the whole peak of the C1 spectra will, however, broaden and a tail at higher binding energies will appear. Through XPS analysis further introduced functional groups can be determined, making XPS analysis a powerful tool for composition analysis. This is especially useful when differentiating graphene from its deviates like graphene oxide (GO) and reduced graphene oxide (rGO) (Figure 1.18), as well as validating surface modifications.

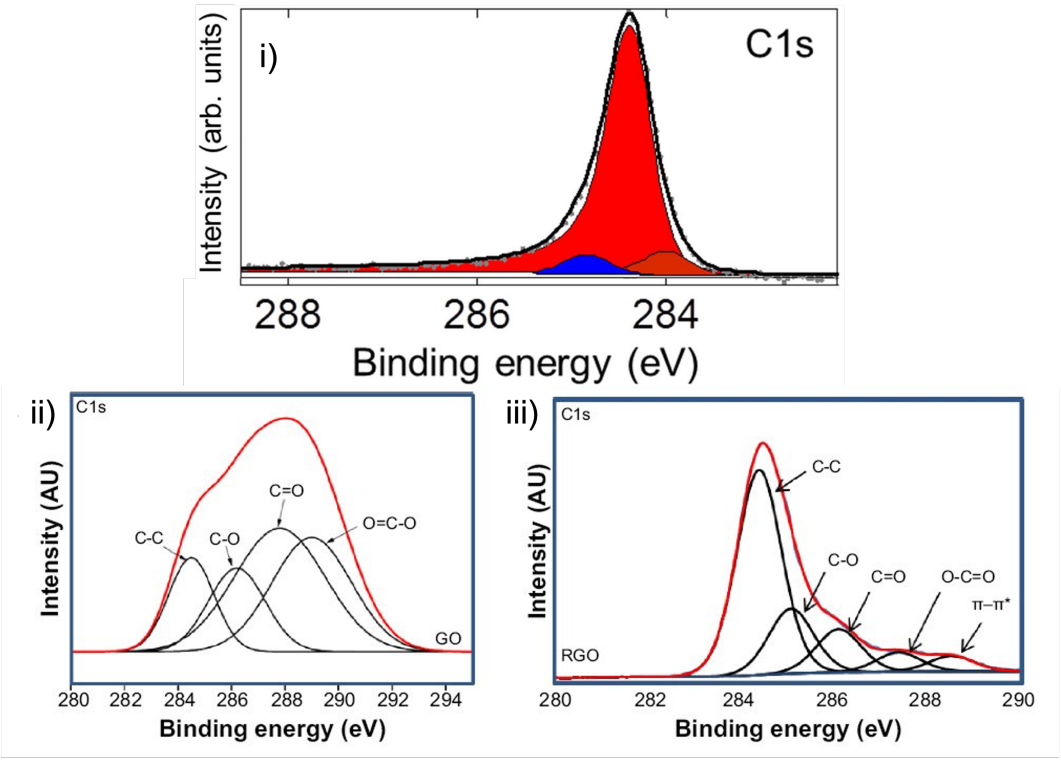

Figure 1.18.: i) XPS C1 spectra of pristine graphene (from [21]) ii) XPS C1 spectra of GO iii) XPS C1 spectra of rGO (both from [80])

1.3.3. Electrical characterisations

As already pointed out before the gFET-based biosensor gives information about the electric current passing the device channel - in this case the graphene layer. The change in electrical current due to binding events at the channel is therefore used as the detection mechanisms of this kind of sensor. The electrical current, however, is not only altered by the chemical environment and biomolecules interacting with the surface, but also by the voltages applied at the source, drain and gate electrode. While the potential between the source and the drain generates the flow of charge carriers along the channel, the gate voltage modulates the electric field across the channel [5]. For an electrolyte-gated gFET setup three standard curves can be used to characterise the gFET device. Those rely on the following combinations: plotting the current against the gate voltage (V_G) (transfer curve), the current against the source-drain voltage (output curve) or the current against the time (time series) [5]. For obtaining transfer curves the V_G is swept while maintaining a fixed bias V_{DS} between the source and drain electrodes. This sweeping results in a V-like shaped curve (Figure1.19), with the left branch representing an increasing density in holes (positive charge carriers) and the right branch an increase in electrons (negative charge carriers). The point of minimum current thereby being the Dirac point, where the charges are evenly balanced. This point is also refereed to as the charge neutrality

point (CNP). The CNP is the most commonly used electrical metric in gFET based biosensing (principle shown in Figure 1.19). The formed V-shape of the transfer curve is a result of the ambipolar nature of graphene and expresses the exchange in the polarity of the major charge carriers. Therefore the shape of the transfer curve yields information about electric aspects and their alterations. If the Dirac point is shifted (to the left/right) this means that doping is taking place, which is the addition of holes or electrons (p- or n-doping). If the branches move closer together or broaden this is due to a change in the transconductance of holes or electrons. If the curve as a whole moves up or down this is a change in the current amplitude. The modulation of each specific device is the delta between the respective maxima and minima of current.

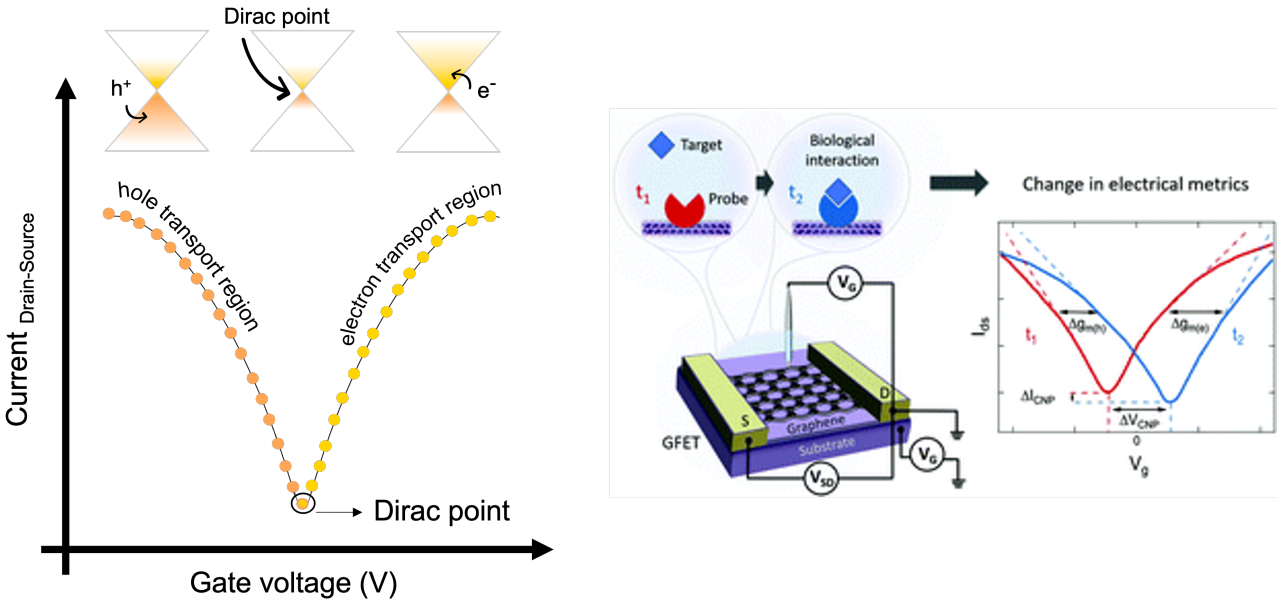

Figure 1.19.: Schematic transfer curve (left) (graphic created by the author using PowerPoint ©) and principle of biosensing comparing the CNP (from [5]) (right)

Theoretically the Dirac point of graphene is close to 0 V, but this is hardly the case in practical experience, as graphene is often p-or n-doped [5]. This doping is the consequence of residues that are presents at the graphene surface and are leftovers of the fabrication and transfer process.

1.3.4. Electrochemical properties of graphene and implications for biosensing

In the configuration of an electrolyte-gated gFET the graphene film, as well as the reference/gate electrode are in direct contact with a solution containing ions. Although this electrode can vary in it's shape, material and the relative position to the graphene

film it will attract ions from the solution. Which ions the electrode attracts is depending on its own charge. When sweeping V_G the charges will also be redistributed at the surface of the gate electrode due to the potential difference displayed by the gate electrode. Silver/silver-chloride (Ag/AgCl) electrodes are most commonly used as electrodes for electrolyte-gated gFET set-ups as they generally provide stable measurements in buffered conditions [74]. But also other metal electrodes are used [5]. Independently of the used material the gate electrode and the graphene film are coupled via an electrical double layer (EDL) resulting of the redistribution of ions in the electrolyte.The phenomenon of the EDL has been refined several times, since it was first described by Helmholtz [56]. Helmholtz started stating that, when a charged electrode is immersed in a solution containing ions, this will result in the electrode attracting ions that are differently charged than its own surface [42]. Consequently these attracted and accumulated ions themselves will attract ions than are of opposite charge, resulting in a double layer (DL). This model was extended by Gouy and Chapman in the early 1910s, which included considerations about diffusion. A few years later the theory was further revised by Stern, who essentially fused the two preceding models into one, also taking adsorption of ions onto the surface into account [103]. Although this model underwent revisions the Stern model is still referred to in the literature frequently today (Figure 1.20) and graphene that is exposed to an electrolyte also encounters the same principles.

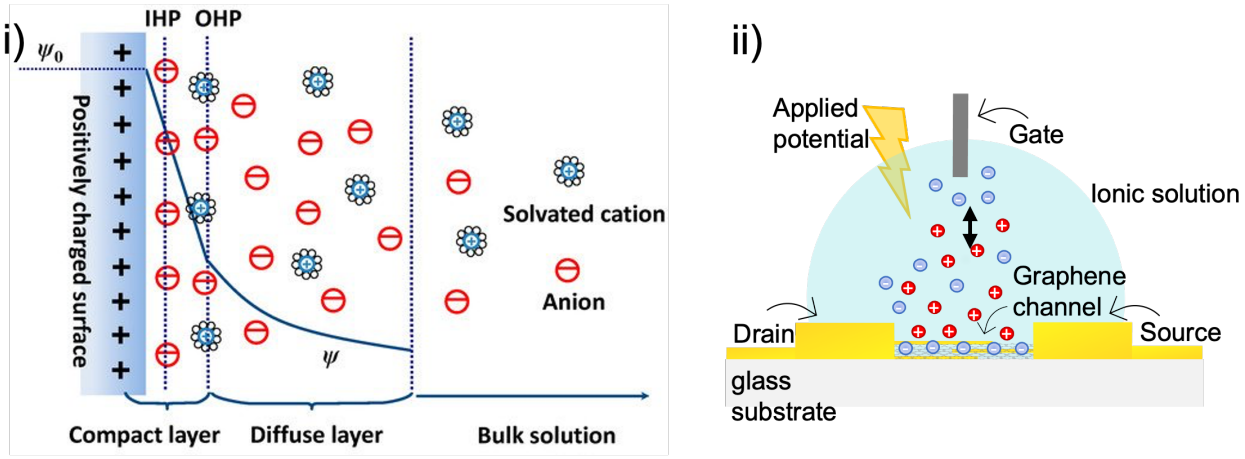

Figure 1.20.: i) EDL according to Stern (from [66]), showing the inner Helmholtz plane (IHP) and the outer Helmholtz plane (OHP) that form the compact layer, the diffusion layer and the bulk solution ii) Illustration of charge distribution on the gFET in an electrolyte gated configuration (adapted from [73])

When using graphene for a electrolyte gated FET one of the challenges that have to be considered is a phenomenon that is a main feature of this EDL, which is described as Debye screening length (λD) and is defined as:

$$\lambda_D = \sqrt{\frac{\varepsilon_0 \varepsilon_r k_B T}{2 N_A e^2 I}}$$

with ε_0 being the permittivity of the free space ($8,85419 * 10^{12} A^2 s^4 kg 1 m^3$) and ε_r the dielectric constant of the electrolyte (for aqueous solutions this can be assumed to be the one of water (80 (depending on the temperature), k_B the Boltzmann constant ($1,380649 * 10^{23} J/K$), T the temperature (in K), N_A the Avogadro constant ($6.022 * 10^{23} mol^{-1}$, e the electron charge and I the ionic strength. The highly relevant part of this equation in the context of biosensing is the ionic strength (I), which is expressed as:

$$I = \frac{1}{2} \sum_i c_i z_i^2$$

with i being the total number of ion species, z_i the number of the charges carried by the ion, and c_i is the concentration of ions. The ionic strength is presented in mol/l, meaning that in order to insert it into the equation, multiplying the the Avogadro constant additionally by 10^3 is required.
But why is this information important in the context of biosensing?
According to the Debye model charged molecules in solution are screened by counter-ions. This results in their electric potential being dampened exponentially with distance from the surface (debye-length). Therefore the Debye-length essentially describes the distance (usually in nm) from the channel surface at which charges can be detected. This distance is depending on the ionic concentration of the used electrolyte or buffer and is inversely proportional to it. Meaning that the higher the concentration of the solution, the closer the molecule has to be to the surface in order to be detectable. This effect is the result of the increase of thickness in the EDL with increasing ionic strength, which leads to the charged particles diffusing slower. To pose an example one can take a buffer system that is commonly used in biological research: Phosphate-buffer saline (PBS). The standard PBS solution used is referred to as 1xPBS and can be further diluted reducing the ionic strength and consequently the debye-length:

Buffer	Ionic strength	λD
1xPBS	177mM	0.74nm
0.1xPBS	17.7mM	2.35nm
0.01xPBS	1.77mM	7.45nm

This is further illustrated in the following graphic (Figure 1.21), which exemplifies that buffers of lower ionic concentration are intuitively more favourable for biosensing applications, as they pose greater sensitivity. This is, however, contradicting the inherent nature of biological fluids, which are predominantly of higher ionic concentrations. This poses a problem, as samples of patients will be obtained in biological fluids (e.g blood, blood plasma, saliva) and are due to this debye-length limitations difficult to be investigated, especially when considering that the graphene film still has to undergo

bio-functionalization for granting selectivity. Which holds even more true when considering that proteins are very sensitive to their environment and can undergo structural changes/defolding when required buffer conditions are not met.

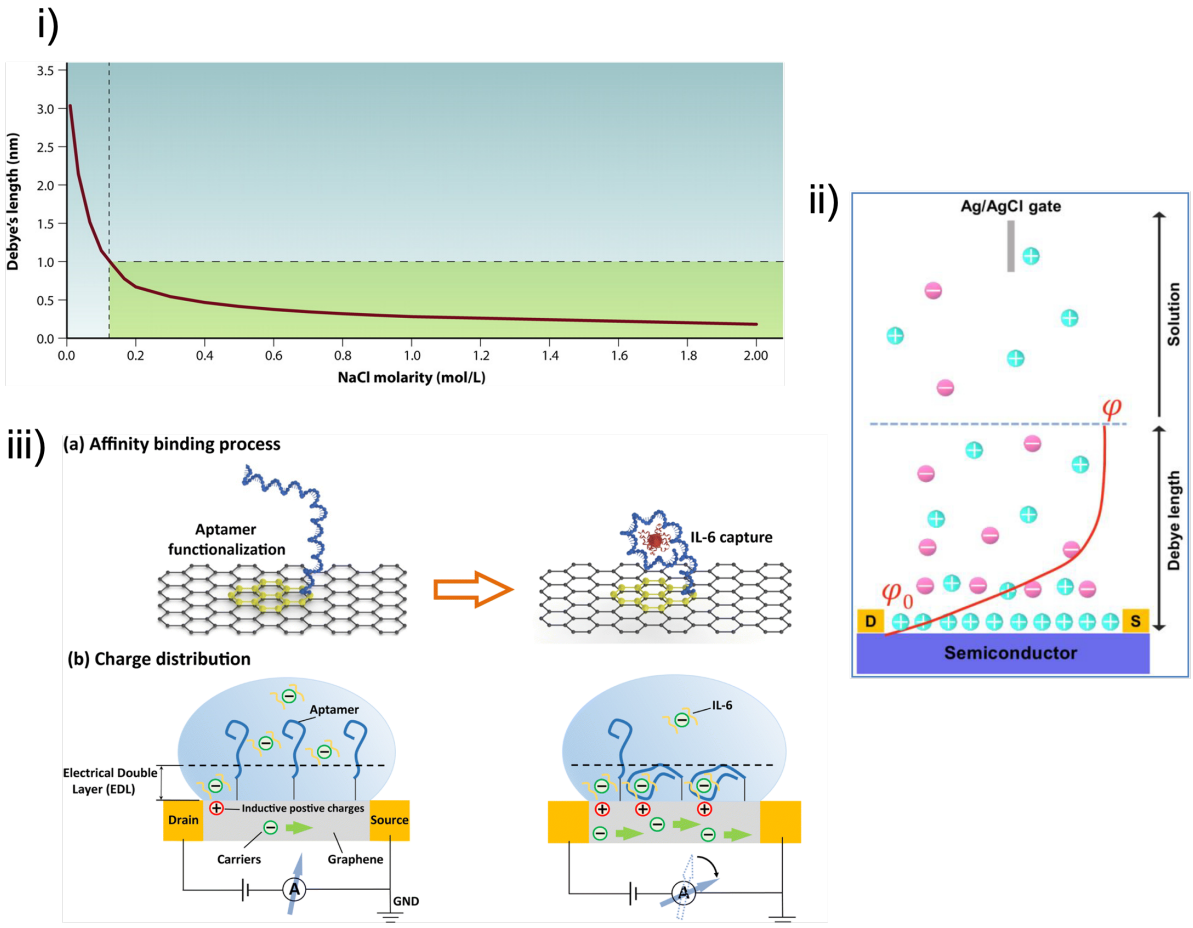

Figure 1.21.: i) Debye-length as a function of the ionic strength of the buffer (here NaCl) (from [49] ii) Formation of the EDL and debye-length at the interface of an electrolyte-gated FET (from [125] iii) Reorganisation of biorecognition element upon binding (from [40])

This is why great efforts are directed towards overcoming this Debye-length screening effect [18],[125], [27], which include reorganisation of the biorecognition elements upon binding [81, 40], using crumpled graphene [46, 47] or opting for smaller recognition elements [69].

Now that the properties of graphene are explained, the device is characterised and the importance of the chemical environment with respect to the detection-possibilities are highlighted, the next section will proceed describing the further functionalizing the

graphene surface.

1.4. Surface modification

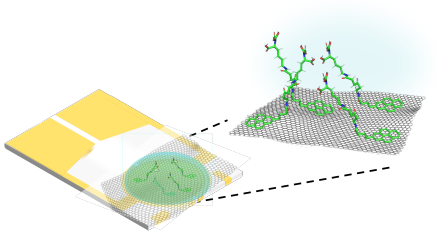

At this point the now prepared gFET is ready for modifications that subsequently allow for the further attachment of biorecognition elements and thus the use of the device as biosensor. These modifications will target the surface architecture and are therefore referred to as surface modifications. The surface of graphene can be modified in different manners [34] of which the arguably most important ones shall now be further introduced:

1. **Covalent surface modifications**: Covalent surface modifications of graphene can be introduced by electrochemically grafting of diazonium salts and Dienophiles [34], [43]. These modifications alter the sp_2 structure of graphene and change the hybridization state to sp_3 for the respective carbon atoms that are attacked by the radicals. This also changes the electrical properties of graphene. Addition of diazonium salts, for example, decreases the conductivity [101]. The big advantage of these kind of modifications is the great stability that is due to the formation of the covalent bonds [43].In the context of biosensing covalent surface modifications have, for example, been used to attach antibodies [25], or aptamers [93] to the graphene linked diazonium salts via click-chemistry protocols. The diazonium salts can be electrografted onto the graphene film, granting great stability [76]. Another way to modify graphene by covalent modifications is to oxidize graphite and exfoliating it in acidic solutions to produce graphene oxide (GO). GO has many functional groups (e.g. hydroxyl (–OH), carboxyl (–COOH), carbonyl (C=O)) that can be used for further modifications and reactions. GO can also be reduced to reduced graphene oxid (rGO) by, for example, hydrazin. This process is supposed to remove the oxygen-containing groups, while at the same time recovering the conjugated structure of graphene. The problem with this approach is that it's difficult to fully understand how reproducible the introduction of these functional groups really is. Although this can be analysed using e.g. X-ray photoelectron spectroscopy (XPS) to get a picture of the abundance of functional groups introduced, this only will provide limited information to which extent those are homogeneous or consistent for every iteration of production.

2. **Non-covalent surface modifications**: While the covalent binding of molecules to a graphene modified surface provides a very stable linkage, this kind of modifications also heavily alters the properties of the respective graphene film. This can be avoided when opting for surface modifications that take advantage of the intrinsic π-system of graphene.The following interactions are based on this principle:
   a) Gas-π Interaction
   b) H-π Interaction
   c) Cation-π Interaction

d) $\pi_{Cation} - \pi$ Interaction

e) Anion-π Interaction

f) Graphene-Ligand non-covalent Interaction

g) $\pi - \pi$ Interaction: Similar to electrostatic interactions the diffuse electron clouds of a π-system exhibits an attractive force to other molecules or to other π-systems. This phenomenon is widespread and responsible for many structure-stabilising interactions in biological systems, such as base stacking or protein folding. Due to this $\pi - \pi$ interaction or π stacking pyrene motifs which are terminated by different functional groups can be used for the modification of graphene.

1.4.1. Pyrene motifs as surface modifications

Commonly used as florescent probe within the context of spectroscopically-based applications, pyrene and it's differently terminated variations are becoming increasingly important as a straightforward way to modify graphene in a non-covalent manner. Relying on $\pi - \pi$ stacking, rather than hybridisation of the carbon atoms, this approach also takes advantage of the aromaticity of the pyrene units, but instead of utilising the fluorescent properties of the molecule, it exploits the interaction of the π-orbital system of the pyrene molecule core with graphene. This mimics the same principle also naturally occurring for the multilayer graphene sheets forming graphite and are solely stable due to the accumulative effect of van der Waals forces. Based on this, pyrene moieties can be seen as small elements employed to conveniently modify the graphene surface, while at the same time preserving the structural and electrical properties of graphene. Many differently terminated pyrene molecules are commercially available or can be synthesised using protocols (Figure 1.22). The seemingly most popular pyrene derivative for CVD graphene modification is the 1-pyrenebutanoic acid succinimidyl ester (PBASE) [59, 110, 99, 112, 98] This pyrene linker features an N-hydroxysuccinimide (NHS) ester that is conveniently reactive with primary amines, forming stable amide bonds. This is of outmost practicability considering that primary amines are one of the most abundant functional groups within proteins, peptides, and many other macromolecules. The downfall, however, being that hydrolysis of the ester group limits the stability and the general possibility to even link biomolecules. The linker system should therefore be carefully selected considering that there are pros and cons to each option, depending on the biorecognition strategies used later on [75].

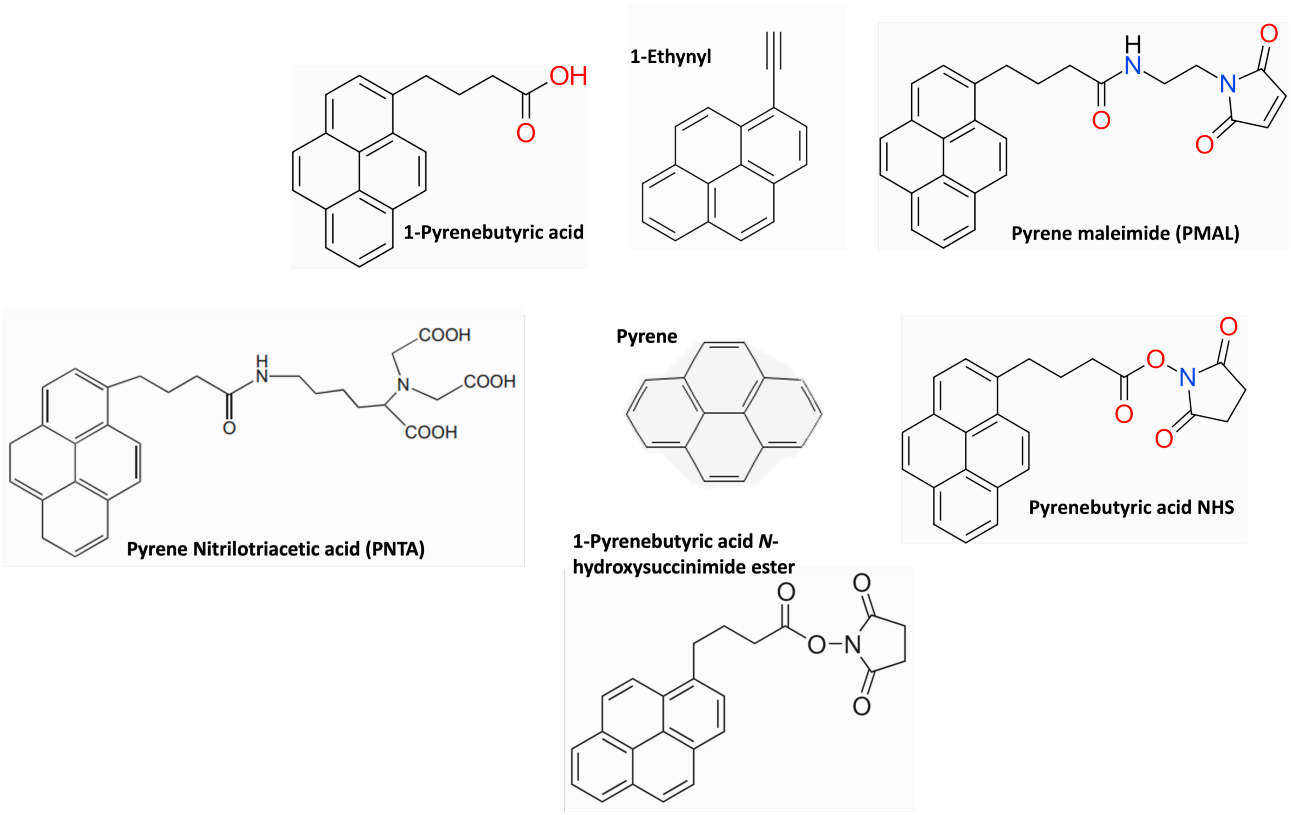

Figure 1.22.: Illustration of different pyrene linkers, with the basic structure of a pyrene molecule in the middle, these different linkers are commercially available from Lumiprobe © (PMAL and PBA-NHS ester), Merck © (PBASE, PBA), AxisPharm © (PETH) and Nanocs © (structure presented here from [44]) (other structures from the indicated company)

The pyrene linker that will now be further introduced has very interesting properties and is, although not completely unknown in the context of biosensing [44, 53, 100], still rather unfamiliar, especially for gFET applications.

Pyrene nitrilotriacetic acid (Pyrene NTA)

Nitrilotriacetic acid (NTA) is no stranger to everyone working with protocols that include protein purification. NTA is commonly used as metal chelator in immobilized-metal affinity-chromatogrophy (IMAC) - the key part to this are nickel ions that are immobilized via the NTA (NiNTA). Through the NTA the nickel ions are partially coordinated, leaving two interaction sites free for interaction (principle shown in Figure 1.23 ii)) with protein sidechains, specifically proteins that contain a histidine tag (His-tag). Histidin has six π-electrons, two from which are from the nitrogen lone pair in the imidazole ring, this allows the nitrogen to bind with the nickel ion. Importantly, working conditions below

a pH of 6 would be problematic, as the nitrogen be protonated due to its PK_A of 6. After this binding step of the his-tagged protein to the NiNTA the solution is washed with imidazole, which competitively binds to nickel ions, leading to the elution of the protein of interest. The exact same principle can also be employed to bind a protein with a his-tag to a pyrene NTA that is immobilized on a graphene film. Thereby the pyrene core interacts with the graphene via π-π-stacking (illustrated in Figure 1.23 i)) and the sidechain containing the NTA is free to bind to nickel ions and is consequently able to coordinate his-tag moieties on a protein.

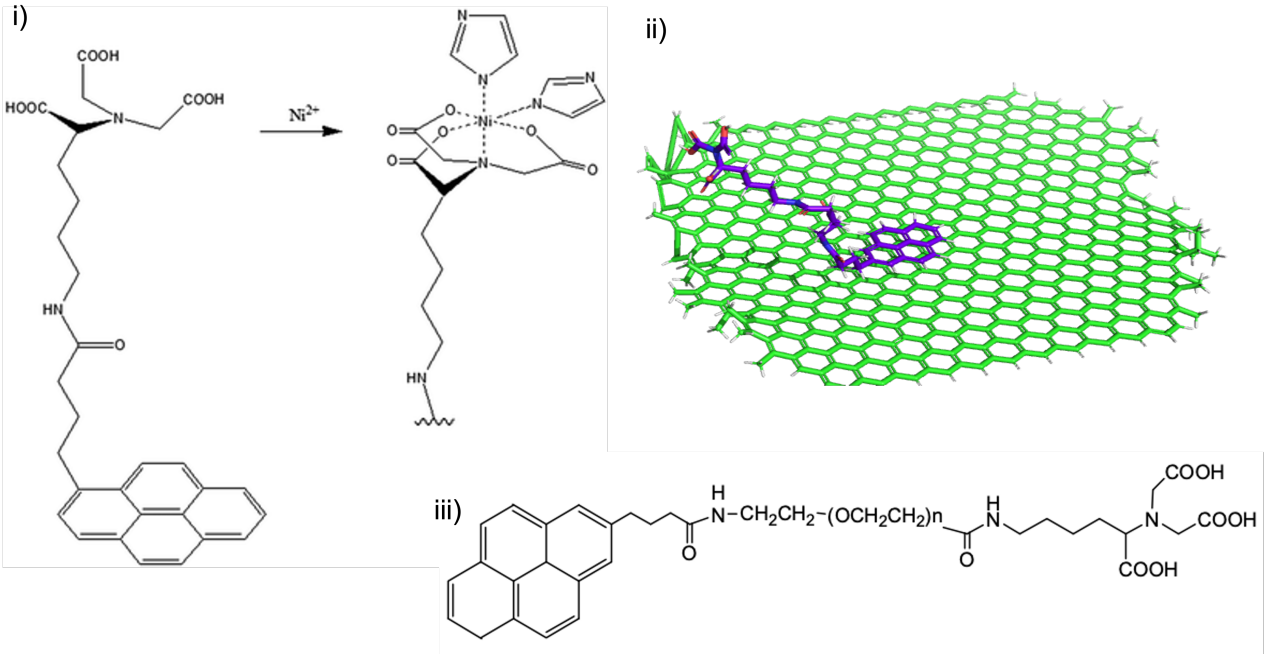

Figure 1.23.: i) Nickel coordination through NTA structure (from [85] ii) Pyrene NTA on graphene simulation using the PyMOL © software (structure created by the author) iii) Structure of Pyrene PEG NTA (used in this work) from Nanocs ©

Due to the properties of graphene discussed earlier having only a layer of graphene will always yield a signal when exposed to biomolecules, resulting in a non-specific response. It is therefore mandatory to add a specific biorecognition element to the now modified surface that will introduce a binding site which is specif to the biomolecule that should be detected. The next section will be dedicated to introducing possible biorecognition elements.

1.5. Biorecognition elements

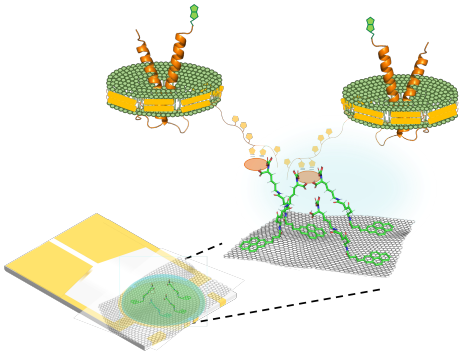

Choosing the appropriate biorecognition element is crucial to the success of a biosensor. The main purpose of the biorecognition element is to supply the biosensor with selectivity to the target biomolecule. As a response of the biosensor should be exclusively detectable when a specif analyte is presented. When deciding for a biorecognition element one therefore has to consider the size - also in respect to the debye length, the selectivity, maybe the easy access or the possibility for mass-fabrication. It is therefore clever to, as suggested by Morales et. al [77] to follow a decision map, focusing on selecting a biosensor paradigm based on the desired application and target rather than they already familiar and used elements. Numerous biorecognition elements are available, which can either be naturally occurring or synthetically produced once or which can lie somewhere in-between as pseudo-natural constructs. Of course all of these elements posses different qualities and recognition mechanisms and we shall now introduce some of the more commonly used ones in this field.

Antibodies/Nanobodies

Antibodies are a pivotal part of the immune response, aimed at recognising foreign molecules (antigens), binding them and thus marking them for degradation. They have a Y-shaped form and consist of two heavy-chains and two light chains. The N-terminal parts of both light and heavy chains form the two antigen-binding sites, while the more C-terminal parts of the heavy chains form the tail. Not surprisingly the region were the binding site is found is highly variable and is also referred to as *hypervariable region*. This grants great diversity making the binding sites of antibodies, which are ultimately only made up of 5-10 amino acids, highly specific for their target. Although this aspects would be desirable for biosensing applications, the downside of antibodies is their size ∼150kDa. This is why also fragmented antigen-binding (Fab/Fab') and even smaller fragment variable (Fv) elements are used [20]. These elements only consist of parts of the former antibodies, containing only parts of the variable regions. Even smaller than those elements are nanobodies, that are essentially just made up of the variable region of one heavy side chains and are ∼15kDa in size. Even though antibodies are bigger in size, expensive and work-intensive in their production, the are still very popular in gFET based biosensing applications, and can also be referred to as ImmunoFETs [98, 126, 65, 70, 59, 87].

Nucleic acids

Nucleic acids are one of the core structures of life. Most relevant in the form of RNA and DNA, nucleic acids are composed of polynucleotide chains. Each nucleotide consists

of a sugar, a phosphate group and a base. All double-stranded nucleic acids are made up of complementary sequences, where the bases interact through base pairing. When nucleic acids are used for biosensing applications, the product is called a genosensor and FETs become GenFETs. Regardless of the type of nucleic acid used (DNA, RNA, LNA and PNA) the general detection principle remains the same: the immobilized sequence on surface the biosensing device binds to it's complementary sequence present on the target. While these hybridization studies are highly sensitive and specific and are also of great interest and presence [116, 36, 12, 33, 46] their range of application as biosensors is limited as they are only optimal for targeting nucleic acids.

Aptamers

Aptamers are single-stranded oligonucleotides that are designed to bind selectively to their target molecules. The process of their development is called Systemic Evolution of Ligands by Exponential Enrichment (SELEX) [127] This is an iterative process aligning the target analyte and oligonucleotide sequence against randomly generated sequences from a library. If there is sufficient binding affinity, the molecule and the aptamer stay bound and pass to the next round and are amplified, which creates the library for the next round. This is continued until the required specificity is achieved. The SELEX process enables the use of aptamers for a broad range of targets as the probes can be readily modified in a sequence-specific manner and are very small 6–30 kDa in size and less than 3 nm [121] long. Additionally granting greater specificity due to their selection process[20]. Although these are very promising prospects and aptamers are also commonly used in gFET configurations [52, 40, 111, 81, 47, 84], they still have not reached clinical relevance due to their lack of quality as well as thorough characterization (folding behaviour etc.) [127].

Enzymes

Enzymes are another group of biomolecules undertaking a vital part of life, as they serve as catalysts for chemical reactions occurring in cells. This boost in chemical reactivity is necessary as many of the reaction would otherwise not take place in the required rate. For catalyzing a reaction the enzyme binds to a substrate and facilitates the breakdown of this substrate into the product. To be able to recognise the substrate, each enzyme has a specif binding site. Due to their nature biosensors using enzymes as biorecognition element will always be enzymatic biosensors. When scanning the literature for enzymes on gFET, we also commoly meet an old acquaintance, the GOx [122, 113, 45], depicting how important glucose detection is. This, however, also illustrates the problem with enzymes based approaches, as they can only be employed for existing enzyme-substrate systems.

Biomimetic elements

It is certainly debatable whether the term biomimetic elements is only applicable to the elements that follow in this paragraph, as it could also be argued that the biorecognition elements mentioned before can be seen under this umbrella term. Biomimetic, however, refers more to a set-up simulating and mimicking the function and performance of biological organs [68]. As regards to biosensing these biomimetic elements can for example be cells as a whole [38], nanovesicles [3, 89] or bioreceptors [8, 24], although bioreceptor is also a term that is a bit to imprecise, as this can also simply mean a biomolecule that binds to a target, but let's get this to a preciser description. Many of the receptor proteins within a cell are situated inside the cell membrane. The cell membrane is a ∼5nm thick lipid bilayer that is essential for the compartmentalization of the cell and thus a structural feature. The function providing feature are the membrane proteins that span through or are unilaterally anchored in the cell membrane. They are essential for transport and communication between extra-and intracellular matrix. Proteins embedded in the cell membrane and passing through it need this surrounding of the lipid bilayer to retain their function, making it very difficult to study them outside their social-cell context. In order to investigate the working principles of one of these proteins it is however necessary to look at them separately (or only in a limited combination). This is why so called nanodisc were invented.

Nanodiscs embedded proteins

Nanodiscs are model membrane systems that consist of phospholipid molecules that are held together by a membrane scaffold protein (MSP). They were first introduced as carriers for reconstituting membrane proteins after they were solubilized from the cell membrane using detergents. The possibility to use those kind of membrane embedded proteins as biosensing devices is a extremely promising one, as this would, theoretically make any membrane protein that is soluble deployable as biorecognition element. Although some examples of Nanodisc embedded protein on FETs are known (on gFET [78], on carbon-nanotubes (CNT) [79, 62, 119, 63], this area is by far not well understood yet. This is why it's especially exciting to be presented with the opportunity to test the nanodisc gFET combination within this work (Figure 1.5). The practical steps as well as the experimental workflow for using nanodisc embedded proteins as biorecognition elements on a gFET will now be topic of the following chapter.

2. Results and Discussion

The main objective of this thesis was to test whether a nanodisc embedded protein can successfully be immobilized on a gFET device using pyrene NTA and further be used as biorecognition element. This section is presenting the experimental details of the approach and will further discuss the results.

2.1. Sample preparation

2.1.1. FET devices

The FET used in the context of this work is a commercially available device from the company Micrux Technologies © (Figure 2.1)). These devices are characterised by 90 interdigitated gold electrodes on a gold substrate. They are recommended for the use of impedance, capacitance and conductivity measurements as well as fuel cells. Further these devices have already been established in the context of biosensing, for example for the biomarker cTnI [93]. The contacts for source and drain are the gold patches vis-à-vis of the sensing area (which is the round area containing the interdigitated electrodes). This sensing area containing the interdigitated electrodes will be further modified with a graphene film thus acting as the conducting channel between the source and drain electrodes.

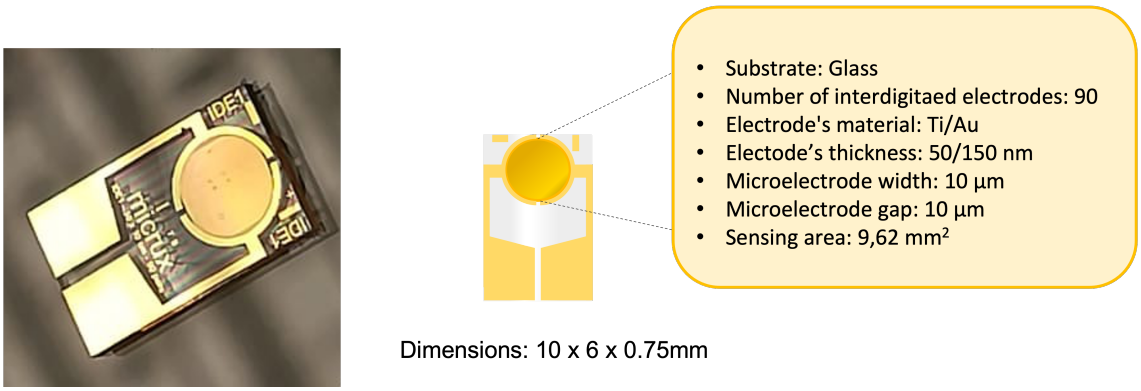

Figure 2.1.: Micrux device (picture and graphic taken/created (using PowerPoint ©) by the author)

2.1.2. gFET fabrication

The obtained devices provided the substrates for the following fabrication process. A detailed explanation of this process is provided in the appendix. In brief: The micrux substrates with the interdigitated microelectrodes are thoroughly cleaned using UV-Ozone treatment, followed by several washing steps, and drying. They are further modified with trimethoxyphenylsilane (2 % solution in ethanol) for 1 h. Afterwards, the chips are extensively incubated and rinsed with fresh ethanol, dried, and baked for 1h at 120°C in the oven. When cooled down these chips can be used as substrates for a graphene film. For this graphene is directly transferred onto these chips. To make graphene transferable the commercially acquired copper/CVD grown graphene/copper foil gets treated with reactive ion etching (RIE) to remove one of the cooper foils sides. Onto this side (so directly on the graphene film) a layer of polymethyl methacrylate (PMMA) with a 200 nm thickness is spin coated. This gets carefully annealed at 110°C with small increments and decrements for heating and cooling. Following this the now available sheet of PMMA/graphene/Cu is cut into small pieces (approximately 1cmx1cm) which shall later fully cover the sensing area. From these pieces the copper foil is etched overnight using a 0.2M ammonium persulfate solution. The floating PMMA/graphene films is thoroughly rinsed with deionized water (DIW) by scooping them in and out of beakers with fresh DIW. After these washing steps PMMA/graphene film can be transferred onto the micrux substrate by submerging the chip under the floating film and very gently taking it out of the water. The chips are then dried for 90min at room-temperature (RT). After this the graphene layer is annealed to the substrate by putting the chips on a hot plate and baking for 1 1/2h (30min to reach 90°C, 30min at 90°C and 30min to cool down to RT). As last step the PMMA layer is removed from the graphene layer using a UV-Ozone cleaning step, which is followed by an acetone bath. Finally, the chips are rinsed with acetone, ethanol and DIW and gently dried. The now bare graphene film is thus ready for characterization, electronic measurements, and further modification.

2.1.3. Graphene characterization

Raman spectroscopy

In the context of this work Raman Spectroscopy was firstly used to obtain information about the quality of the graphene film on the devices after transfer and PMMA removal (Figure 2.2. The 2D/G peak ratio is at 2.45 indicating a monolayer of graphene at the spot of observation. Further the spectra suggest the investigated graphene film to be relatively defect-free due to only a small D peak. It must be noted however that, to truly have a full picture one should opt for a technique called Raman mapping where many spots are sampled, instead of just purposefully selected spots. Due to the design of the devices used here, mapping was not possible, as always spots between the electrodes had to be selected.

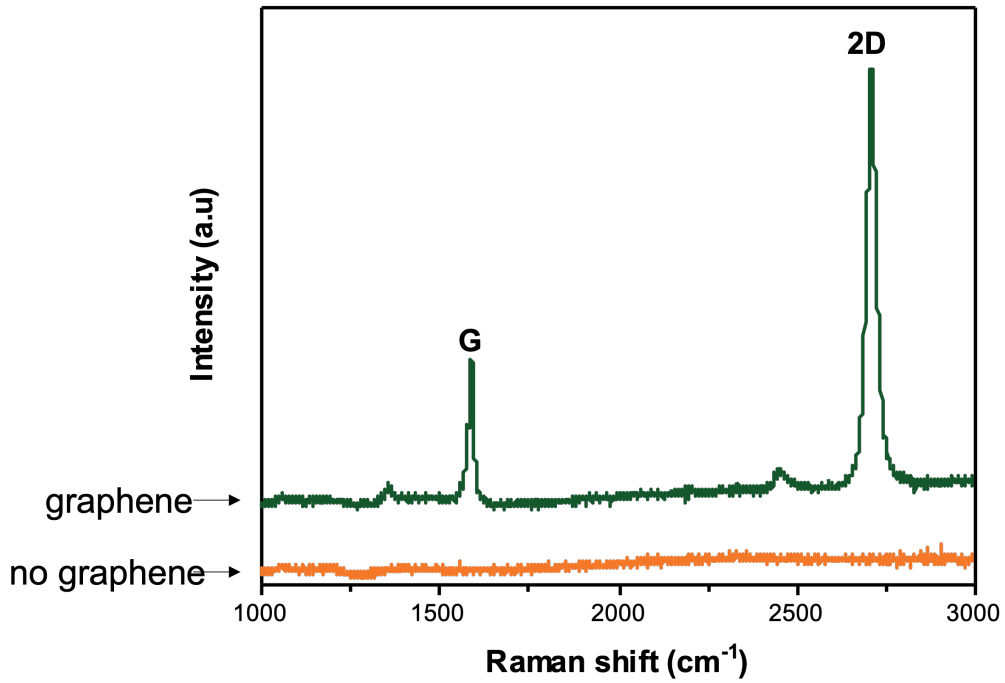

Figure 2.2.: Raman spectra of graphene film on micrux devices

Scanning electron microscopy (SEM)

As visible in the subsequently obtained SEM pictures (Figure2.4) and as validated by Raman Spectroscopy the investigated devices for this work show holes within the graphene film. These holes are most likely results of the layout of the devices: As the surface of the sensing area is not flat, but has height differences due to the electrodes, creating a landscape with elevations and decrements. This likely creates a lot of surface tension on the transferred graphene film, which can only be relived through partial ruptures. Next to the design also the transfer process itself can lead to these disruptions, as the mechanical stress of transferring the graphene film onto the substrate is high and trapped water residues that are maybe still left after the drying step and that are then exposed to the baking step could be the cause for these holes (Figure 2.3). This however was investigated using longer drying times (up to 24h), which did not result in a more continuous film or better electrical properties. At the higher magnification picture one can clearly see the boarder region being folded and multilayered as a result of the rupture. It can also be observed that the film along the boarder of the gold electrode seems slightly damaged, indicating that the film is not flexible enough to bridge this step size without being

impacted. These kind of damages seem to be problematic, as they pose a source of non-replicability, that can not be controlled consistently. The intact graphene film gives an expected visual impression, meaning that the graphene that covers the device is of desired quality.

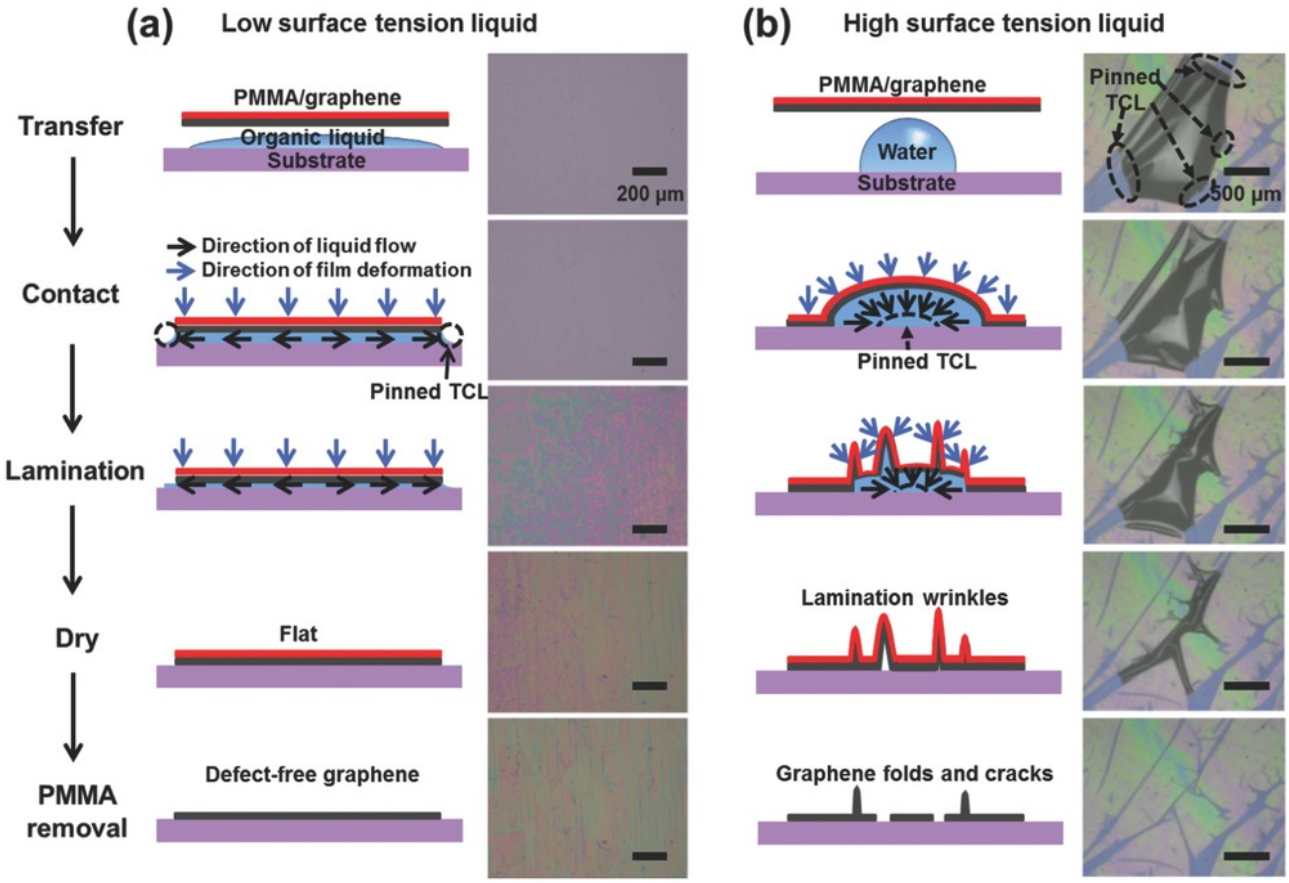

Figure 2.3.: Transfer process under a) low (heptane) or b) high (water) surface tension [54] - illustrating the consequences of the surface tension for the graphene film

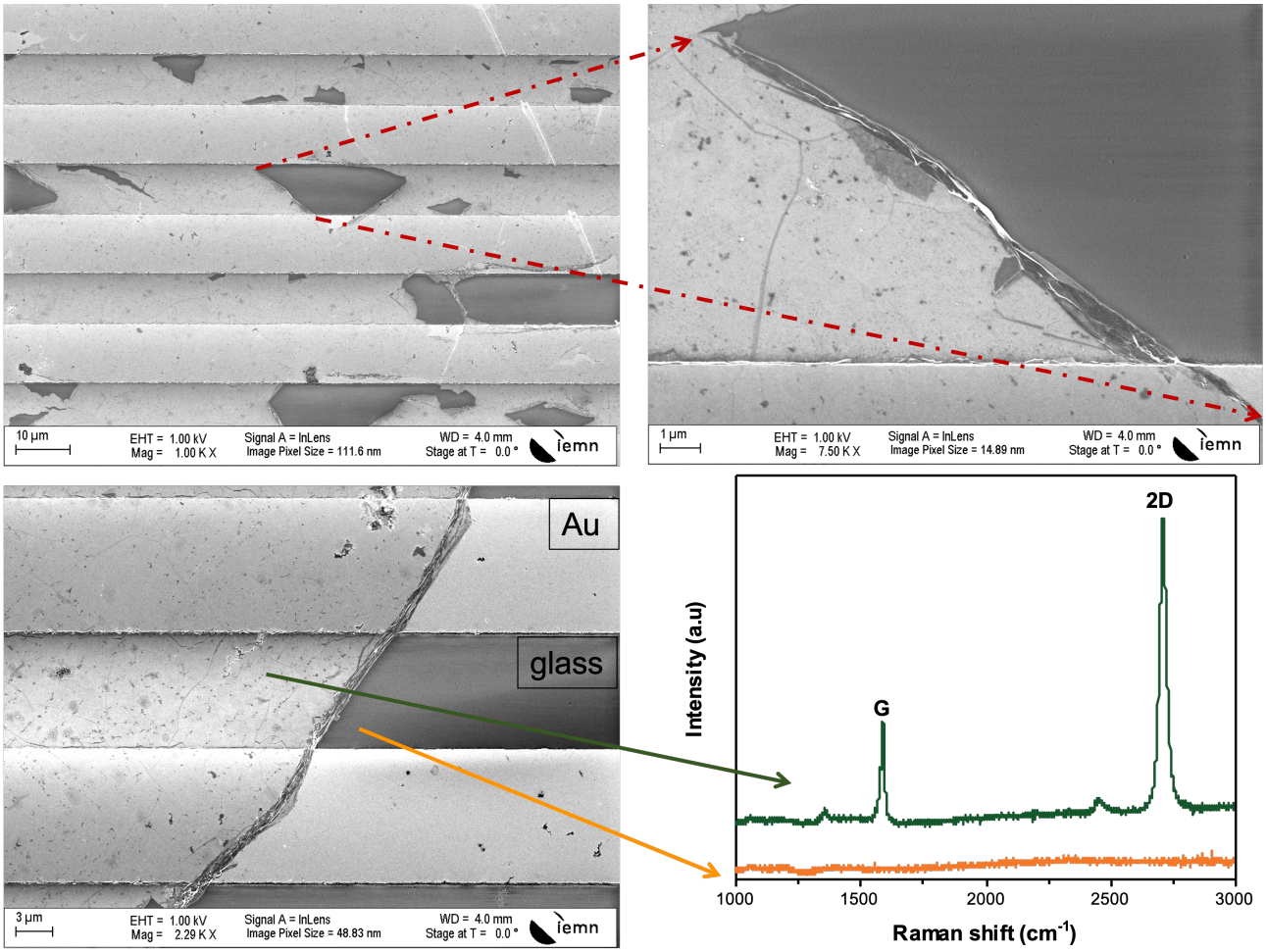

Figure 2.4.: Validation of graphene on substrate, also exhibiting defects in the graphene film, as indicated via Raman spectroscopy

Atomic force microscopy (AFM)

Next to Raman spectroscopy and SEM, AFM images were obtained allowing for the further investigation of surface properties. When looking at the paradigmatic images obtained for the devices used (Figure 2.5), one can appreciate the surface topology showing defect-free spots, as well as cracks and folds that ultimately also lead to the observed height differences.

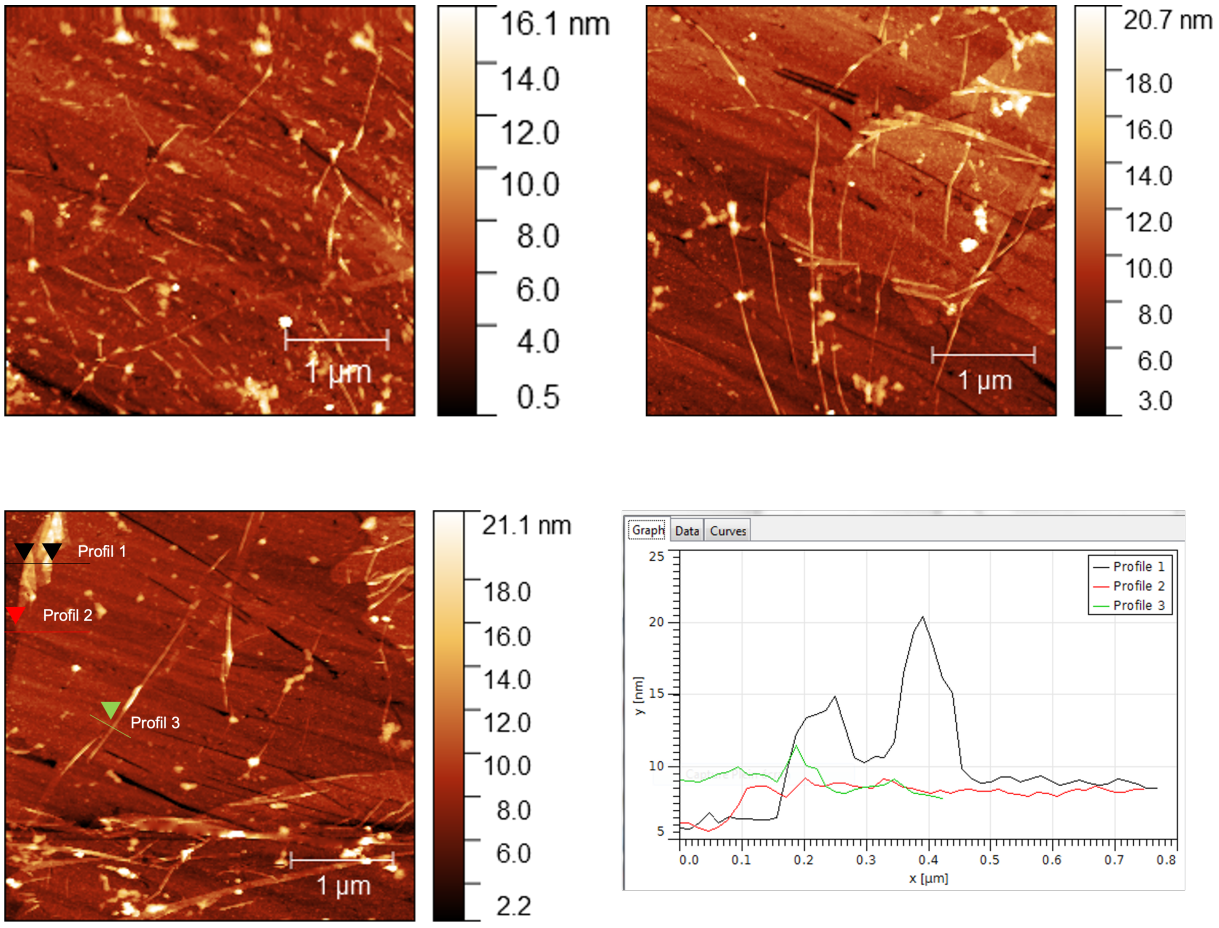

Figure 2.5.: Atomic force microscopy images of graphene film on micrux device (LMB40), obtained at different spots of this one sample

Now that a first characterisation of the properties of the graphene layer on the device is done, it is time to investigate the devices concerning their electrical properties.

2.1.4. Electrical characterization

For this work the effect of the biomolecules was determined by comparing the transfer curves (Figure 2.6) before and after exposing the sensor to the sample. For this the (V_G) is swept between two voltages with a selected step size (e.g. 5mV) and a specified scan rate (e.g. 20mV/s). Before biosensing measurements were performed each device was electrically characterized using 1xPBS buffer. This was done to examine whether the devices were comparable after the fabrication process.

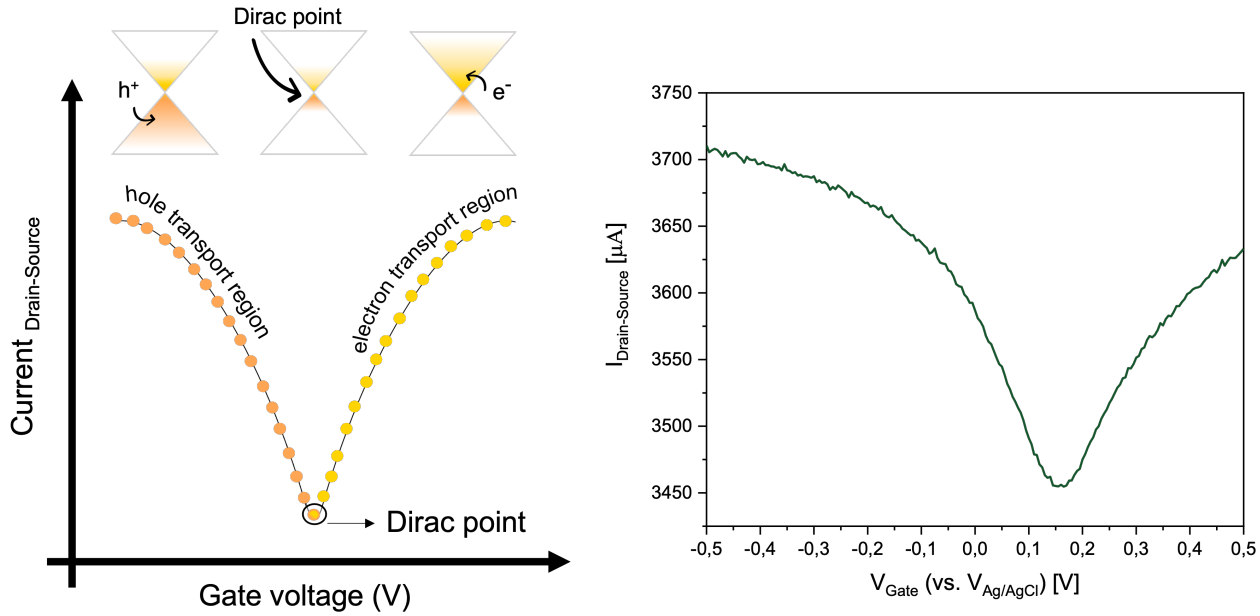

Figure 2.6.: Schematic (left) and representative device (LMB 26) (data obtained in 1xPBS buffer) (right)

The devices investigated in the context of this work showed a tendency to be p-doped (Figure 2.7 and Figure2.8), which is very likely due to remaining residues of PMMA [60]. The mean Dirac point was found to be at 0.123 V, with a standard deviation of 0.064 V and the median being at 0.131 V. The most negative-doped device was found to have it's Dirac point at -0.009 V and the most positive-doped one at 0.238 V. These results clearly indicate that for the most devices residues of the transfer process were still remaining on the graphene film, even despite the cleaning step using UV-ozon and acetone. Further the devices show a mean modulation of 253,5 μA with a standard deviation of 139,2 μA and the median being at 220,5 μA. The lowest performing device exhibited a modulation of 80,3 μA and the highest performing one a modulation of 770,9 μA (Figure2.8).

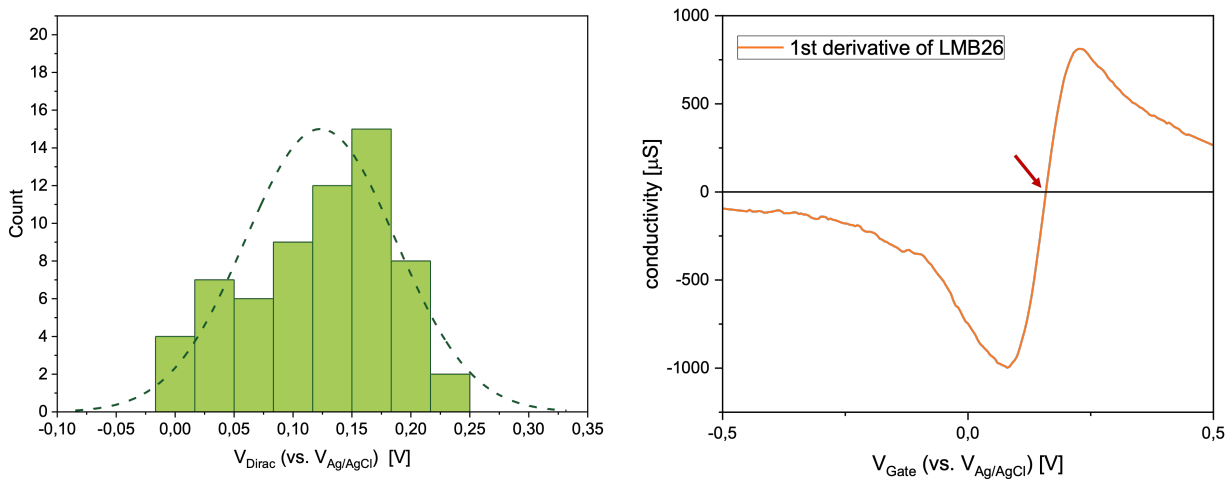

Figure 2.7.: Distribution of Dirac points of the devices (N=63) (normal distribution is given as visual indication that there is a bias towards p-doping) (left) and visual explanation of how the Dirac point is obtained from the data (right)

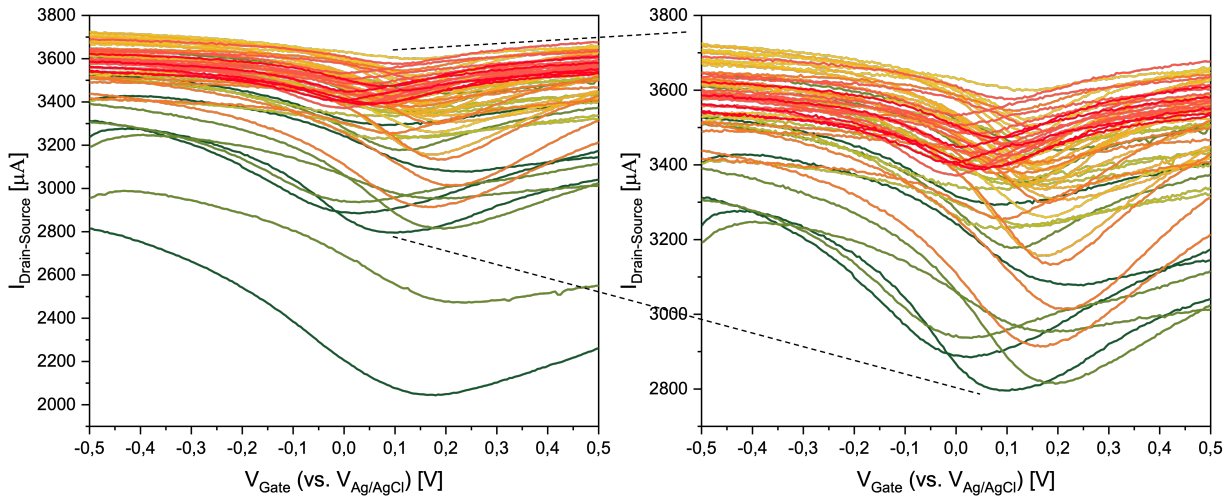

Figure 2.8.: Transfer curves of all devices that were fabricated with a 90min drying step (N=63)

All in all the devices showed significant variability concerning their Dirac point and

their modulation. Indicating that the fabrication process results in varying characteristics and demonstrating the necessity to obtain baseline measurements to ensure device quality.

2.1.5. Surface modifications

The presence of various pyrene linkers can be verified by raman spectroscopy, as was done for various linkers (all after an incubation period of 2h on the device) (Figure 2.9). The appearance of new bands, as well as G band splitting (in the case of PETH) and the emergence of the D' band indicate the successful immobilization of the different linkers.

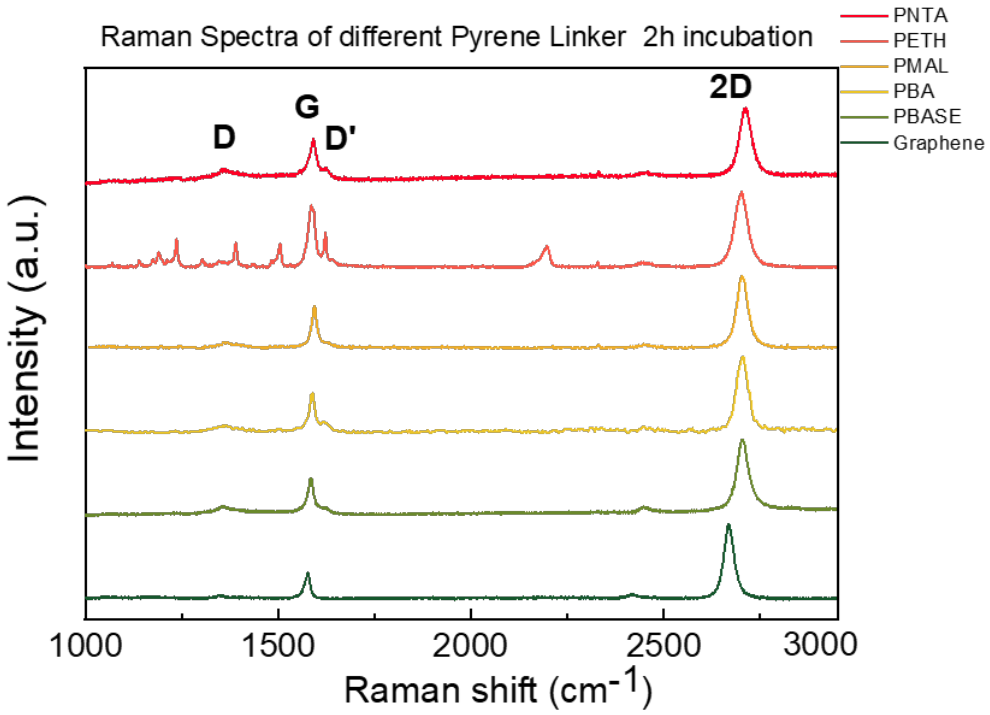

Figure 2.9.: Raman spectra of various pyrene linkers on graphene

The linker relevant for this work, pyrene NTA, was obtained from Nanocs © and had a molecular weight of 2000g/mol. Considering the molecular composition it's calculable that the molecule contains 32 polyethylene glycol (PEG) units. PEG increases the solubility, making the bought powder water soluble. Pyrene NTA was therefore dissolved in MQ water at a concentration of 5mM. Then 15-20μl of this solution were put on the sensing area of the graphene modified micrux devices and incubated for 2h. This was done in a glass petri dish bedded with a wet tissue in order to prevent evaporation. After the incubation the device was carefully rinsed with MQ and buffer. The presence of pyrene NTA on the graphene film was validated using raman spectroscopy (Figure 2.10). The raman spectra of pyrene NTA displays a clear reduction in 2D peak intensity,

compared to unmodified graphene with a ratio (2_D/G) of 1.15. Further the D' peak becomes visible and the D peak starts to appear, which is not detectable or very minor in pristine graphene. It has to be mentioned, that dissolving pyrene NTA in MQ might also pose a possible difficulty: as graphene is highly hydrophobic it's not quite clear how stable the interaction can be over time, especially when working in a flow cell set-up which also includes mechanical forces. The general immobilization, however, seems to be successful.

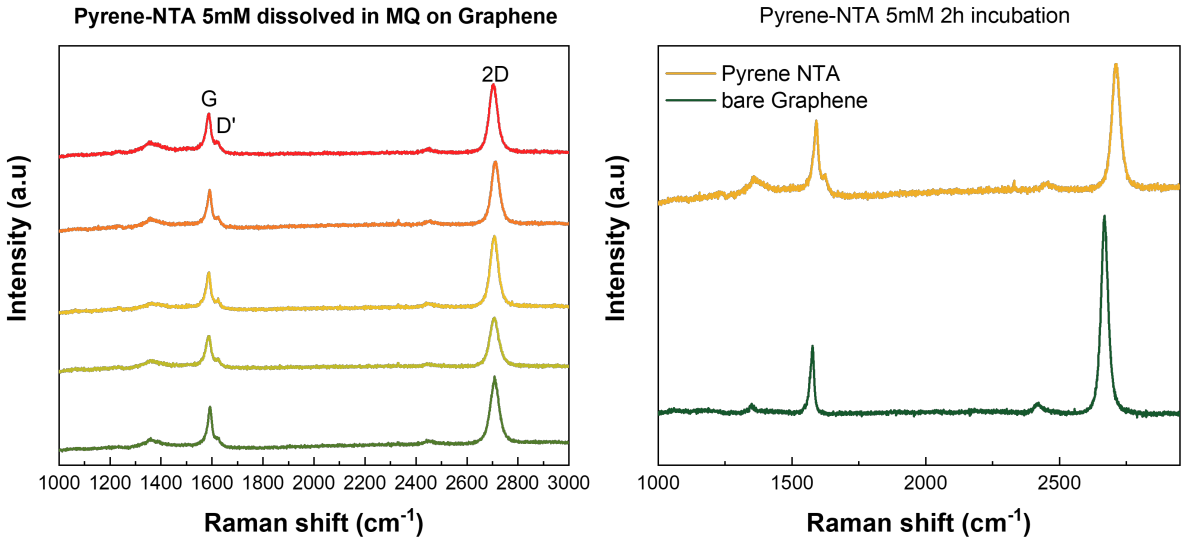

Figure 2.10.: Raman spectra of pyrene nta on graphene, different spots on one chip indicating the homogeneous immobilization of pyrene nta (left) Raman spectra of bare garphene compared to pyrene nta on graphene (right)

2.1.6. Biorecognition elements

Nanodisc containing glycophorin A were used as biorecognition elements is this work. The nanodisc were kindly provided by a cooperation of the group of Frank Rosenau in Ulm and the Biosensor Technologies group from the Austrian Institute of Technology (AIT) in Tulln. The nanodisc were reconstitued in a nanodisc buffer (20mM TRIS, 0.5mM EDTA, 100mM NaCl @pH 7.22). They were shipped in two compositions, one as empty nanodiscs and the other containing a glycophorin A domain with a biotin-tag. The MSP1D1 protein was used as MSP and included a his-tag. The nanodisc were at a concentration of 160 μM and ~150-180kDa in size. In order to test whether this can be used as biorecognition element the following approach was laid-out: Through the his-tag on the MSP the nanodisc should be immobilized on the graphene using the pyrene NTA properties. For this the graphene + pyrene NTA incubated chip was presented with a 100mM nickel sulphate ($NiSO_4$) solution for 1h and afterwards incubated with

the nanodisc solution. The device should then be tested against a ligand that has a high affinity towards biotin: streptavidin. The next section will cover the results of this proof-of-principle biosensing approach.

2.2. Biosensing

In order to test whether the devices are successfully applicable for sensing measurements, they were tested against ranging concentrations of streptavidin. The avidin/streptavidin-biotin affinity is extremely high ($K_D = \sim 10^{-14}$) and is regularly used in a proof-of-principle way to check biosensing devices or in a surface modifying fashion [108, 114, 82, 37, 94, 9]. The measurements were performed in a flow cell set-up (as shown in Figure 2.11). For this the microfluidic pump was filled up with buffer until the tubes were wetted, the chip was carefully inserted into the commercially available cell (Micrux ©) and the cap (containing the gate electrode) was closed. With a flow rate of 20μL/min buffer was pumped through the cell from inlet to outlet. The liquid from the outlet was collected as waste. This set-up resulted in the electrolyte-gated gFET configuration required for the measurements. Transfer curves using the same buffer were obtained before the experiment started, after every modification step and after every exposure to streptavidin in buffer at increasing concentrations. For the recording of the transfer curves the measurement cell and the gate were connected to a source meter unit (SMU) U2722A (Keysight Technologies ©) and a silver chloride wire was used a the gate electrode. For the electrical measurements the SMU was controlled via the software Dirac time (© Patrik Aspermair). The source-drain bias (V_{DS}) was kept constant at 0.05 V and the gate voltage (V_{GS}) was swept between -0.5 and 0.5 V, with a scan rate of 20mV/s and a step size of 5mV. For each steps three $I_D V_G$ curves were recorded consecutively (always the last one is shown in the following graphs).

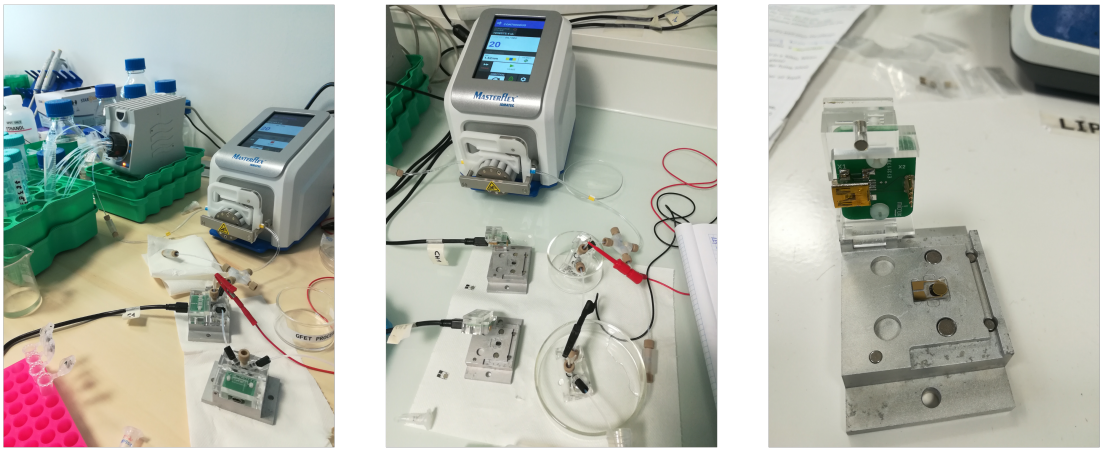

Figure 2.11.: Experimental set up, showing the flow cell from Micrux ©, with and without cap and the placement of the devices

Since the nanodisc were reconstituted in nanodisc buffer this buffer was used for the baseline measurements and as diluent for the streptavidin stock solution. As described before this buffer contained: 20mM TRIS, 0.5mM EDTA and 100mM NaCl @pH 7.22. Which corresponds to an ionic strength of I=0.19M and a debye length of 0.68nm, which is similar to 1xPBS. This is actually already problematic, as the pyrene linker and the subsequent attachment of the nanodisc are already exceeding this distance. With that being said, in a comparable approach 1xPBS was used and biosensing experiments were successfully conducted [78], indicating that it is not really well understood what happens at the surface regarding spatial orientation. It can also be argued that this might make electrostatic gating effects non-significant, because those are screened due to the small debye length [79]. In any case was the buffer kept to ensure the stability of the nanodiscs. The first $I_D V_G$s were recorded on bare graphene. Afterwards the device was presented with the nanodisc + glycophorin A solution. Following the 2h incubation, the chip was carefully rinsed with buffer, placed back into the measurement cell, flushed with buffer and measurements were obtained. The immobilization of pyrene NTA resulted in a positive shift (+42.5 mV) (presented in Figure 2.12. This p-doping effect can be explained by the electron withdrawing functional group of nta, but this also could indicate that the functional group is in fact close to the surface and can therefore have this effect that is similar to the p-doping effect found for other pyrene linkers (predominantly PBASE) [115, 109, 128, 117, 67].

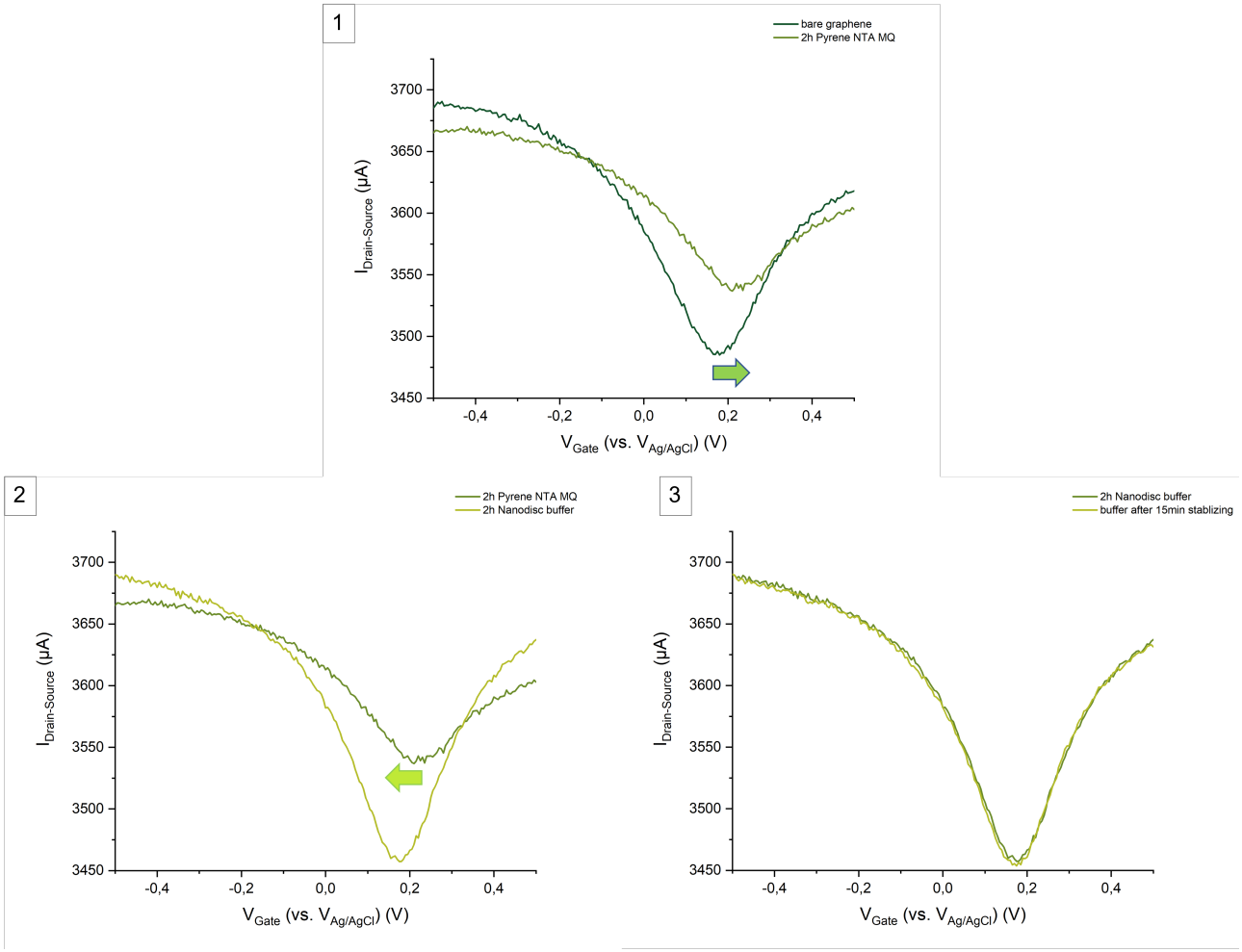

Figure 2.12.: Transfer curves of immobilization steps on gFET (LMB8): 1) indicating a positive shift for pyrene NTA, 2) a negative shift for the nanodiscs (middle) and 3) stability of nanodiscs in buffer (15min)

Following the immobilization of pyrene NTA on the graphene surface the device was immersed in the 100mM ($NiSO_4$) solution for 1h. The chip was carefully rinsed with MQ and immediately afterwards incubated with the nanodisc solution containing glycophorin A for 2h. After the incubation with the nanodics + glycophorin A solution the chip was placed back into the measurement set-up, flushed with buffer and I_DV_Gs were recorded. Here a negative shift (-45mV) was observed (Figure 2.12. This can arguable be due to the amino acids from the protein which can partially donate electrons to the graphene channel [41, 10, 90, 11]. This n-doping upon immobilization of nanodics containing a protein was also observed by Murugathas et al. [78]. They further observed a significant reduction in current modulation, which was not the case in this experiment. We further

also observed n-doping when using only empty nanodiscs, which still however contain a MSP. The device was then left for 15min in the cell, before another round of I_DV_Gs were recorded in order to check whether the immobilization was stable (Dirac point: 0,1742). As this was the case the experiment could be continued (Figure 2.12. For this a dilution series of streptavidin was prepared. Starting with a stock solution at 100μM and further diluted with ND buffer. These solutions were then presented to the device with increasing concentrations. This was done using the microfluidic pump. Each concentration was presented to the device for 15min using a flow rate of 20μL/min. Afterwards I_DV_G curves were recorded. With increasing concentrations a negative shift was observed (Figure 2.13. The obtained Dirac points were then plotted against the concentration (Figure 2.14), the

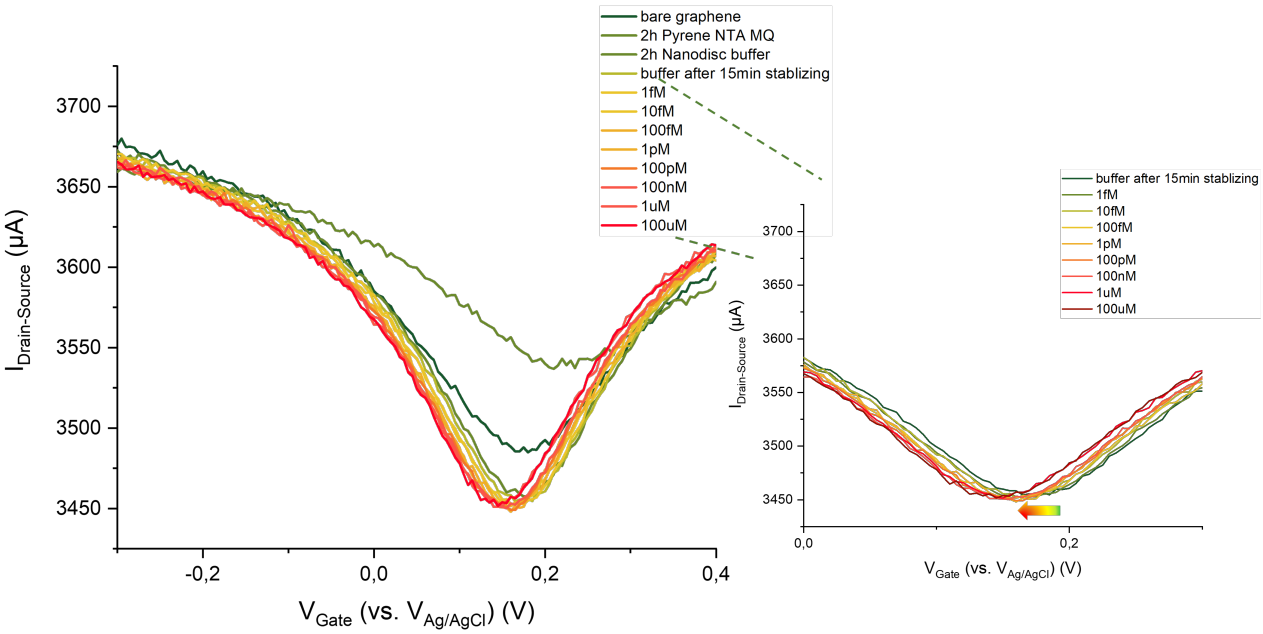

Figure 2.13.: Biosensing data presenting the device with increasing concentrations of streptavidin

same was done for the calculated △Dirac, which is the change in mV from the starting point (Dirac point of nanodiscs in buffer) as absolute value (Figure in linear scale and in log scale 2.14). Comparing the delta, rather than absolute values, is preferable as the respective system is taken into account. This also makes experiment performed on different devices comparable.

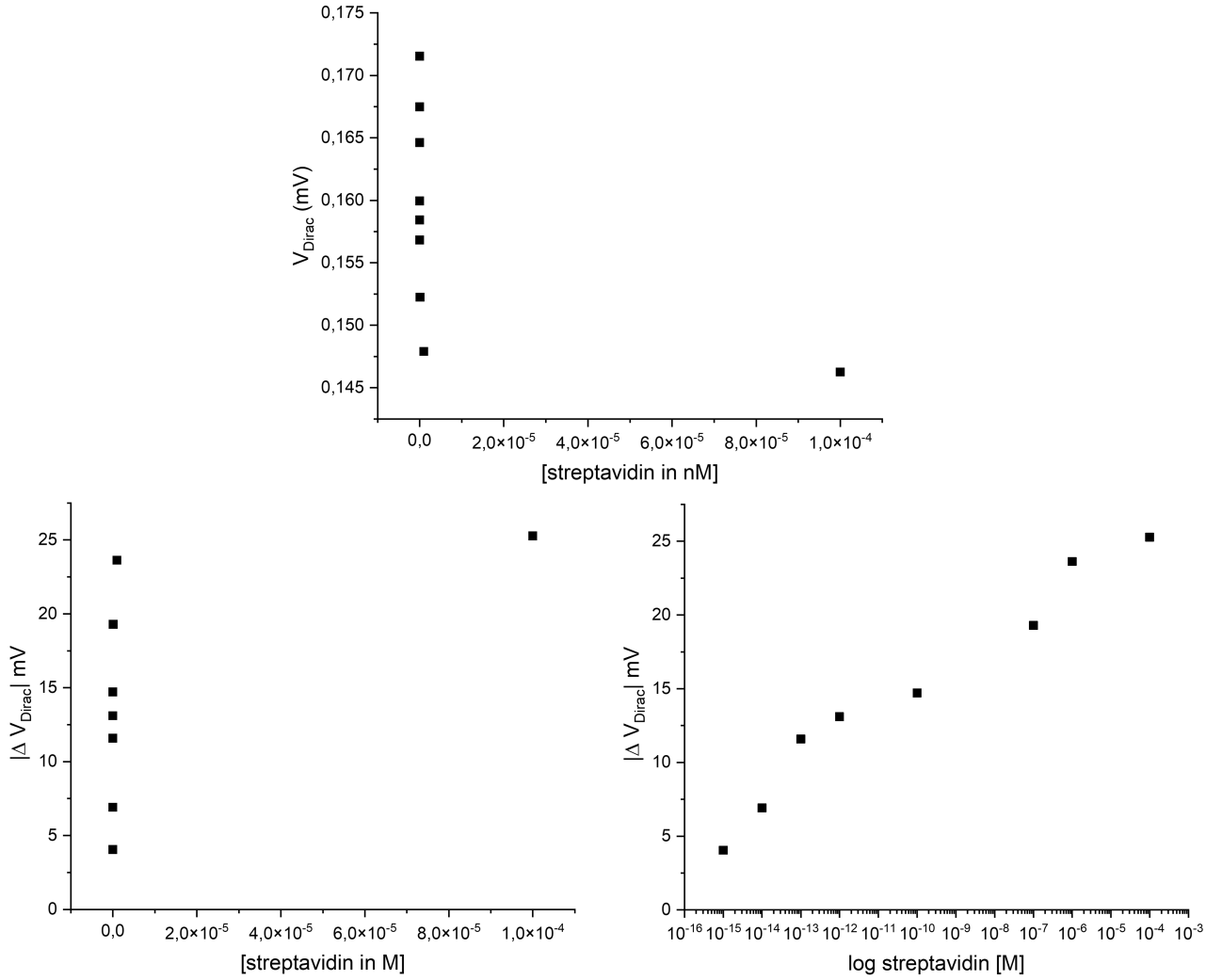

Figure 2.14.: Data Vdirac LMB 8

Since the expected K_D is $\sim 10^{-14}$, and thus very low one can argue that going up to a concentrations as high as 100 μM is an excessive measure, but at the same time this has to be seen as a process-oriented approach trying to gather preliminary data. Moreover it is essential to reach saturation of the sensor in order eventually evaluate the correct binding affinity (as illustrated in Figure 2.15). Further it has to be noted that the response is rather small (max. $\sim 25mV$), although still distinguishable from noise.

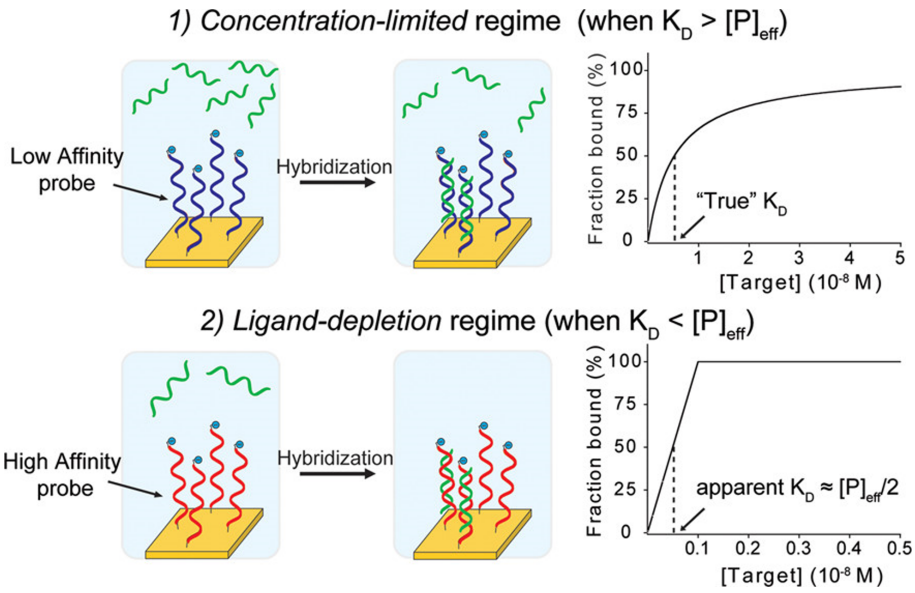

Figure 2.15.: Operation regimes of surface-based biosensors: concentration-limited regime vs. Ligand-depletion regime (from [28])

As every experiment is only ever as good as its control experiments, the following questions should be raised after evaluating the data obtained for each biosensing experiment:

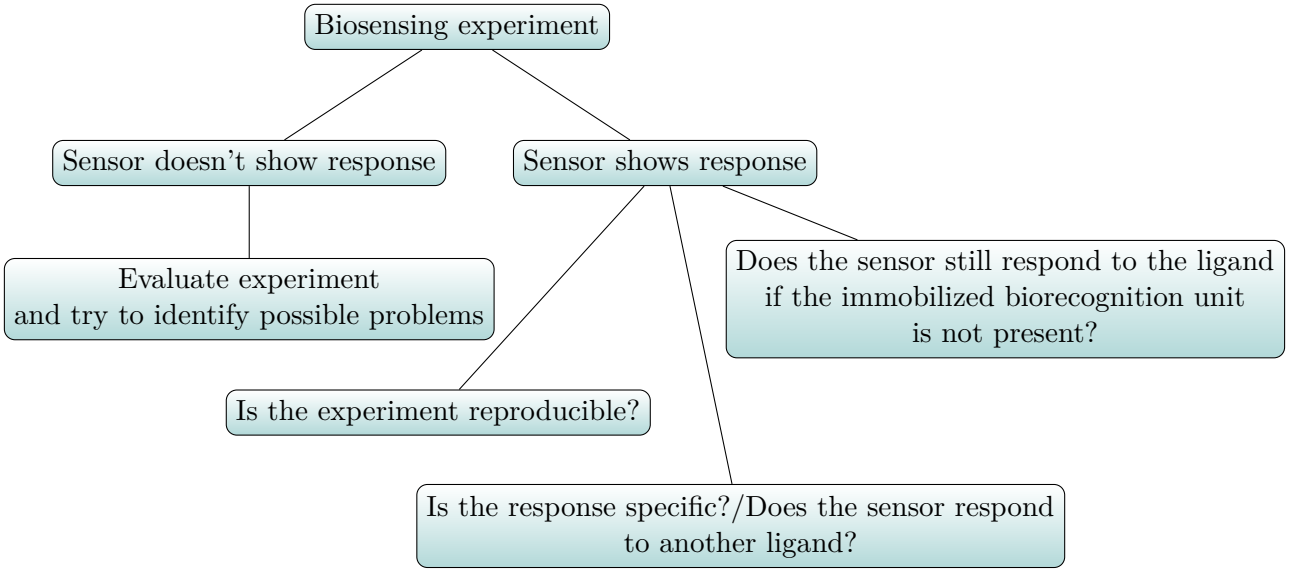

Figure 2.16.: Decision tree for biosensing experiment evaluation (created by the author using PowerPoint ©)

Hence the obvious control experiments for this experiment were: 1. reproducing the experiment using a maybe more suitable concentration range (only up to around 100pM); 2. Test another device that underwent the same modification steps against a different ligand 3. Use a device which has the empty nanodiscs immobilized and test it against the same concentration range of streptavidin. Although this approach seemed rather straight forward, there were several issues encountered. The first and most problematic being that follow up experiments seemed to face reoccurring stability issues regarding the connection of the set-up with resulted in unreliable measurements. After repeated attempts to fix this connection issues, it was discovered that the gate electrode might be the cause of problems and indeed, after searching for plausible reasons it was found that the nanodisc buffer which contained tris(hydroxymethyl)aminomethane (TRIS) was very likely destabilizing the silver-chloride wire used as gate electrode [72]. Since the biosensing measurements of the most relevant benchmark study were conducted in 1xPBS [78] (although they as well used a TRIS/NaCl buffer for elution, resulting in the assumptions that the nanodiscs stay stable over time, even when the bufffer is changed from nanodics buffer to PBS), this approach was subsequently also tried for the experiments that followed the realization that the combination of buffer and gate electrode was unsuitable. But the results obtained when using the nanodisc buffer were not reproducible with the PBS based configuration (Data not shown). This could also possible be due to destabilization of the nanodisc, although this is only an assumption. This lack of reproducibility combined with the running out of time, lead to the unsatisfactory outcome of only having interpretable data from one biosensing experiment performed. Additionally to the electrical measurements, however, surface investigations were conducted providing supplementary data.

2.2.1. Surface investigation for biosensing approach

AFM measurements were performed, investigated one sample with bare graphene, one with graphene + pyrene nta and one sample with graphene + pyrene nta + nickel-ions + nanodiscs containing glycophorin A. Although an increase in surface roughness and clusters of different diameters were observed (Figure 2.17), which are an indication of successful immobilization ([78]-supporting information), this data should be interpreted with caution, as it can not be unambiguously assumed that what we see here are indeed nanodics.

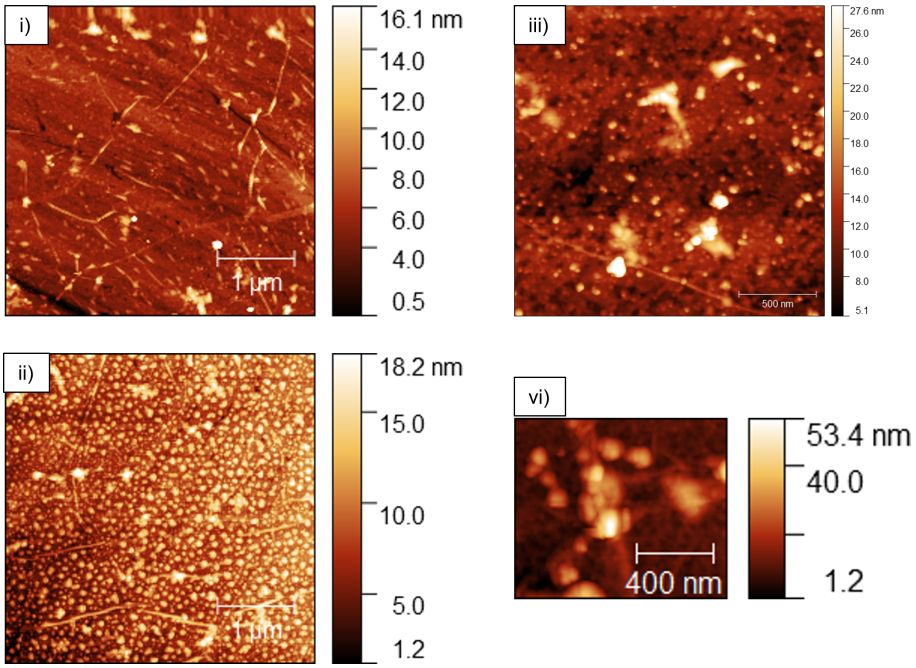

Figure 2.17.: AFM images of i) bare graphene ii) graphene + pyrene nta iii) and vi) graphene + pyrene nta immobilized nanodiscs (with glycophorin A)

In addition to these measurements X-ray photoelectron spectroscopy (XPS) was carried out. XPS was performed for one sample of pyrene nta alone, one sample of pyrene nta immobilized on graphene on a micrux device as well as one with additionally immobilized nanodiscs containing glycophorin A. The results of this investigation (Figure 2.18) indicate the successful immobilization of nanodics on the graphene film using the pyrene nta functionalization strategy. This can be reasoned because of the relative decrease in C=C bonds accompanied by a relative increase in "shake-up" (plasmon $\pi - \pi*$), as well as an increase in peptide-bonds. Again with the limitation that, since the data is fitted according to the data obtained, this can only be regarded as an evidence that the nanodisc are immobilized, not a proof. It has also to be mentioned that this kind of investigation, although very powerful, doesn't tell us anything about the way the elements are present on the sample, just that they are present. Meaning that we can only assume that it

was,in fact, the functionalization strategy used which is not responsible for the signal possible corresponding to the nanodiscs and not simply unspecific absorption on the surface.

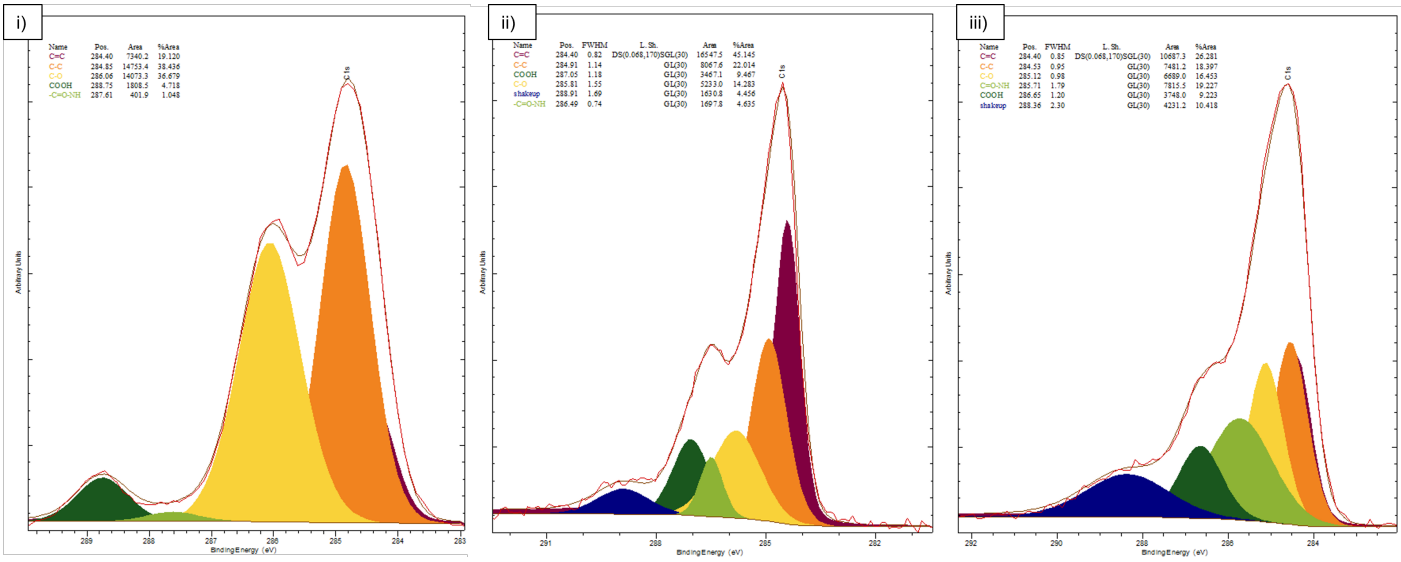

Figure 2.18.: XPS analysis of i) pyrene nta ii) graphene + pyrene nta iii) graphene + pyrene nta + nanodiscs

With all that being said, it can be argued that these results indicate that indeed the nanodics can be immobilized onto the presented gFET. Regarding the potential for biosensing applications, however, no meaningful final conclusion can be drawn. Although the immobilisation strategy using pyrene NTA and therefore taking advantage of the often already available his-tag seems, in theory, rather straight-forward and appealing, several aspects remain unclear. One of them being the question whether the specific pyrene NTA used, with it's long PEG chain was the best choice. This argument is due to the fact that it is not yet understood how this long chain behaves - does it stay upright in the electrolyte solution? Does it lay flat and potentially interact with the graphene film (as possible indicated by the electron withdrawing properties). What happens upon binding of the his-tag of the nanodisc to the pyrene NTA? How are defects within the graphene film influencing these observations? All these questions can not be answered with the data presented here. Therefore it can be assessed that, although biosensing with gFET certainly is a very powerful tool due to the high sensitivity that can be achieved, the field graphene based biosensors still might have to undergo some alterations until robust, reusable, selective devices are available, which can be illustrated on the basis of this work here. In case of the devices presented in this work it would arguable be a reasonable idea to invest time in re-designing the layout - reducing height step and thus levelling electrodes and substrate in order to also reduce defects in the long-run, as this is the first step that can be undertaken towards reproducibility. Further,

in order to use nanodisc for this application one might still have to dedicate time to better understand possible interactions between graphene itself and the nanodiscs, as well as understanding the impact the different immobilization strategies might have. Also the problem of the debye length has to be considered in this context, especially when thinking about clinical biosensing applications that inevitable demand the use of solutions with high ionic strength. Therefore it has to be better understood what exactly is happening at the surface concerning spatial orientation. For all of these purposes devices exhibiting less variances would be beneficial, as the lesser aberrations that occur, the more insightful investigations regarding the aforementioned topics can be conducted. In the end only devices providing all the required criteria will be acceptable in terms of medical applications pushing the standard for scientific research into that direction and raising the bar to really understand the biophysical and biochemical processes involved.

Noteworthy remarks

At this point several aspects that also play a part in the output of a biosensor have not been mentioned yet and will also not be covered in this work. However it has to made clear that these are also contributing factors and some of them should at least be mentioned to flag their relevance.

- Layout of gFET: Since the contact width (W) and the contact length (D) play a critical role in the intrinsic performance of the gFET, as their ratio influences the resistance of the device and its electrical sensitivity [35]. Therefore the respective design will always have an impact on the performance of the device.

- Microfluidic set-up: Of course the settings of the microfluidic set-up are something that can be addressed. On the one hand mass transport should not be limited thus a sufficient flow rate has to be selected, but higher flow-rates are potentially destabilizing to the surface architecture. Simulations of different flow-rates in different surface architectures could therefore be helpful to understand what the surface is exposed to. Also the entrapment of air can be fatal for measurements. Further challenges include non-specific absorption/binding (NSA/NSB) and integration and automation [17].

- Unspecific absorption: This aspect has only be touched upon in the context of this work, but its highly significant, as biosensors don't provide the same compartmentalization as biological systems do, making non-specific absorption more abundant in biosensing settings [30]. This is even more relevant, as biological fluids represent crowded environments and are thus tricky samples to work with.

- Data fitting: Although this facet does not play a big part in this particular work it should still be mentioned that this is a relevant part of data treatment in the context of biosensing. With every model used one has to consider the assumptions this model makes about the system in interrogation. In the case of the often used Langmuir-isotherm, the assumptions are that the surface is homogeneous (also only

providing one type of interaction site), each of these sites are equivalent and only provide one binding site is available per molecule. This is of course a simplified way of regarding binding interactions as molecules can also have more than one binding site, something that has to be taken into account when fitting your data. It is then mandatory to think of what kind of Model is used and why and be aware that different models will also make the results appear differently [15].

Even these points are by far not covering the whole complexity of biosensors and although even simplified approaches often result into representing reality quite well, it should just be kept in mind that there are many more aspects to consider.

3. Conclusion and outlook

The work of this thesis was focused on testing an already quite established set-up concerning a new combination of surface modification and biorecognition element. Although nanodisc have already been successfully immobilized and tested as biosensing directed biorecognition elements on gFET, the functionalization strategy used here was a different one, taking advantage of the NTA-His-tag relation. Further, due to differences in design of the devices not every biosensing device will show the same outcome when presented with functionalization strategies as well as biosensing approaches, making it indispensable to test different approaches on different devices. A successful nanodics immobilization strategy would open the door to conveniently utilizing membrane proteins in the context of biosensing. Hence explaining the motivation for this work. Before this could be realized a considerable amount of time was dedicated to better understanding of the device properties and fabrication steps. This resulted in evaluating parameters such as the drying time during the fabrication process and performing substantial quality control that included SEM pictures and raman spectroscopy and thus quite some time spent in the clean room. This was absolutely indispensable as it provided great insight into the reasons behind inconsistent electrical measurements. This was followed by a period of time in which several surface modifications strategies were carried out (pyrene linkers and covalent-modification strategies) and combined with biorecognition elements (predominately aptamers) ans tested against their respective ligand. Finally, I decided to focus on the pyrene NTA nanodisc combination as this sparked the highest intrinsic motivation and curiosity, likely due to the fact that membrane proteins play such a fascinating role in the organisation of cells and are thus very fascinating. Particularly because many receptors are membrane bound and transmit signals from the extracellular to the intracellular matrix upon ligand binding. This also means that they often have a high affinity towards their ligand and are therefore also of considerable interest for biosensing applications. This dedication to the topic resulted in some preliminary results that can be considered an interesting, although minor contribution to understanding how these protein containing lipid-bilayer constructs can be utilized as biorecognition units in the future. In general will it be intriguing to see in which direction the vast field of biosensors in general and graphene based biosensors in particular will develop. This is accompanied by ethical considerations as the development towards point-of-care (POC) devices in medical settings can be regarded positive when individual fluctuations of patients are taken into consideration. Since this has the potential to take health care to a new individualized low-cost level. However, personal/every-day biosensing devices should still be handled with caution as they might promise more than they deliver, taking advantage of the hopes of their customers to improve their health by providing a lot of personal data as well as possibly being without medical supervision. Of course, in an ideal

world were biosensing would be used in the optimized and supervised way, healthcare could move away from treating people upon already having a disease towards prevention strategies that are based on highly sensitive and selective devices. This becomes especially important when considering that the trend towards POC devices is constantly advancing and that the need for fast and reliable diagnostics that is financially accessible to the broad population is more essential than ever. This need will further pave the way for interdisciplinary research that will be required to address the complex problems posed by the discipline of biosensing.

Bibliography

[1] *Molecular biology of the cell*, sixth edit ed. Garland Science, New York, NY, 2015.

[2] What are Biosensors? Principle, Working, Types and Applications, 2019.

[3] Ahn, S. R., An, J. H., Lee, S. H., Song, H. S., Jang, J., and Park, T. H. Peptide hormone sensors using human hormone receptor-carrying nanovesicles and graphene FETs. *Scientific Reports 10*, 1 (2020), 388.

[4] Bankar, S. B., Bule, M. V., Singhal, R. S., and Ananthanarayan, L. Glucose oxidase — An overview. *Biotechnology Advances 27*, 4 (7 2009), 489–501.

[5] Béraud, A., Sauvage, M., Bazán, C. M., Tie, M., Bencherif, A., and Bouilly, D. Graphene field-effect transistors as bioanalytical sensors: design, operation and performance. *Analyst 146*, 2 (2021), 403–428.

[6] Bergveld, P. Development of an ion-sensitive solid-state device for neurophysiological measurements. *IEEE transactions on bio-medical engineering 17*, 1 (1 1970), 70–71.

[7] Bhalla, N., Jolly, P., Formisano, N., and Estrela, P. Introduction to biosensors. *Essays in biochemistry 60*, 1 (6 2016), 1–8.

[8] Bohbot, J. D., and Vernick, S. The Emergence of Insect Odorant Receptor-Based Biosensors. *Biosensors 10*, 3 (3 2020).

[9] Bontempi, N., Chong, K., Orton, H., Staude, I., Choi, D., Alessandri, I., Kivshar, Y., and Neshev, D. Highly sensitive biosensors based on all-dielectric nanoresonators. *Nanoscale 9* (4 2017).

[10] Bradley, K., Briman, M., Star, A., and Grüner, G. Charge Transfer from Adsorbed Proteins. *Nano Letters 4*, 2 (2 2004), 253–256.

[11] Bradley, K., Gabriel, J.-C. P., Briman, M., Star, A., and Grüner, G. Charge Transfer from Ammonia Physisorbed on Nanotubes. *Physical Review Letters 91*, 21 (11 2003), 218301.

[12] Cai, B., Huang, L., Zhang, H., Sun, Z., Zhang, Z., and Zhang, G.-J. Gold nanoparticles-decorated graphene field-effect transistor biosensor for femtomolar MicroRNA detection. *Biosensors and Bioelectronics 74* (2015), 329–334.

[13] Chakraborty, M., and Hashmi, M. Graphene as a Material – An Overview of Its Properties and Characteristics and Development Potential for Practical Applications. 1 2018.

[14] Cheema, J. A., Carraher, C., Plank, N. O. V., Travas-Sejdic, J., and Kralicek, A. Insect odorant receptor-based biosensors: Current status and prospects. *Biotechnology Advances 53* (2021), 107840.

[15] Chen, C. Evaluation of Equilibrium Sorption Isotherm Equations. *The Open Chemical Engineering Journal 7* (1 2014), 24–44.

[16] Childres, I., Jauregui, L. A., Park, W., Cao, H., and Chen, Y. P. Raman spectroscopy of graphene and related materials. *New developments in photon and materials research 1* (2013).

[17] Choi, S., Goryll, M., Sin, L. Y. M., Wong, P. K., and Chae, J. Microfluidic-based biosensors toward point-of-care detection of nucleic acids and proteins. *Microfluidics and Nanofluidics 10*, 2 (2011), 231–247.

[18] Chu, C.-H., Sarangadharan, I., Regmi, A., Chen, Y.-W., Hsu, C.-P., Chang, W.-H., Lee, G.-Y., Chyi, J.-I., Chen, C.-C., Shiesh, S.-C., Lee, G.-B., and Wang, Y.-L. Beyond the Debye length in high ionic strength solution: direct protein detection with field-effect transistors (FETs) in human serum. *Scientific Reports 7*, 1 (2017), 5256.

[19] CLARK, L. C. J., and LYONS, C. Electrode systems for continuous monitoring in cardiovascular surgery. *Annals of the New York Academy of Sciences 102* (10 1962), 29–45.

[20] Crivianu-Gaita, V., and Thompson, M. Aptamers, antibody scFv, and antibody Fab' fragments: An overview and comparison of three of the most versatile biosensor biorecognition elements. *Biosensors and Bioelectronics 85* (2016), 32–45.

[21] Cunge, G., Ferrah, D., Petit-Etienne, C., Davydova, A., Okuno, H., Kalita, D., Bouchiat, V., and Renault, O. Dry efficient cleaning of poly-methyl-methacrylate residues from graphene with high-density H2 and H2-N2 plasmas. *Journal of Applied Physics 118*, 12 (9 2015), 123302.

[22] DeLeon, C., Wang, D. Q.-H., and Arnatt, C. K. G Protein-Coupled Estrogen Receptor, GPER1, Offers a Novel Target for the Treatment of Digestive Diseases. *Frontiers in Endocrinology 11* (2020).

[23] Deng, S., and Berry, V. Wrinkled, rippled and crumpled graphene: an overview of formation mechanism, electronic properties, and applications. *Materials Today 19*, 4 (2016), 197–212.

[24] D'Agostino, M., Pavoni, E., Romagnoli, A., Ardiccioni, C., Motta, S., Crippa, P., Biagetti, G., Notarstefano, V., Barocci, S., Costabile, B. K., Colasurdo, G., Caucci, S., Mencarelli, D., Turchetti, C., Farina, M., Pierantoni, L., Teana, A. L., Hadi, R. A., Chinappi, M., Trucchi, E., Mancia, F., Morozzo della Rocca, B., D'Annessa, I., and Marino, D. D. SARS-CoV-2 multi-variant graphene biosensor based on engineered dimeric ACE2 receptor. *medRxiv* (1 2021), 2021.10.02.21264210.

[25] Eissa, S., Jimenez, G. C., Mahvash, F., Guermoune, A., Tlili, C., Szkopek, T., Zourob, M., and Siaj, M. Functionalized CVD monolayer graphene for label-free impedimetric biosensing. *Nano Research 8*, 5 (2015), 1698–1709.

[26] Eivazzadeh-Keihan, R., Bahojb Noruzi, E., Chidar, E., Jafari, M., Davoodi, F., Kashtiaray, A., Ghafori Gorab, M., Masoud Hashemi, S., Javanshir, S., Ahangari Cohan, R., Maleki, A., and Mahdavi, M. Applications of carbon-based conductive nanomaterials in biosensors. *Chemical Engineering Journal 442* (2022), 136183.

[27] Elnathan, R., Kwiat, M., Pevzner, A., Engel, Y., Burstein, L., Khatchtourints, A., Lichtenstein, A., Kantaev, R., and Patolsky, F. Biorecognition Layer Engineering: Overcoming Screening Limitations of Nanowire-Based FET Devices. *Nano Letters 12*, 10 (10 2012), 5245–5254.

[28] Esteban Fernández de Ávila, B., Watkins, H. M., Pingarrón, J. M., Plaxco, K. W., Palleschi, G., and Ricci, F. Determinants of the Detection Limit and Specificity of Surface-Based Biosensors. *Analytical Chemistry 85*, 14 (7 2013), 6593–6597.

[29] FDA-NIH Biomarker Working Group. BEST (Biomarkers, EndpointS, and other Tools) Resource [Internet].

[30] Frutiger, A., Tanno, A., Hwu, S., Tiefenauer, R. F., Vörös, J., and Nakatsuka, N. Nonspecific Binding—Fundamental Concepts and Consequences for Biosensing Applications. *Chemical Reviews 121*, 13 (7 2021), 8095–8160.

[31] Fuentes, N., and Silveyra, P. Estrogen receptor signaling mechanisms. *Advances in protein chemistry and structural biology 116* (2019), 135–170.

[32] Gao, B., Rojas Chávez, R. A., Malkawi, W. I., Keefe, D. W., Smith, R., Haim, H., Salem, A. K., and Toor, F. Sensitive detection of SARS-CoV-2 spike protein using vertically-oriented silicon nanowire array-based biosensor. *Sensing and Bio-Sensing Research 36* (2022), 100487.

[33] Gao, J., Wang, C., Wang, C., Chu, Y., Wang, S., Sun, M. y., Ji, H., Gao, Y., Wang, Y., Han, Y., Song, F., Liu, H., Zhang, Y., and Han, L. Poly-l-Lysine-Modified Graphene Field-Effect Transistor Biosensors for Ultrasensitive

Breast Cancer miRNAs and SARS-CoV-2 RNA Detection. *Analytical Chemistry 94*, 3 (1 2022), 1626–1636.

[34] Georgakilas, V., Otyepka, M., Bourlinos, A. B., Chandra, V., Kim, N., Kemp, K. C., Hobza, P., Zboril, R., and Kim, K. S. Functionalization of Graphene: Covalent and Non-Covalent Approaches, Derivatives and Applications. *Chemical Reviews 112*, 11 (11 2012), 6156–6214.

[35] Giubileo, F., and Bartolomeo, A. D. The role of contact resistance in graphene field-effect devices. *arXiv: Mesoscale and Nanoscale Physics* (2017).

[36] Green, N. S., and Norton, M. L. Interactions of DNA with graphene and sensing applications of graphene field-effect transistor devices: A review. *Analytica Chimica Acta 853* (2015), 127–142.

[37] Guo, P., Xiong, J., Zheng, D., Zhang, W., Liu, L., Wang, S., and Gu, H. A biosensor based on a film bulk acoustic resonator and biotin–avidin system for the detection of the epithelial tumor marker mucin 1. *RSC Adv. 5* (7 2015).

[38] Gupta, N., Renugopalakrishnan, V., Liepmann, D., Paulmurugan, R., and Malhotra, B. D. Cell-based biosensors: Recent trends, challenges and future perspectives. *Biosensors and Bioelectronics 141* (2019), 111435.

[39] Han, Q., Pang, J., Li, Y., Sun, B., Ibarlucea, B., Liu, X., Gemming, T., Cheng, Q., Zhang, S., Liu, H., Wang, J., Zhou, W., Cuniberti, G., and Rümmeli, M. H. Graphene Biodevices for Early Disease Diagnosis Based on Biomarker Detection. *ACS Sensors 6*, 11 (11 2021), 3841–3881.

[40] Hao, Z., Pan, Y., Huang, C., Wang, Z., and Zhao, X. Sensitive detection of lung cancer biomarkers using an aptameric graphene-based nanosensor with enhanced stability. *Biomedical Microdevices 21*, 3 (2019), 65.

[41] Heller, I., Janssens, A. M., Männik, J., Minot, E. D., Lemay, S. G., and Dekker, C. Identifying the Mechanism of Biosensing with Carbon Nanotube Transistors. *Nano Letters 8*, 2 (2 2008), 591–595.

[42] Helmholtz, H. Ueber einige Gesetze der Vertheilung elektrischer Ströme in körperlichen Leitern mit Anwendung auf die thierisch-elektrischen Versuche. *Annalen der Physik 165*, 6 (1 1853), 211–233.

[43] Hetemi, D., Noël, V., and Pinson, J. Grafting of Diazonium Salts on Surfaces: Application to Biosensors. *Biosensors 10*, 1 (1 2020).

[44] Holzinger, M., Baur, J., Haddad, R., Wang, X., and Cosnier, S. Multiple functionalization of single-walled carbon nanotubes by dip coating. *Chemical Communications 47*, 8 (2011), 2450–2452.

[45] Huang, C., Hao, Z., Qi, T., Pan, Y., and Zhao, X. An integrated flexible and reusable graphene field effect transistor nanosensor for monitoring glucose. *Journal of Materiomics 6*, 2 (2020), 308–314.

[46] Hwang, M. T., Heiranian, M., Kim, Y., You, S., Leem, J., Taqieddin, A., Faramarzi, V., Jing, Y., Park, I., van der Zande, A. M., Nam, S., Aluru, N. R., and Bashir, R. Ultrasensitive detection of nucleic acids using deformed graphene channel field effect biosensors. *Nature communications 11*, 1 (3 2020), 1543.

[47] Hwang, M. T., Park, I., Heiranian, M., Taqieddin, A., You, S., Faramarzi, V., Pak, A. A., van der Zande, A. M., Aluru, N. R., and Bashir, R. Ultrasensitive Detection of Dopamine, IL-6 and SARS-CoV-2 Proteins on Crumpled Graphene FET Biosensor. *Advanced Materials Technologies 6*, 11 (11 2021), 2100712.

[48] Idumah, C. I. Novel trends in conductive polymeric nanocomposites, and bionanocomposites. *Synthetic Metals 273* (3 2021), 116674.

[49] Jan, S., and Bert, P. The Role of Biomacromolecular Crowding, Ionic Strength, and Physicochemical Gradients in the Complexities of Life's Emergence. *Microbiology and Molecular Biology Reviews 73*, 2 (6 2009), 371–388.

[50] Joshi, P., Mishra, R., and Narayan, R. J. Biosensing applications of carbon-based materials. *Current Opinion in Biomedical Engineering 18* (2021), 100274.

[51] K., G. A. Graphene: Status and Prospects. *Science 324*, 5934 (6 2009), 1530–1534.

[52] Khan, N. I., and Song, E. Detection of an IL-6 Biomarker Using a GFET Platform Developed with a Facile Organic Solvent-Free Aptamer Immobilization Approach. *Sensors (Basel, Switzerland) 21*, 4 (2 2021).

[53] Kiliszek, M., Harputlu, E., Szalkowski, M., Kowalska, D., Unlu, C. G., Haniewicz, P., Abram, M., Wiwatowski, K., Niedziółka-Jönsson, J., Maćkowski, S., Ocakoglu, K., and Kargul, J. Orientation of photosystem I on graphene through cytochrome c553 leads to improvement in photocurrent generation. *Journal of Materials Chemistry A 6*, 38 (2018), 18615–18626.

[54] Kim, H. H., Lee, S. K., Lee, S. G., Lee, E., and Cho, K. Wetting-Assisted Crack- and Wrinkle-Free Transfer of Wafer-Scale Graphene onto Arbitrary Substrates over a Wide Range of Surface Energies. *Advanced Functional Materials 26*, 13 (4 2016), 2070–2077.

[55] Koshino, M., and Ando, T. Orbital diamagnetism in multilayer graphenes: Systematic study with the effective mass approximation. *Physical Review B 76*, 8 (8 2007), 85425.

[56] Kurzweil, P. Chapter 19 - Electrochemical Double-layer Capacitors. Elsevier, Amsterdam, 2015, pp. 345–407.

[57] Kwon, O. S., Song, H. S., Park, S. J., Lee, S. H., An, J. H., Park, J. W., Yang, H., Yoon, H., Bae, J., Park, T. H., and Jang, J. An Ultrasensitive, Selective, Multiplexed Superbioelectronic Nose That Mimics the Human Sense of Smell. *Nano Letters 15*, 10 (10 2015), 6559–6567.

[58] Kwon, W., Do, S., Won, D. C., and Rhee, S.-W. Carbon Quantum Dot-Based Field-Effect Transistors and Their Ligand Length-Dependent Carrier Mobility. *ACS Applied Materials & Interfaces 5*, 3 (2 2013), 822–827.

[59] Kwong Hong Tsang, D., Lieberthal, T. J., Watts, C., Dunlop, I. E., Ramadan, S., del Rio Hernandez, A. E., and Klein, N. Chemically Functionalised Graphene FET Biosensor for the Label-free Sensing of Exosomes. *Scientific Reports 9*, 1 (2019), 13946.

[60] Lee, H., Paeng, K., and Kim, I. S. A review of doping modulation in graphene. *Synthetic Metals 244* (2018), 36–47.

[61] Lee, J., Zheng, X., Roberts, R. C., and Feng, P. X.-L. Scanning electron microscopy characterization of structural features in suspended and non-suspended graphene by customized CVD growth. *Diamond and Related Materials 54* (2015), 64–73.

[62] Lee, M., Yang, H., Kim, D., Yang, M., Park, T. H., and Hong, S. Human-like smelling of a rose scent using an olfactory receptor nanodisc-based bioelectronic nose. *Scientific Reports 8*, 1 (2018), 13945.

[63] Lee, S. H., Lee, M., Yang, H., Cho, Y., Hong, S., and Park, T. H. Bioelectronic sensor mimicking the human neuroendocrine system for the detection of hypothalamic-pituitary-adrenal axis hormones in human blood. *Biosensors and Bioelectronics 154* (2020), 112071.

[64] Lee, Y. H., and Mutharasan, R. Biosensors. *Sensor Technology Handbook* (1 2005), 161–180.

[65] Lei, Y.-M., Xiao, M.-M., Li, Y.-T., Xu, L., Zhang, H., Zhang, Z.-Y., and Zhang, G.-J. Detection of heart failure-related biomarker in whole blood with graphene field effect transistor biosensor. *Biosensors and Bioelectronics 91* (2017), 1–7.

[66] Liu, N., Chen, R., and Wan, Q. Recent Advances in Electric-Double-Layer Transistors for Bio-Chemical Sensing Applications, 2019.

[67] Liu, Y., Yuan, L., Yang, M., Zheng, Y., Li, L., Gao, L., Nerngchamnong, N., Nai, C. T., Sangeeth, C. S. S., Feng, Y. P., Nijhuis, C. A., and Loh,

K. P. Giant enhancement in vertical conductivity of stacked CVD graphene sheets by self-assembled molecular layers. *Nature Communications 5*, 1 (2014), 5461.

[68] Lu, L., Hu, X., and Zhu, Z. Biomimetic sensors and biosensors for qualitative and quantitative analyses of five basic tastes. *TrAC Trends in Analytical Chemistry 87* (2017), 58–70.

[69] Maehashi, K., Katsura, T., Kerman, K., Takamura, Y., Matsumoto, K., and Tamiya, E. Label-Free Protein Biosensor Based on Aptamer-Modified Carbon Nanotube Field-Effect Transistors. *Analytical Chemistry 79*, 2 (1 2007), 782–787.

[70] Maidin, N. N. M., Rahim, R. A., Halim, N. H. A., Abidin, A. S. Z., Ahmad, N. A., and Lockman, Z. Interaction of graphene electrolyte gate field-effect transistor for detection of cortisol biomarker. *AIP Conference Proceedings 2045*, 1 (12 2018), 20022.

[71] Manimekala, T., Sivasubramanian, R., and Dharmalingam, G. Nanomaterial-Based Biosensors using Field-Effect Transistors: A Review. *Journal of electronic materials 51*, 5 (2022), 1950–1973.

[72] Mettler Toledo. How to Measure pH in TRIS-Containing Samples.

[73] Miklos Bolza. Graphenea.

[74] Minot, E. D., Janssens, A. M., Heller, I., Heering, H. A., Dekker, C., and Lemay, S. G. Carbon nanotube biosensors: The critical role of the reference electrode. *Applied Physics Letters 91*, 9 (8 2007), 93507.

[75] Mishyn, V., Hugo, A., Rodrigues, T., Aspermair, P., Happy, H., Marques, L., Hurot, C., Othmen, R., Bouchiat, V., Boukherroub, R., Knoll, W., and Szunerits, S. The holy grail of pyrene-based surface ligands on the sensitivity of graphene-based field effect transistors. *Sensors & Diagnostics 1*, 2 (2022), 235–244.

[76] Mishyn, V., Rodrigues, T., Leroux, Y. R., Aspermair, P., Happy, H., Bintinger, J., Kleber, C., Boukherroub, R., Knoll, W., and Szunerits, S. Controlled covalent functionalization of a graphene-channel of a field effect transistor as an ideal platform for (bio)sensing applications. *Nanoscale Horizons 6*, 10 (2021), 819–829.

[77] Morales, M. A., and Halpern, J. M. Guide to Selecting a Biorecognition Element for Biosensors. *Bioconjugate chemistry 29*, 10 (10 2018), 3231–3239.

[78] Murugathas, T., Hamiaux, C., Colbert, D., Kralicek, A. V., Plank, N. O. V., and Carraher, C. Evaluating Insect Odorant Receptor Display Formats for Biosensing Using Graphene Field Effect Transistors. *ACS Applied Electronic Materials 2*, 11 (11 2020), 3610–3617.

[79] Murugathas, T., Zheng, H. Y., Colbert, D., Kralicek, A. V., Carraher, C., and Plank, N. O. V. Biosensing with Insect Odorant Receptor Nanodiscs and Carbon Nanotube Field-Effect Transistors. *ACS Applied Materials & Interfaces 11*, 9 (3 2019), 9530–9538.

[80] Muthoosamy, K., Geetha Bai, R., Abubakar, I., Sudheer, S., Lim, H., Loh, S. H.-S., Ming, H., Chia, C.-h., and Manickam, S. Exceedingly biocompatible and thin-layered reduced graphene oxide nanosheets using an eco-friendly mushroom extract strategy. *International Journal of Nanomedicine* (12 2014).

[81] Nakatsuka, N., Yang, K.-A., Abendroth, J. M., Cheung, K. M., Xu, X., Yang, H., Zhao, C., Zhu, B., Rim, Y. S., Yang, Y., Weiss, P. S., Stojanović, M. N., and Andrews, A. M. Aptamer-field-effect transistors overcome Debye length limitations for small-molecule sensing. *Science (New York, N.Y.) 362*, 6412 (10 2018), 319–324.

[82] Nimse, S. B., Song, K., Sonawane, M. D., Sayyed, D. R., and Kim, T. Immobilization Techniques for Microarray: Challenges and Applications, 2014.

[83] O'Driscoll, B.; Raghavan, V. B. T. W. T. D. P. A. S. G. S. Aptamer functionalisation of back-gated graphene field effect transistors for Pb2+ sensing. *Proceedings of the 2nd International Electronic Conference on Biosensors* (2022).

[84] Ohno, Y., Maehashi, K., and Matsumoto, K. Label-Free Biosensors Based on Aptamer-Modified Graphene Field-Effect Transistors. *Journal of the American Chemical Society 132*, 51 (12 2010), 18012–18013.

[85] Osella, S., Kiliszek, M., Harputlu, E., Unlu, C. G., Ocakoglu, K., Kargul, J., and Trzaskowski, B. Controlling the charge transfer flow at the graphene/pyrene–nitrilotriacetic acid interface. *Journal of Materials Chemistry C 6*, 18 (2018), 5046–5054.

[86] Oshin, O., Kireev, D., Akinwande, D., Adetiba, E., Idachaba, F., and Atayero, A. Advancing PoC Devices for Early Disease Detection using Graphene-based Sensors. *Journal of Physics: Conference Series 1378*, 3 (2019), 32031.

[87] Oshin, O., Kireev, D., Hlukhova, H., Idachaba, F., Akinwande, D., and Atayero, A. Graphene-Based Biosensor for Early Detection of Iron Deficiency, 2020.

[88] Park, S. J., Kwon, O. S., Lee, S. H., Song, H. S., Park, T. H., and Jang, J. Ultrasensitive Flexible Graphene Based Field-Effect Transistor (FET)-Type Bioelectronic Nose. *Nano Letters 12*, 10 (10 2012), 5082–5090.

[89] Park, S. J., Song, H. S., Kwon, O. S., Chung, J. H., Lee, S. H., An, J. H., Ahn, S. R., Lee, J. E., Yoon, H., Park, T. H., and Jang, J. Human

dopamine receptor nanovesicles for gate-potential modulators in high-performance field-effect transistor biosensors. *Scientific Reports 4*, 1 (2014), 4342.

[90] Podila, R., Vedantam, P., Ke, P. C., Brown, J. M., and Rao, A. M. Evidence for Charge-Transfer-Induced Conformational Changes in Carbon Nanostructure–Protein Corona. *The Journal of Physical Chemistry C 116*, 41 (10 2012), 22098–22103.

[91] Pumera, M. Graphene in biosensing. *Materials Today 14*, 7 (2011), 308–315.

[92] ROBERTS, C., MACKENZIE, A., MORT, M., ATKINSON, T., KRAGH-FURBO, M., and WILKINSON, J. *Living Data*, 1 ed. Bristol University Press, 7 2019.

[93] Rodrigues, T., Mishyn, V., Bozdoğan, A., Leroux, Y., Happy, H., Kasry, A., Boukherroub, R., Dostalek, J., Aspermair, P., Bintinger, J., Kleber, C., Szunerits, S., and Knoll, W. On The Detection of Ctni -A Comparison of Surface-Plasmon Optical -Electrochemical, and Elec-tronic Sensing Concepts. *Annals of Vascular Surgery 6* (3 2021), 1–16.

[94] Ryu, B., Nam, H., Oh, B.-R., Song, Y., Chen, P., Park, Y., Wan, W., Kurabayashi, K., and Liang, X. Cycle-Wise Operation of Printed MoS2 Transistor Biosensors for Rapid Biomolecule Quantification at Femtomolar Levels. *ACS Sensors 2* (1 2017).

[95] Sadighbayan, D., Hasanzadeh, M., and Ghafar-Zadeh, E. Biosensing based on field-effect transistors (FET): Recent progress and challenges. *TrAC - Trends in Analytical Chemistry 133* (2020), 116067.

[96] Schöning, M. J., and Poghossian, A. Recent advances in biologically sensitive field-effect transistors (BioFETs). *Analyst 127*, 9 (2002), 1137–1151.

[97] Sengupta, J., and Hussain, C. M. Graphene-based field-effect transistor biosensors for the rapid detection and analysis of viruses: A perspective in view of COVID-19. *Carbon Trends 2* (2021), 100011.

[98] Seo, G., Lee, G., Kim, M. J., Baek, S.-H., Choi, M., Ku, K. B., Lee, C.-S., Jun, S., Park, D., Kim, H. G., Kim, S.-J., Lee, J.-O., Kim, B. T., Park, E. C., and Kim, S. I. Rapid Detection of COVID-19 Causative Virus (SARS-CoV-2) in Human Nasopharyngeal Swab Specimens Using Field-Effect Transistor-Based Biosensor. *ACS Nano 14*, 4 (4 2020), 5135–5142.

[99] Sheibani, S., Capua, L., Kamaei, S., Akbari, S. S. A., Zhang, J., Guerin, H., and Ionescu, A. M. Extended gate field-effect-transistor for sensing cortisol stress hormone. *Communications Materials 2*, 1 (2021), 10.

[100] Singh, M., Holzinger, M., Tabrizian, M., Winters, S., Berner, N. C., Cosnier, S., and Duesberg, G. S. Noncovalently functionalized monolayer graphene for sensitivity enhancement of surface plasmon resonance immunosensors. *Journal of the American Chemical Society 137*, 8 (2015), 2800–2803.

[101] Sinitskii, A., Dimiev, A., Corley, D. A., Fursina, A. A., Kosynkin, D. V., and Tour, J. M. Kinetics of Diazonium Functionalization of Chemically Converted Graphene Nanoribbons. *ACS Nano 4*, 4 (4 2010), 1949–1954.

[102] Smolyarova, T. E., Shanidze, L. V., Lukyanenko, A. V., Baron, F. A., Krasitskaya, V. V., Kichkailo, A. S., Tarasov, A. S., and Volkov, N. Protein biosensor based on Schottky barrier nanowire field effect transistor. *Talanta 239* (2022), 123092.

[103] Stern, O. ZUR THEORIE DER ELEKTROLYTISCHEN DOPPELSCHICHT. *Zeitschrift für Elektrochemie und angewandte physikalische Chemie 30*, 21-22 (11 1924), 508–516.

[104] Suvarnaphaet, P., and Pechprasarn, S. Graphene-Based Materials for Biosensors: A Review. *Sensors (Basel, Switzerland) 17*, 10 (9 2017), 2161.

[105] Szunerits, S., and Boukherroub, R. Graphene-based biosensors. *Interface Focus 8*, 3 (2018), 20160132.

[106] Thanihaichelvan, M., Surendran, S. N., Kumanan, T., Sutharsini, U., Ravirajan, P., Valluvan, R., and Tharsika, T. Selective and electronic detection of COVID-19 (Coronavirus) using carbon nanotube field effect transistor-based biosensor: A proof-of-concept study. *Materials Today: Proceedings 49* (2022), 2546–2549.

[107] Valota, A. T., Toth, P. S., Kim, Y.-J., Hong, B. H., Kinloch, I. A., Novoselov, K. S., Hill, E. W., and Dryfe, R. A. W. Electrochemical investigation of chemical vapour deposition monolayer and bilayer graphene on the microscale. *Electrochimica acta 110* (2013), 9–15.

[108] Wang, S., Hossain, M. Z., Shinozuka, K., Shimizu, N., Kitada, S., Suzuki, T., Ichige, R., Kuwana, A., and Kobayashi, H. Graphene field-effect transistor biosensor for detection of biotin with ultrahigh sensitivity and specificity. *Biosensors and Bioelectronics 165* (2020), 112363.

[109] Wang, X., Hao, Z., Olsen, T. R., Zhang, W., and Lin, Q. Measurements of aptamer–protein binding kinetics using graphene field-effect transistors. *Nanoscale 11*, 26 (2019), 12573–12581.

[110] Wang, X., Zhu, Y., Olsen, T. R., Sun, N., Zhang, W., Pei, R., and Lin, Q. A graphene aptasensor for biomarker detection in human serum. *Electrochimica Acta 290* (2018), 356–363.

[111] Wang, Z., Hao, Z., Yu, S., De Moraes, C. G., Suh, L. H., Zhao, X., and Lin, Q. An Ultraflexible and Stretchable Aptameric Graphene Nanosensor for Biomarker Detection and Monitoring. *Advanced Functional Materials 29*, 44 (11 2019), 1905202.

[112] Wang, Z., Hao, Z., Yu, S., Huang, C., Pan, Y., and Zhao, X. A Wearable and Deformable Graphene-Based Affinity Nanosensor for Monitoring of Cytokines in Biofluids, 2020.

[113] Wang, Z., Yu, H., and Zhao, Z. Silk fibroin hydrogel encapsulated graphene filed-effect transistors as enzyme-based biosensors. *Microchemical Journal 169* (2021), 106585.

[114] Windbacher, T., Sverdlov, V., and Selberherr, S. Biotin-Streptavidin Sensitive BioFETs and Their Properties BT - Biomedical Engineering Systems and Technologies. A. Fred, J. Filipe, and H. Gamboa, Eds., Springer Berlin Heidelberg, pp. 85–95.

[115] Wu, G., Tang, X., Meyyappan, M., and Lai, K. W. C. Doping effects of surface functionalization on graphene with aromatic molecule and organic solvents. *Applied Surface Science 425* (2017), 713–721.

[116] Xia, Y., Sun, Y., Li, H., Chen, S., Zhu, T., Wang, G., Man, B., Pan, J., and Yang, C. Plasma treated graphene FET sensor for the DNA hybridization detection. *Talanta 223* (2021), 121766.

[117] Xu, S., Zhan, J., Man, B., Jiang, S., Yue, W., Gao, S., Guo, C., Liu, H., Li, Z., Wang, J., and Zhou, Y. Real-time reliable determination of binding kinetics of DNA hybridization using a multi-channel graphene biosensor. *Nature Communications 8*, 1 (2017), 14902.

[118] Yang, G., Li, L., Lee, W. B., and Ng, M. C. Structure of graphene and its disorders: a review. *Science and Technology of Advanced Materials 19*, 1 (12 2018), 613–648.

[119] Yang, H., Kim, D., Kim, J., Moon, D., Song, H. S., Lee, M., Hong, S., and Park, T. H. Nanodisc-Based Bioelectronic Nose Using Olfactory Receptor Produced in Escherichia coli for the Assessment of the Death-Associated Odor Cadaverine. *ACS Nano 11*, 12 (12 2017), 11847–11855.

[120] Yang, Y., Han, C., Jiang, B., Iocozzia, J., He, C., Shi, D., Jiang, T., and Lin, Z. Graphene-based materials with tailored nanostructures for energy conversion and storage. *Materials Science and Engineering: R: Reports 102* (2016), 1–72.

[121] Yoo, H., Jo, H., and Oh, S. S. Detection and beyond: challenges and advances in aptamer-based biosensors. *Materials Advances 1*, 8 (2020), 2663–2687.

[122] You, X., and Pak, J. J. Graphene-based field effect transistor enzymatic glucose biosensor using silk protein for enzyme immobilization and device substrate. *Sensors and Actuators B: Chemical 202* (2014), 1357–1365.

[123] Zhang, J. X. J., and Hoshino, K. *Molecular Sensors and Nanodevices: Principles, Designs and Applications in Biomedical Engineering*. Micro and nano technologies series. Elsevier Science & Technology Books, Saint Louis, 2013.

[124] Zhang, Y., Tang, T.-T., Girit, C., Hao, Z., Martin, M. C., Zettl, A., Crommie, M. F., Shen, Y. R., and Wang, F. Direct observation of a widely tunable bandgap in bilayer graphene. *Nature 459*, 7248 (2009), 820–823.

[125] Zheng, Z., Zhang, H., Zhai, T., and Xia, F. Overcome Debye Length Limitations for Biomolecule Sensing Based on Field Effective Transistors†. *Chinese Journal of Chemistry 39*, 4 (4 2021), 999–1008.

[126] Zhou, L., Wang, K., Sun, H., Zhao, S., Chen, X., Qian, D., Mao, H., and Zhao, J. Novel Graphene Biosensor Based on the Functionalization of Multifunctional Nano-bovine Serum Albumin for the Highly Sensitive Detection of Cancer Biomarkers. *Nano-Micro Letters 11*, 1 (2019), 20.

[127] Zhou, W., Huang, P.-J. J., Ding, J., and Liu, J. Aptamer-based biosensors for biomedical diagnostics. *The Analyst 139*, 11 (6 2014), 2627–2640.

[128] Zhu, Y., Hao, Y., Adogla, E. A., Yan, J., Li, D., Xu, K., Wang, Q., Hone, J., and Lin, Q. A graphene-based affinity nanosensor for detection of low-charge and low-molecular-weight molecules. *Nanoscale 8*, 11 (2016), 5815–5819.

A. Appendix

Fabrication protocol

This protocol should provide a comprehensive "recipe" depicting all the preparation steps for fabricating the graphene field-effect transistors used in this work. The graphics for this protocol were created by the author using PowerPoint © and BioRender ©, as well as camera pictures obtained by the author.

1. Purchase of substrates:
   For this work commercially available devices from MicruX Technologies were purchased. Specifically Thin-film Gold InterDigitated Electrode (10/10 µm) without the epoxy resin SU-8 (ED-IDE1-Au).

2. Quality check:
   In a first step the purchased devices have to be checked for their quality. Each box contains 50 devices and although industrial-fabricated there can be size aberrations or damaged electrodes, which disqualify the devices for further use. Therefore the chips are individually placed in the measurement cell in order to check for size. During that the devices are also optically checked for severe damages. Depending on the batch it can also be valuable to further do random checks of the electrodes under a light microscope to validate the intactness.

3. Cleaning:
   In order to remove organic residues from the substrates they are placed into a glass beaker with acetone for 15 minutes, covered with a glass plate and put on a shaker for gentle oscillation of the liquid. Afterwards the substrates are individually rinsed with MQ and placed into a glass beaker with MQ, covered and shaken for another 15 minutes. Finally the substrates are individually rinsed again using Ethanol and immersed into a glass beaker with Ethanol, which is again put on the shaker for 15 minutes with a glass plate as coverage. After that the substrates are blow-dried with the air gun. For that the back of the substrate is held with the tweezers and the right (or left - depending on handedness) corner of the substrate is held against a paper towel on the table. Then the air-flow is appropriately applied to completely dry the substrate. Although maybe seemingly counterintuitive, it is important to finish the washing step with ethanol, as water residues are incompatible with the chemical used for the next step.

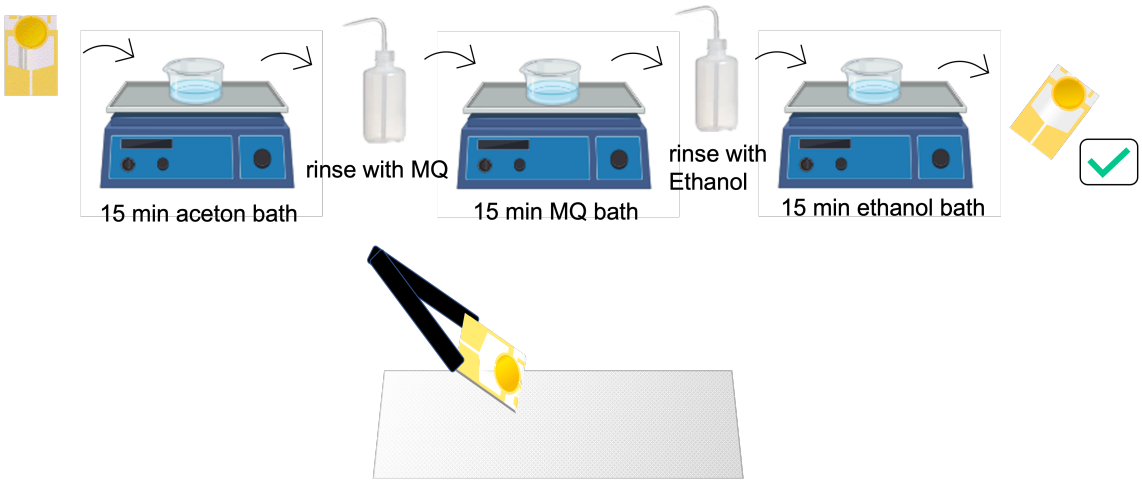

Figure A.1.: Schematic of device cleaning steps

4. Silanization
   In order to improve the adhesion of graphene onto the substrate a silanization step is implemented. For this a 2% solution of trimethoxyphenylsilane (TMPS) in ethanol is mixed and poured in a plastic petri dish. It is highly relevant that plastic is used for this step as silane sticks to glass. The chips are then carefully immersed in this solution for 1h and sealed with an aluminium foil under the fume hood. Afterwards the chips are immersed in a beaker of fresh ethanol, rinsed with ethanol, immersed in another beaker of fresh ethanol and again rinsed with ethanol before they are dried and placed into a glass petri dish. Finally the chips are put in the oven for baking at 120°C, again being covered under an aluminium foil. After baking the glass petri dish containing the chips is removed from the oven and left for cool down (usually this was done as overnight step). When the chips are cooled down they can be stored in petri dishes or gel boxes. The chips are now ready for graphene transfer.

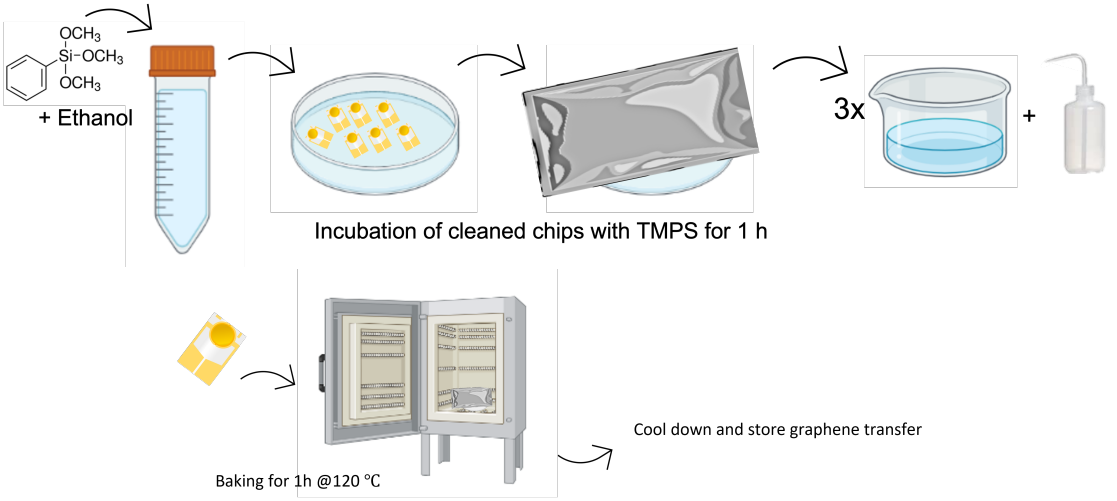

Figure A.2.: Schematic illustration of the silanization process

5. Graphene transfer
   In order to make graphene transferable, the commercially acquired cooper (Cu) - graphene - cooper sheet from Graphenea © was cut and treated in the clean room. Because the bottom layer of cooper is already retreated for easier removal, this layer was removed via reactive ion etching (RIE). Onto this side (so directly on the graphene film) a layer of polymethyl methacrylate (PMMA) with a 200 nm thickness was spin-coated and annealed. The Cu/graphene/PMMA pieces were then brought to the lab, where they could be cut into smaller pieces that would well cover the whole sensing area of the devices. For removing the remaining Cu-layer, a 0.2M ammonium persulfate solution was prepared, by dissolving the required amount of

ammonium persulfate ($(NH_4)_2S_2O_8$) in DIW. As every film requires it's own beaker, one can calculate with 80-100ml per film. Each small piece of Cu/graphene/PMMA was then individually put into a teflon beaker containing the $NH_4)_2S_2O_8$ solution with the Cu side facing the solution. This was left overnight for allowing the full etching process to be finished. On the next day this is proceeded by five rinsing steps, carefully scooping out the floating graphene film using a small falcon tube cap and each time placing it in a new beaker of fresh DIW. These washing steps will remove remaining residues from the etching solution. The graphene film is then transferred onto one of the cleaned and silanized chips by extremely carefully submerging the chip under the graphene film and moving it toward the edge of the beaker. While holding the chip in a tilted manner with the tweezers the graphene film can be positioned correctly and slowly and carefully removed from the water. This requires great attention, as any folding will result in defects on the film. When successfully transferred onto the chips, the chips are left for drying on a glass slide at room temperature for 90min, while covering them with a glass petri dish, but positioning it unleveled, so that air can still circulate. Following this drying step the chips on the glass slide are put on the hotplate for graphene annealing. This is done by slowly heating up the hotplate to 90°C, which is done over 30min. Then the chips are left for 30min at 90°C and are afterwards slowly cooled down again to RT. So 30min to reach 90°C, 30min at 90°C and then 30min (or more when required) to cool down to RT. Now the graphene film is annealed and only the PMMA layer has to be removed before the devices can be used. This should ideally rather be done promptly before doing experiments to avoid the longer exposure of graphene to air. Alternatively the chips can also be stored under nitrogen after the removal.

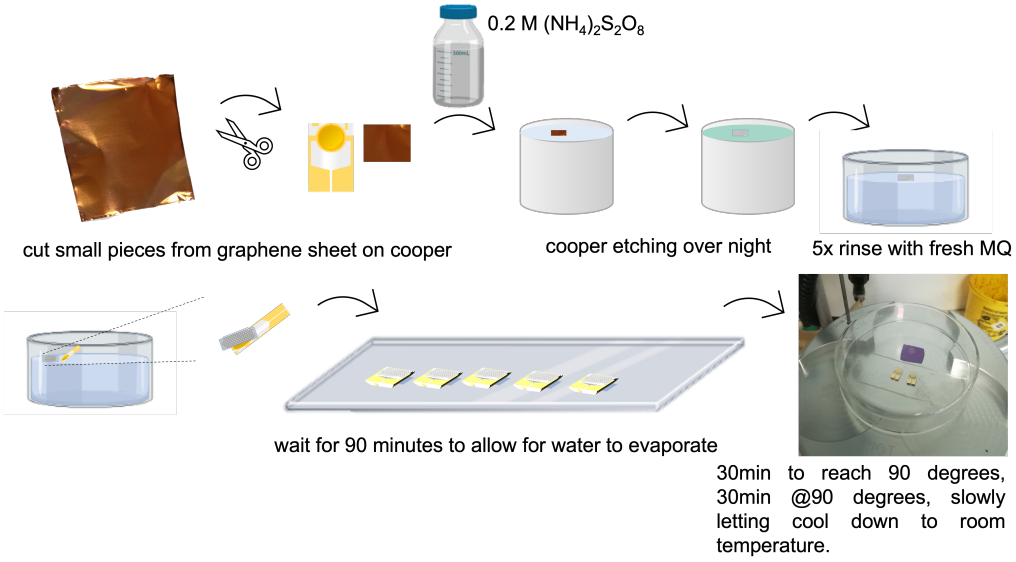

Figure A.3.: Schematic of graphene film preparation and transfer

6. Polymer removal
   The PMMA polymer layer is removed to make the graphene film accessible for further surface modification. For this the chips are put on a glass slide which is placed in the UV-ozone chamber, where the chips are then under plasma cleaning for 10min. Afterwards the chips are immersed in a beaker with fresh acetone that is put on the shaker for 30min. The rotations should be moderate, so that the liquid only moves in slow circles. After the acetone bath the chips are individually rinsed with acetone, ethanol and MQ and gently dried. The chips are now ready to use. Usually this is also a good time to check some properties of the device like measuring the resistance (Ω) and recording a transfer curve ($I_D V_G$) using a standard buffer.

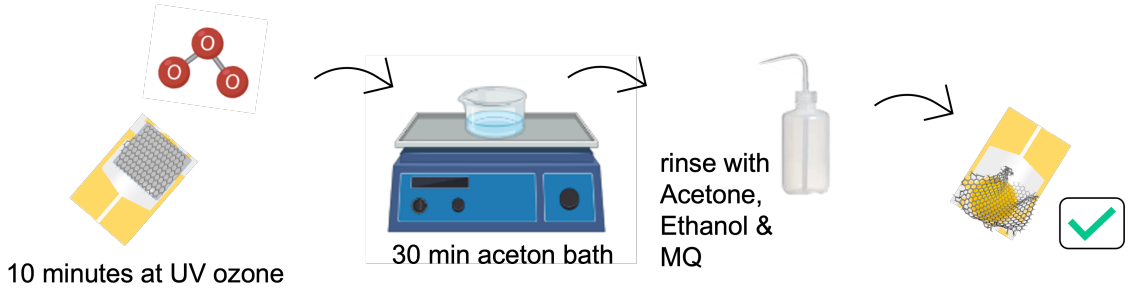

Figure A.4.: Schematic of PMMA removal steps

Declaration of work contribution

All biosensing data was obtained and analysed by the author. Concerning the fabrication process all steps excluding the ones in the clean room (RIE and spin-coating) were also done by the author. The clean-room treated graphene sheets were kindly provided by Adrien Hugo. Raman spectroscopy data was obtained by the author under the supervision of Adrien Hugo and analysed by the author. The SEM pictures were obtained by the author after receiving complete training on the apparatus. AFM pictures were obtained by Dominique Deresmes in the presence of the author and the data was analysed by the author. XPS samples were investigated by the team in charge and the data was subsequently analysed by the author. The nanodiscs were kindly provided by the Group of Frank Rosenau in Ulm and the Biosensor Technologies group from the Austrian Institute of Technology (AIT) in Tulln, in particular Jakob Andersson and David Kleinheinz.

List of Figures